

Fall 1-31-2009

Optimizing fare structure and service frequency for an intercity transit system

Feng-Ming Tsai
New Jersey Institute of Technology

Follow this and additional works at: <https://digitalcommons.njit.edu/dissertations>



Part of the [Transportation Engineering Commons](#)

Recommended Citation

Tsai, Feng-Ming, "Optimizing fare structure and service frequency for an intercity transit system" (2009). *Dissertations*. 898.
<https://digitalcommons.njit.edu/dissertations/898>

This Dissertation is brought to you for free and open access by the Electronic Theses and Dissertations at Digital Commons @ NJIT. It has been accepted for inclusion in Dissertations by an authorized administrator of Digital Commons @ NJIT. For more information, please contact digitalcommons@njit.edu.

Copyright Warning & Restrictions

The copyright law of the United States (Title 17, United States Code) governs the making of photocopies or other reproductions of copyrighted material.

Under certain conditions specified in the law, libraries and archives are authorized to furnish a photocopy or other reproduction. One of these specified conditions is that the photocopy or reproduction is not to be “used for any purpose other than private study, scholarship, or research.” If a user makes a request for, or later uses, a photocopy or reproduction for purposes in excess of “fair use” that user may be liable for copyright infringement,

This institution reserves the right to refuse to accept a copying order if, in its judgment, fulfillment of the order would involve violation of copyright law.

Please Note: The author retains the copyright while the New Jersey Institute of Technology reserves the right to distribute this thesis or dissertation

Printing note: If you do not wish to print this page, then select “Pages from: first page # to: last page #” on the print dialog screen



The Van Houten library has removed some of the personal information and all signatures from the approval page and biographical sketches of theses and dissertations in order to protect the identity of NJIT graduates and faculty.

ABSTRACT

OPTIMIZING FARE STRUCTURE AND SERVICE FREQUENCY FOR AN INTERCITY TRANSIT SYSTEM

**by
Feng-Ming Tsai**

This study presents an approach to jointly optimize service headway and differentiated fare for an intercity transit system with an objective of total profit maximization and with consideration given to the economic and social sustainability of the system. Service capacity and fleet size constraints are considered. The optimization problem is structured into four scenarios which are comprised of the combinations of whether the Ranges of Travel Distance (RTD) is fixed or variable and if the time period is for a single period or for multiple periods. A successive substitution method (specifically, a modified Gauss Southwell method) is applied to solve for the optimal solutions when the RTD is considered fixed, while a heuristic solution algorithm (specifically, a Genetic Algorithm) is developed to find the optimal solutions when the RTD is considered to be optimized.

The methodology discussed in this dissertation contributes to the field of transportation network modeling because it establishes how to solve the fare and headway design problem for an intercity transit system. Intercity transit agencies are faced with the challenge of determining fares for a very complicated setting in which demand elasticity, realistic geographic conditions, and facility locations of the transit system all must be taken into account.

A real world case study - Taiwan High Speed Rail is used to demonstrate the applicability of the developed methodology. Numerical results of optimal solutions and sensitivity analyses are presented for each scenario. The sensitivity analyses enable

transit planners to quantify the impact of fare policies and address social equity issues, which can be a major hurdle of implementing optimal fare policy to achieve maximum profit operation. According to the sensitivity analysis, the total profit surfaces for various headways, fares, and RTD are relatively flat near the optimum. This indicates that the transit operator has flexibility in shifting the solution marginally away from the optimum without significantly reducing the maximum profit. By varying the elasticity parameters of fare and demand one can observe how these variables affect the optimized RTD. The results indicate that as the elasticity parameters of fare increase or demand decreases, the optimal number of RTD increase while the boundaries of RTD are concentrated in the range of shorter travel distances.

**OPTIMIZING FARE STRUCTURE AND SERVICE FREQUENCY
FOR AN INTERCITY TRANSIT SYSTEM**

**by
Feng-Ming Tsai**

**Dissertation Advisor
Dr. Steven I-Jy Chien**

**A Dissertation
Submitted to the Faculty of
New Jersey Institute of Technology
in Partial Fulfillment of the Requirements for the Degree of
Doctor of Philosophy in Transportation**

Interdisciplinary Program in Transportation

January 2009

**OPTIMIZING FARE STRUCTURE AND SERVICE FREQUENCY
FOR AN INTERCITY TRANSIT SYSTEM**

**by
Feng-Ming Tsai**

**A Dissertation
Submitted to the Faculty of
New Jersey Institute of Technology
in Partial Fulfillment of the Requirements for the Degree of
Doctor of Philosophy in Transportation**

Interdisciplinary Program in Transportation

January 2009

Copyright © 2009 by Feng-Ming Tsai

ALL RIGHTS RESERVED

APPROVAL PAGE

**OPTIMIZING FARE STRUCTURE AND SERVICE FREQUENCY
FOR AN INTERCITY TRANSIT SYSTEM**

Feng-Ming Tsai

11/13/08

Dr. Steven I-Jy Chien, Dissertation Advisor Date
Professor of Civil and Environmental Engineering, NJIT

11/13/08

Dr. Athanassios Bladikas, Committee Member Date
Associate Professor of Industrial and Manufacturing Engineering, NJIT

11/13/08

Dr. Lazar Spasovic, Committee Member Date
Professor of Civil and Environmental Engineering, NJIT

11/13/08

Dr. Janice R. Daniel, Committee Member Date
Associate Professor of Civil and Environmental Engineering, NJIT

11/13/2008

Dr. Jian Yang, Committee Member Date
Associate Professor of Industrial and Manufacturing Engineering, NJIT

BIOGRAPHICAL SKETCH

Author: Feng-Ming Tsai
Degree: Doctor of Philosophy
Date: January 2009

Undergraduate and Graduate Education:

- Doctor of Philosophy in Transportation Engineering
New Jersey Institute of Technology, Newark, NJ, 2009
- Master of Science in Transportation Engineering
New Jersey Institute of Technology, Newark, NJ, 2002
- Bachelor of Science in Civil Engineering
Chung Yung Christian University, Chun-Li, Taiwan, 1998

Major: Transportation Engineering

Presentations and Publications:

Bladikas, Athanassios, Chuck Feng-Ming Tsai, and Steven I-Jy Chien. "Evaluation of Bus Travel Time and Schedule Adherence under Adverse Weather." Presentation at Transportation Research Board, 88th Annual Meeting, 2009.

Tsai, Chuck Feng-Ming, Steven I-Jy Chien, and Lazar N. Spasovic. "Optimizing Distance-Based Fares and Headway of an Intercity Transportation System with Elastic Demand and Trip Length Differentiation," Journal of the Transportation Research Board, 2008. (Accepted for publication)

Chien, Steven I-Jy and Chuck Feng-Ming Tsai. "Optimization of Fare Structure and Service Frequency for Maximum Profitability of Transit Systems." Transportation Planning and Technology, Vol. 30, No. 5, pp. 477-500, 2007.

Chien, Steven, Chuck Feng-Ming Tsai, and Edwin Hou. "Optimization of Multiple-Route Feeder Bus Service - Application of Geographic Information Systems (GIS)," Journal of the Transportation Research Board, TRR No. 1857, pp. 56-64, 2003.

Daniel, Janice, Chuck Feng-Ming Tsai, and Steven I-Jy Chien. "Factors in Truck Crashes on Roadways with Intersections," Journal of the Transportation Research Board, TRR No. 1818, pp. 54-59, 2002.

To my beloved parents and family,
thanks for their unwavering support and concern.

Especially thank my dearest wife for her countless sacrifices and immense love,
she has made this work possible.

僅以此成果獻給我最深愛的老婆, *Nathan* 及最關心我的家人

唯有他們的鼓勵與支持我才可以順利完成

ACKNOWLEDGMENT

I am greatly indebted to my dissertation advisor, Dr. Steven I-Jy Chien, who constantly supported, inspired and encouraged me with his insight, dedication and understanding during my Ph.D. study. Special thanks are given to Dr. Athanassios Bladikas, Dr. Lazar Spasovic, Dr. Janice Daniel, and Dr. Jian Yang for serving as committee members and providing me with precious suggestions on research and industrial practice.

I also extend my thanks to Dr. Yi-Ta Wu, Dr. Yimin Tang, Dr. Rajat Rajbhandari, Mr. Kitae Kim, and Ms. Patricia DiJoseph for their informative discussion on the wide range of transportation problems.

I also appreciate support from the New Jersey Department of Transportation, National Center for Transportation and Industrial Productivity, New Jersey Institute of Technology, and the International Road Federation (IRF) Fellowship Program.

TABLE OF CONTENTS

Chapter	Page
1 INTRODUCTION	1
1.1 Problem Statement	3
1.2 Objective and Work Scope.....	5
1.3 Research Approach	8
1.4 Dissertation Organization	9
2 LITERATURE REVIEW	10
2.1 Transit Fare Structures	10
2.2 Fare Optimization	16
2.3 Optimization Algorithms and Heuristics	22
2.4 Transit Demand.....	25
2.5 Fare Elasticities.....	29
2.6 Summary	32
3 METHODOLOGY	34
3.1 Fixed RTD and Single Time Period – Scenario I.....	34
3.1.1 System Assumptions	34
3.1.2 Model Formulation	37
3.1.3 Constraints	39
3.1.4 Optimization Problem.....	42
3.2 Variable RTD and Single Time Period – Scenario II.....	45
3.2.1 System Assumptions	45
3.2.2 Model Formulation	47
3.2.3 Constraints	47

TABLE OF CONTENTS
(Continued)

Chapter	Page
3.2.4 Optimization Problem.....	48
3.3 Fixed RTD for Multiple Time Periods – Scenario III.....	49
3.3.1 System Assumptions.....	49
3.3.2 Model Formulation.....	51
3.3.3 Constraints.....	52
3.3.4 Optimization Problem.....	54
3.4 Variable RTD for Multiple Time Periods – Scenario IV.....	56
3.4.1 System Assumptions.....	57
3.4.2 Model Formulation.....	58
3.4.3 Constraints.....	59
3.4.4 Optimization Problem.....	59
3.5 Summary.....	61
4 SOLUTION ALGORITHMS.....	63
4.1 Fixed RTD in Scenarios I and III.....	64
4.1.1 Successive Substitution Method.....	64
4.1.2 The Hessian Matrix.....	68
4.2 Variable RTD in Scenarios II and IV.....	71
4.2.1 Genetic Algorithm.....	71
4.2.2 Encoding and Decoding Schemes.....	78
4.2.3 Reproduction, Crossover, and Mutation.....	82
4.3 Summary.....	85

TABLE OF CONTENTS
(Continued)

Chapter	Page
5 CASE STUDY	86
5.1 The Taiwan High Speed Rail System	86
5.2 Fixed RTD and Single Time Period – Scenario I.....	91
5.3 Variable RTD and Single Time Period – Scenario II.....	95
5.4 Fixed RTD and Multiple Time Periods – Scenario III.....	100
5.5 Variable RTD and Multiple Time Periods – Scenario IV	105
5.6 Optimal Results Comparison.....	110
5.7 Sensitivity Analysis.....	117
6 CONCLUSION AND FUTURE RESEARCH.....	140
6.1 Conclusions.....	141
6.2 Future Research	143
REFERENCES	145

LIST OF TABLES

Table	Page
1.1 Definitions of the Study Fare Optimization Scenarios	5
2.1 Characteristics of Various Fare Structures	12
2.2 Fare Structures of Transit Systems in North America	14
2.3 Analytical Models for Transit System and Fare Optimization	21
3.1 Weight Factors of Unit Fare by Different RTD (Single Time Period)	46
3.2 Weight Factors of Unit Fare for Different RTD (Multiple Time Periods)	58
3.3 Characteristics of Models for Scenarios I through IV	62
3.4 Decision Variables in the Models for Scenarios I through IV	62
4.1 Number of Decision Variables and Principal Minors	71
4.2 Number of Decision Variables for Different RTD	73
4.3 Usage of the Genes in Part 1	80
4.4 Representation of the genes in Part 2	81
4.5 Representation of the Genes in Part 3	82
4.6 One-Point and Two-Point Crossover	84
4.7 One-Point and Two-Point Mutations	84
5.1 Station-to-Station Distances and Travel Times	89
5.2 Baseline Values of Input Parameters for All Scenarios	90
5.3 Potential Demand in Passengers per Hour	91
5.4 Optimized Fares and Weighted Unit Fares of Scenario I	93
5.5 Ridership under Optimal Operation of Scenario I	94
5.6 Ridership and Average Revenue under Optimal Operation of Scenario I	94
5.7 Load Factor under Optimal Operation of Scenario I	95

LIST OF TABLES
(Continued)

Table	Page
5.8 Elasticity Parameter of Fare of Scenario II.....	95
5.9 Optimized Fares and Weighted Unit Fares of Scenario II.....	98
5.10 Ridership under Optimal Operation of Scenario II.....	98
5.11 Ridership and Revenue under Optimal Operation of Scenario II.....	99
5.12 Load Factor under Optimal Operation of Scenario II.....	99
5.13 Potential Demand in Passengers per Hour (Peak)	100
5.14 Potential Demand in Passengers per Hour (Off-peak).....	101
5.15 Optimized Fares and Weighted Unit Fares of Scenario III (Peak)	102
5.16 Optimized Fares and Weighted Unit Fares of Scenario III (Off-peak)	102
5.17 Ridership under Optimal Operation of Scenario III (Peak Hour).....	103
5.18 Ridership under Optimal Operation of Scenario III (Off-peak Hour)	103
5.19 Ridership and Revenue under Optimal Operation of Scenario III.....	104
5.20 Load Factor under Optimal Operation of Scenario III.....	105
5.21 Optimized Fares and Weighted Unit Fares of Scenario IV (Peak).....	107
5.22 Optimized Fares and Weighted Unit Fares of Scenario IV (Off-Peak).....	107
5.23 Ridership under Optimal Operation of Scenario IV (Peak).....	108
5.24 Ridership under Optimal Operation of Scenario IV (Off-peak)	108
5.25 Average Revenue under Optimal Operation of Scenario IV	109
5.26 Load Factor under Optimal Operation of Scenario IV	110
5.27 Optimized Results of Scenarios I and II	111
5.28 Optimized Results of Scenarios III and IV	113
5.29 Optimized Results of Scenario I by Various Solution Algorithms.....	117

LIST OF FIGURES

Figure	Page
3.1 Studied transit route configuration and station-to-station distance.....	36
3.2 Configuration of outbound travel demand at link m	41
3.3 Configuration of inbound travel demand at link m	41
3.4 Optimal headway for various feasible conditions (Single time period)	44
3.5 Optimal headway for various feasible conditions (Multiple time periods)	56
4.1 Flow chart of the modified Gauss-Southwell method	67
4.2 Total number of decision variables vs. RTD of Scenario II	73
4.3 Flow chart of the developed Genetic Algorithm.....	77
4.4 Encoding scheme of a chromosome representation.....	78
5.1 Configuration of the Taiwan High Speed Rail line	87
5.2 Maximum profit vs. number of RTD of Scenario II by GA	97
5.3 Maximum profit vs. number of RTD of Scenario IV by GA.....	106
5.4 Optimized fares of Scenarios I and II	111
5.5 Load factor under optimal operation of Scenarios I and II.....	112
5.6 Optimized fares of Scenarios III and IV	113
5.7 Load factor under optimal operation of Scenarios III and IV.....	114
5.8 Optimized numbers and RTD of Scenarios I through IV	115
5.9 Profit achieved in each iteration of Scenario I.....	116
5.10 Profit vs. headway for Scenarios I and II.....	118
5.11 Profit vs. unit fare (δ) for Scenarios I and II.....	119
5.12 Profit vs. headway for Scenarios III and IV	119
5.13 Profit vs. unit fare (δ') for Scenarios III.....	121
5.14 Profit vs. unit fare (δ') for Scenarios IV.....	121

LIST OF FIGURES
(Continued)

Figure	Page
5.15 Profit vs. unit fares γ_s and γ_m for Scenario I.....	122
5.16 Profit and ridership vs. $E_{F_{zy}}$ in each RTD for Scenario I	124
5.17 Profit and ridership vs. $E_{F_{zy}}$ in each RTD for Scenario III.....	124
5.18 Maximized profit and ridership vs. E_{F_y} multiplier for Scenario II.....	125
5.19 Maximized profit and ridership vs. E_{F_y} multiplier for Scenario IV.....	126
5.20 Optimal number of RTD vs. E_{F_y} multiplier for Scenarios II and IV	127
5.21 Optimal RTD for various $E_{F_{zy}}$ multipliers for Scenario II.....	128
5.22 Optimal RTD for various $E_{F_{zy}}$ multipliers for Scenario IV	129
5.23 Maximized profit and optimal headway vs. E_w for Scenarios I and II.....	130
5.24 Maximized profit and optimal headway vs. E_w for Scenarios III and IV	131
5.25 Maximized profit and optimal headway vs. demand multiplier for Scenarios I and II.....	131
5.26 Maximized profit and optimal headway vs. demand multiplier for Scenarios III and IV	133
5.27 Optimal weighted unit fare vs. demand multiplier for Scenarios I and III.....	134
5.28 Optimal unit fare vs. demand multiplier for Scenarios II and IV	135
5.29 Maximized profit and optimal fleet size vs. demand multiplier for Scenario IV	136
5.30 Maximized profit and optimal number of RTD vs. demand multiplier for Scenarios II and IV	137
5.31 Optimal RTD for various demand multipliers for Scenario II.....	138
5.32 Optimal RTD for various demand multipliers for Scenario IV	139

CHAPTER 1

INTRODUCTION

Public transit systems are an integral part and essential feature of urban mobility in developed as well as developing countries. An efficient transit service may attract travelers from riding automobiles, which has been recognized as a potential way of alleviating traffic congestion, improving mobility, reducing air pollution, and reducing energy consumption. One of the key issues in developing an efficient transit system is to set a fare combined with good service quality to stimulate passenger demand and increase revenue.

As indicated in a report by the American Public Transportation Association (APTA, 2005), transit ridership increases by 3.3 percent across all public transit systems for every 10 percent increase in fuel prices, with particularly high ridership growth experienced by light rail (e.g., 8.8 percent). A similar study conducted by Litman (2004) based on selected European public transit systems was found that a 10 percent rise in fuel prices increased transit ridership of 1.6 percent in the short run and 1.2 percent over the long run. In another study, it was found that due to a drastic increase of fuel price from 1.07 dollars per gallon in 1998 to 3.61 dollars per gallon in 2008 (until August), commuters changed their travel habits and relied more on public transit (Currie et al. 2007). APTA announced that Americans took more than 2.8 billion trips on public transportation in the second quarter of 2008. This is almost 140 million more trips than last year for the same time period. In 2007, there were 10.3 billion passenger trips served by U.S. public transportation, which reach the highest ridership over the past 50 years.

Therefore, transit agencies have to adjust their service frequency and fare to justify increasing demand and the associated operating expenses. Optimizing a transit system with proper service operation and fare is therefore an important goal of the public transportation industry.

Transit fare policies are established mostly in response to a particular issue or problem (e.g., a revenue shortfall, a new competitive transit system, etc.). According to a report by APTA (1994), only 3% of transit agencies made fare changes on a regularly scheduled basis while the remaining 97% reported making fare changes only as needed. However, a later APTA report (1998) indicated that more than half of the transit agencies have a regular fare review process on an unexpected revenue shortfall.

The out-of-pocket cost (e.g., fare) and its relationship to service quality greatly influence transit ridership. The transit fare is a key source of revenue and is essential to the operation of a reasonable service. However, structuring the fare is a challenging task to fulfill different objectives, such as maximizing profit and/or minimizing operator cost subject to practical constraints of operable fleet size.

The parameters for setting transit fare are correlated with three major factors, including fare strategy, payment/collection options, and pricing levels (Fleishman, 1996). Although each parameter is typically evaluated separately, these are all interrelated, and decisions must be made by considering the joint impact from all parameters. Basic fare strategies are in general either flat or differentiated. In a flat fare, riders are charged the same fare regardless of the length of the trip, time of day, or quality of service. Alternatively, fares can be differentiated by various dimensions, such as distance- or zone-based, time-based (e.g., peak versus off-peak), and service-based (e.g., express

versus local). Payment options include cash, period pass, single or multiple ride tickets, and stored-value/ride fare card. The final piece is the actual pricing levels of each payment option, including discounts for prepaid options.

While considering differentiated fares, a higher fare should be charged to cover the higher operating costs associated with serving longer trips, operating peak period service, or providing express service. Otherwise, the users of the higher cost services are effectively cross-subsidized by the users of short distance, off-peak, or local service. In many cases, differentiated fares are deemed a better approach to generate greater revenue than using a flat fare. If the users are traveling longer distances, they would be considered less price sensitive than those using a shorter distance service.

The ultimate goal of this study is to optimize fare and service to yield a maximum profit operation for an intercity transit system, which relies on substantial revenue to cover the operating cost. Although it is costly to provide convenient service, demand will be stimulated if the fare charged to the users is reasonable.

1.1 Problem Statement

Before evaluating an intercity transit system, a set of performance measures, such as level of service, on-time performance and equitable fare must be identified. The trade-off between economically efficient operation and adequate services for the public is very complex and requires sophisticated analyses. Transit suppliers need to decide what service level to provide (e.g., how frequently vehicles will be dispatched) and what fare to charge. To maintain good financial health, the service provider has a challenging task, maximizing either social welfare or profit (defined as the total fare box revenue minus the

operator's cost). In the case of a profit maximizing objective, when expenditures exceed revenues, as it is the case in many public transportation systems, the objective becomes minimization of the subsidy.

On the other hand, transit riders prefer short wait time (or frequent service) that can be usually achieved by decreasing service headway (i.e., the time between the successive arrivals), which increases fleet size and that escalates the operator's cost. Understandably, most transit agencies would prefer to minimize the number of departures to reduce operating cost. In addition, steady riders prefer lower fares, which in turn may lead to insufficient revenue to cover the cost. The trade-off between the level of fare and operating cost should be carefully considered when transit agencies plan a new intercity transit route or extend an existing intercity transit service.

While designing intercity transit service, transit agencies should have a proper understanding of passenger demand, which is a function of fare and service characteristics. Previous studies (Meyer, 1965; Daskin et al. 1998; Ling, 1998) found that the impact of travel distance on intercity transit fare is diminished as distance increases. If the elasticity of demand is strongly dependent on distance, then differentiated fares can maximize total revenue. Therefore, a potential way to increase the revenue could be handled by using a distance-based fare, which accounts for the sensitivity of passengers traveling within different Ranges of Travel Distance (RTD). This helps transit agencies quantify how much better of, in terms of additional revenue or profit, they can be by comparing this case with charging pure distance-based rates.

It is desirable to develop an analytical model to optimize and evaluate an intercity transit system whose characteristics (i.e., fare, demand, service frequency, and fare

elasticity) vary irregularly over trip length and time. Such a model can reliably evaluate and compare intercity transit systems, especially when demand fluctuates significantly over different time periods.

1.2 Objective and Work Scope

This study presents an optimization approach for an intercity transit service considering demand elasticity, which is sensitive to fare and travel time. The objective of this study is to develop models which jointly optimize headway, differentiated fare, and RTD that yield the maximum total profit for an intercity transit system, subject to service capacity and fleet size constraints. The optimized differentiated fares are based on the trip length and time of the trip (e.g., peak and off-peak periods).

To develop a differentiated fare, four scenarios shown in Table 1.1 are used, which consider given or variable RTD with single period or temporal distance-based fare. The developed model for each scenario is discussed below.

Table 1.1 Definitions of the Study Fare Optimization Scenarios

		Ranges of Travel Distance (RTD)	
		Given	Variable to be optimized
Distance-based Fare	Fixed over time	Scenario I	Scenario II
	Temporal	Scenario III	Scenario IV

- Scenario I: A base model developed in this scenario is to optimize distance-based fare and headway for peak period under the given RTD for fare differentiation.

The peak period considered in this scenario is based on the highest potential hourly demand, and thus the objective is maximizing the hourly profit.

- Scenario II: The model developed in this scenario is enhanced from Scenario I by considering variable RTD for fare differentiation, which optimizes the headway and distance-based fare. The objective is maximizing the hourly profit considering the peak period demand.
- Scenario III: The model developed in this scenario is to optimize temporal distance-based fares and headway for peak and off-peak periods under the given RTD for fare differentiation. The objective is maximizing the daily profit considering daily demand.
- Scenario IV: The model developed in this scenario is enhanced from Scenario III by considering variable RTD for fare differentiation, which optimizes the temporal headway and distance-based fare. The objective is maximizing daily profit considering daily demand.

It is worth noting that fare elasticities in Scenarios I and III are identical within the same RTD, however in Scenarios II and IV, variable elasticity parameters of fare in different origin-destination (O-D) pairs are considered.

The developed models are used for a real-world case study, the Taiwan High Speed Rail (THSR), a 212 - mile long high speed rail line with eight stations connecting three major cities, Taipei, Taichung, and Kaohsiung, on Taiwan's west coast. All numerical data used in this study are based on real world operating data, which include station spacing, vehicle travel time, potential demand, and vehicle capacity. The THSR system began revenue operation in January, 2007, and the optimal solutions from the

developed models may influence future managerial decisions.

The overall framework for this research approach is shown in Figure 1.1. To achieve the objective of this research, various previous studies related to transit network and fare structures, optimization methods, passenger travel behavior, and solution algorithms are thoroughly reviewed and discussed in Chapter 2.

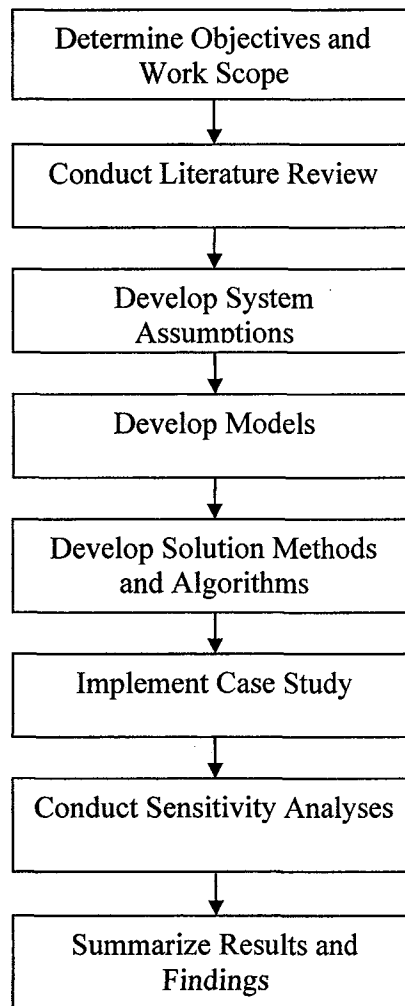


Figure 1.1 Framework of research approach.

1.3 Research Approach

To satisfy the aforementioned objectives of Section 1.2 and models for each scenario, an analytical approach is used to optimize fare and headway under the condition of fixed RTD. This optimization approach relies essentially on the methods of differential calculus. Analytical results are presented for the optimized decision variables and objective functions. However, as model complexity increases, analytical solutions become very difficult to obtain. Thus, a solution algorithm, called Genetic Algorithm, is developed to search for a near optimum solution.

The optimization models developed in Scenarios I and III are multi-dimensional and nonlinear functions, including the decision variables (e.g., headway and fare), which can be solved by numerical methods (e.g., Gauss-Southwell and Powell methods). Thus, a modified Gauss-Southwell method (successive substitution method) is implemented to determine the optimized solutions (i.e., fixed and temporal fares and service headways) numerically.

The optimization models developed in Scenarios II and IV are also multi-dimensional, nonlinear, and have multiple real and integer variables. The determination of fare is a large combinatorial problem where the solution space consists of combinations of distance-based fare and headway (i.e., fixed and temporal) with various RTD. Therefore, a Genetic Algorithm (GA) is developed to solve the optimized RTD (e.g., optimal number of RTD and corresponding travel distance range) as well as service headway and fare for single and multiple time periods (e.g., peak and off-peak).

1.4 Dissertation Organization

This dissertation is organized into six chapters. In Chapter 1, the background of the fare optimization problem, the research objective, and work scope are presented. Previous studies are thoroughly reviewed and discussed in Chapter 2. Chapter 3 presents the formulation of the total profit function for the four scenarios considering both given and variable RTD during single and multiple time periods, while in Chapter 4, the successive substitute method and developed Genetic Algorithm are presented to solve the optimization problems defined in Scenarios I through IV. Chapter 5 presents a case study of the Taiwan High Speed Rail system, in which the applicability and performance of the developed models are tested and assessed. Numerical results, including optimal solutions and sensitivity analyses are conducted. Finally, conclusions and suggestions for future studies are presented in Chapter 6.

CHAPTER 2

LITERATURE REVIEW

Previous studies reviewed in this chapter are summarized in topical sections, which includes transit fare structures, transit system and fare optimization, optimization algorithms and heuristics, transit travel demand functions, and fare elasticities.

2.1 Transit Fare Structures

Fleishman et al. (1996) and Vuchic (2004) classified fare structures based on the relationship between the amount of fare and distance traveled. According to this criterion, fare structures are flat or differentiated. The differentiated fare can be further subdivided into zonal fare, distance-based fare, sectional fare, and time-based fare.

Previous studies on transit fare structures found that the use of flat fare is highly inequitable and penalizing to short-distance or off-peak users (Cervero, 1981). Meyer (1965) found that passengers who travel longer distance are generally in higher income brackets. Hence, to avoid the inequity of short distance riders subsidizing long travel distance riders, implementing differentiated fares not only provides a solution for the equity issue but also bring a potential benefit to generate greater revenue. Thus, a differentiated fare policy was deemed better than a flat fare policy.

For flat fare, transit users are charged a constant fare regardless of trip length or type of services (e.g., express vs. local) throughout the transit network (Fleishman et al. 1996). A flat fare is the simplest and most convenient fare structure for both passengers and transit operators in terms of payment and collection (LaBelle et al. 1995). Travel

distances are relatively uniform in cities with limited geographic size, so that the conveniences of the flat fare outweigh the inequities related to its lack of correlation with trip length (Vuchic, 2004). Therefore, small and medium size systems generally opt for flat fare.

The fare in a differentiated structure may vary with one or multiple factors (e.g., distance, time and service type) and is considered one of many important transit marketing strategies. Differentiated fares can be classified into four categories (Fleishman et al. 1996): (1) Distance- or zonal-based fares, which is based on the distance traversed; (2) Time-based fare, determined by when the trip is made (e.g., peak and off-peak); (3) Service-based fare, determined by the mode (i.e., a higher fare for rail than for bus) or by speed (e.g., express or local service); and (4) Market-based fare, determined by the frequency of use and willingness to use.

The complexity is found in the range of market-based options offered for all of these systems, rather than in the existence of differentials on the basis of distance, time-of-day, or type of service. Other types of differentiated fare structure widely used by the transit industry include quality-based, cost-based, route-based, and patron-based fares. The quality and cost-based fares are determined by the service quality (e.g., business or standard class) and the operator cost (e.g., vehicles with or without air-conditioning systems). The route-based fare is determined by different origin-destination routes, and the patron-based fare is determined by passenger class (e.g., discounted fares for students and senior citizens).

The zone-based and section-based fare structures have been discussed by Vuchic (2004). The main characteristic of a zone-based fare is that it provides a uniform fare

within central business districts (CBD) and non-uniform (e.g., distance-based) fare for longer trips to and from sub-urban areas. This treatment is more equitable by differentiating the fare charged to passengers traveling short and long distances. However in section-based fares, transit routes are divided into sections which are shorter and fare increments smaller than zone-based fares. The comparison among various characteristics of different fare structures is summarized in Table 2.1.

Table 2.1 Characteristics of Various Fare Structures

Characteristics	Fare Structures		
	Flat	Zone-based	Distance-based/ Sectional
Equity	Poor	Good	Very good
Passenger attraction	Good	Very good	Very good
Revenue collected	Variable	Good	Very good
Simplicity of collection	Excellent	Fair-good	Poor
Simplicity of control	Excellent	Fair	Poor
Simplicity of passengers	Excellent	Fair-good	Poor
Line length	Short	Medium	Long
Network type	Ubiquitous	Divisible in zones	Long lines
Travel distance	Short	Variable	Variable

Source: Urban Transit Operation, Planning, and Economics (Vuchic, 2004)

Zone-based or distance-based fare structures are common used by transit agencies, such as NJ Transit, WMATA, D.C. Many large cities still retained zone-based fares without considering the length of the routes even after the government takeover. A case study of zone-based fares and off-peak fare reduction was implemented in Broom County, NY, from 1986 to 1988. The total revenues were down during the 1987 interim

fare changes and increased in 1988 when fares were increased and a zone-based fare was implemented. The fare zones were placed approximately 3 miles away from the Binghamton CBD, in which about 35 percent of passengers paid one zone fare. It was found that transit systems that adopted a fare differentiation (e.g., zone-based fare) suffered no detrimental effect. The zone-based fare may have greater potential to increase revenue in a large-sized system, since more riders would pay zone-based fares (Andrle, 1991).

Over one third of the North American transit systems use distance-based fares (primarily zone-based), and only 5% use time (e.g., peak vs. off-peak) differentials (LaBelle et al. 1995). The distance-based fare was recommended because of the higher operating costs associated with long distance travel services. In addition, higher operating cost services tend to display lower elasticities than lower operating cost services. Hence, the majority of transit agencies (e.g., BART, San Francisco, CA) have adopted either distance-based or time-based fares with the exception of CTA (Chicago, IL) and WMATA (Washington, D.C.), in which an integration of distance- and time-based fares is used. The fare structures employed by transit systems in North America were summarized in the Transit Cooperative Research Program (TCRP) Report 10 (Fleishman et al. 1996) as shown in Table 2.2.

Table 2.2 Fare Structures of Transit Systems in North America

Transit Systems		Fare Structures			
Name	City, State	Flat	Distance-based	Zone-based	Time-based
<i>LA County Metropolitan Transportation Authority (LACMTA)</i>	Los Angeles, CA	√			
<i>Orange County Transportation Authority (OCTA)</i>	Orange Co., CA	√			
<i>Bay Area Rapid Transit District (BART)</i>	San Francisco, CA		√		
<i>Southern California Regional Rail Authority (SCRRA)</i>	CA			√	√
<i>Washington Metropolitan Area Transit Authority (WMATA)</i>	Washington, DC		√		√
<i>Miami-Dade Transit Agency (MDTA)</i>	Miami, FL	√			
<i>Metropolitan Atlanta Rapid Transit Authority (MARTA)</i>	Atlanta, GA	√			
<i>Chicago Transit Authority (CTA)</i>	Chicago, IL	√			√
<i>Greater Lafayette Public Transportation Corp. (GLPTC)</i>	Lafayette, IN	√			
<i>Transit Authority of River City (TARC)</i>	Louisville, KY	√			√
<i>Bi-State Development Agency (BSDA)</i>	St. Louis, MO	√			
<i>Massachusetts Bay Transportation Authority (MBTA)</i>	Boston, MA			√	
<i>Maryland Transit Administration (MTA)</i>	Baltimore, MD			√	
<i>New Jersey Transit (NJ Transit)</i>	NJ			√	
<i>Port Authority of New York and New Jersey (PATH)</i>	NY/NJ	√			
<i>New York City Transit Authority (NYCTA)</i>	NYC, NY	√			
<i>Greater Cleveland Regional Transit Authority (GCRTA)</i>	Cleveland, OH	√			
<i>Miami Valley Regional Transit Authority (MVRTA)</i>	Dayton, OH	√			
<i>Toronto Transit Commission (TTC)</i>	Toronto, ON	√			
<i>Southeastern Pennsylvania Transportation Agency (SEPTA)</i>	Philadelphia, PA	√			
<i>Calgary Transit (CT)</i>	Montreal, QC	√			
<i>Dallas Area Rapid Transit (DART)</i>	Dallas, TX	√			
<i>Metro</i>	Seattle, WA			√	√
<i>Madison Metro</i>	WI	√			

Source: TCRP Report 10 (Fleishman, 1996).

Jorgensen (2004) conducted an empirical analysis of transit systems in Norway to determine the impact of fare and service quality (e.g., passengers' comfort, the speed of transport vehicle) on travel distance for different modes of travel (e.g., buses, trains, planes, and ferries). The study found that transit fares are positively related to traveling distance (e.g., a linear function). The result also indicated that the positive effects of increased transport quality are outweighed by long distance travel. However, for trains the same relationship is weakly concave, meaning fare is less influenced by the increase in travel distance. Furthermore, it was found that if the trip length is less than 360 km, the fare is influenced by travel distance more for trains than buses.

Time-based fares are used when the work-related demand during peak periods tends to be heavier and less elastic to fare than the more discretionary demand during off-peak periods. Hence, reducing off-peak fare may increase overall ridership and minimize potential revenue loss (LaBelle, 1995). The idea of time-based fare was to shift some riders away from peak hours to reduce the operating cost, and increasing the ridership during off-peak hours. Several studies in New York City and London (Mayworm et al. 1980; Collins, 1984) found that fare elasticities during off-peak hours range between -0.11 and -0.84, while the elasticities of peak hours range between -0.04 and -0.32. In CTA (Chicago, IL) fare elasticities during peak and off-peak hours were -0.10 and -0.46, respectively. A similar study conducted by Pham (1991) illustrated that the difference between peak and off-peak fares should be sufficiently large (over 25%) to create a measurable effect which may influence the decision to use the public transit system during the peak period.

2.2 Fare Optimization

A number of studies related to transit fare optimization have been conducted in the past two decades, which include fare optimization for a grid transit network (Kocur and Hendrickson, 1982; Chang and Schonfeld, 1989, 1991; Chien and Spasovic, 2002, etc), irregular geographic areas (Spasovic, Boile, and Bladikas, 1994) and transit lines (Lam and Zhou, 2000; Lee and Tsai, 2004; Chien and Tsai, 2006, etc). The objective functions in the above studies were to maximize either total profit and/or social welfare.

Previous transit optimization models used to over simplify passenger demand distributions and shape of service areas to observe the relationship among decision variables and model parameters. Typically, the assumption of a grid transit network and directional demand to and from a transfer station or central business district (CBD) were assumed to maximize profit or social welfare (i.e., Kocur and Hendrickson, 1982; Chang and Schonfeld, 1989, 1991; Chien and Spasovic, 2002). This assumption enables a model to be solved analytically, but the models were used for a hypothetical, simplified transit system.

Without considering temporal demand, analytical models to assess characteristics of urban public transportation systems, such as stop spacing, service frequency, and fare for bus and tram networks were found in previous studies. Kocur and Hendrickson (1982) analyzed bus service, considering that demand is sensitive to service quality and fare. Closed form solutions for optimal route spacing, headway, and fare were derived based on maximizing objective functions for profit and social welfare on a rectangular grid street network. Using a linearized approximation approach to transit system design, an analytic model considering elastic demand, financial constraints, and the effect of fleet

size on congestion was developed by Oldfield and Bly (1988) to determine the optimal vehicle size for an urban bus system. The study mentioned above did not consider time dependent demand.

Considering temporal demand, Chang and Schonfeld (1991) developed an optimization model for a feeder bus system whose customers are sensitive to service quality and fare. The optimized closed form solutions, including headway, fare, fleet size, and route spacing were derived for different objectives, such as cost minimization and profit/social welfare maximization. The models were formulated and compared on the basis of four demand conditions, which include steady fixed demand, cyclical fixed demand, steady equilibrium demand, and cyclical equilibrium demand. The optimization objective was to maximize operator profit and social welfare. The optimal fare was found to be very sensitive to the fare elasticity parameter for profit maximization and the elasticity was zero for social welfare maximization in equilibrium cases. However, the model can only deal with many-to-one or one-to-many demand.

Chien and Spasovic (2002) developed a model to optimize route and stop spacings, service headway, and fare by maximizing the total profit and social welfare of a grid transit system considering a linear demand function which is sensitive to travel time and fare. It was found that the profit and welfare functions are relatively flat near the optimum. This shallowness of the objective functions gave transit operators flexibility to slightly alter the optimal solution without significantly reducing the profit or social welfare.

In designing transit service, agencies should determine fares that generate revenue to cover the cost of providing the service (van Nes, 2002). When the operator cost

exceeds revenue in profit maximization problems, the objective becomes one of minimizing the subsidy instead of maximizing profit. The most likely situation was that the main objective to maximize social welfare for urban public transport network, whereas profit maximization was used for an interurban network (Berechman, 1993).

The studies mentioned above did not consider more realistic demand distributions and shapes of service areas. Spasovic, Boile, and Bladikas (1994) optimized bus transit service coverage by maximizing operator's profit and social welfare. In marked contrast to the above papers, this paper determined optimal public transit facilities (route and station spacing), operating headway, and fare, while considering the impact of realistically irregular geographic, socio-economic, demand, and traffic characteristics.

Lam and Zhou (2000) proposed a bi-level programming approach based on the method developed by Tobin and Friesz (1988) to determine the optimal fare structure of a transit network with fixed service frequency by maximizing the operator's total revenues, where the passenger route choice behavior was taken into consideration through a stochastic user equilibrium (SUE) transit assignment model. Under a user equilibrium condition, the passenger demand was a function of minimum travel time between each origin-destination. Both flat and distance-based fares were considered for the service line in the study. The difference in degree of passengers' perception of travel time was used as a measurement parameter. The result showed that both demand and fare decreased as the measurement parameter increased, because passengers having additional knowledge of travel cost of each transit line, which were more sensitive to fare charges. Moreover, fare elasticities were found to be more sensitive to fare changes for express service lines than for local service.

Lee and Tsai (2004) developed a product-line pricing method for a simplified Taiwan High Speed Rail in which only 3 stations were considered. A pricing model for two types of service classes (e.g., express and local) and two types of passenger classes (e.g., first and second class) was developed, which considered service choice of passengers and market competition in three intercity transit routes. In the demand model, passengers' service choice was formulated as a logit function, market competition was represented by a linear demand function, and service capacity was used as a constraint to restrict the feasible solution spaces. A bi-level program was developed to maximize profit in the upper level and minimize the generalized cost (e.g., a function of fare, travel time and comfort) in the lower level, while sensitivity analysis and a convergence test were used to test the results.

Yang (1996) presented the transit fare structure as a typical leader-follower problem (Stackelberg Game), in which the transit operator (leader) can predict responses of passengers (follower) before they decide on what fare to charge users. The results showed that the consideration of a market differential (e.g., service at all station vs. each station) seemed more effective in increasing profit and capacity utilization than product differential (e.g., express vs. regular). However, the developed model could not handle temporal transit demand situations.

Considering differentiated fares, Chien and Tsai (2006) developed a model that jointly optimizes temporal headways and differentiated fares to maximize profit for urban light rail transit. The developed model was formulated by considering a general situation (e.g., with or without temporal and differentiated fare structure), and a numerical example was used from the City Subway in Newark, New Jersey. The result showed that

maximum profit can be achieved by temporal headway and differentiated fare. The sensitive analysis was conducted to evaluate the decreasing of the difference between the operating costs for idle and on duty vehicles. It was found that the optimal headway increases during the peak period, but decreases during the off-peak period

Tsai, Chien, and Spasovic (2007) developed an optimization approach for an intercity public transit service under elastic travel demand where the passengers are sensitive to fare and wait time. The approach jointly optimized service headway and distance-based fare structure which maximized the total profit subject to service capacity and fleet size constraints. The optimal fares were differentiated based on trip length. An efficient solution method was developed and used to solve the profit maximization for a real world intercity transit system (e.g., Taiwan High Speed Rail). It was found that the profit surfaces for various headways, unit fares and weight factors for different travel ranges are relatively flat near the optimum. This indicates that the transit operator has flexibility to shift the solution marginally away from the optimum without reducing the optimal profit significantly. This finding could be very useful especially in determining the threshold values of travel distance ranges.

A classification of existing analytic models for transit fare optimization is summarized in Table 2.3, in which most previous studies found that improving transit services (e.g., reduced fare or increased frequency) leads to an increase in passenger demand.

Table 2.3 Analytical Models for Transit System and Fare Optimization

Decision Variables	Objective Function	Transit Network	Demand Pattern	Authors (Year)
Route Spacing, Headway, and Fare	Maximize Profit, and User Benefit	Grid	Elastic, Many-to-One	Kocur and Hendrickson (1982)
Number of Zones, Headway, and Fare	Minimize Operator, User Cost, and Maximize Social Welfare	Grid	Elastic, Many-to-One	Chang and Schonfeld (1989)
Headway, Fare, Fleet Size, and Route Spacing	Minimize Operation Cost, and Maximize Profit/Social Welfare	Grid	Time Dependent, Elastic	Chang and Schonfeld (1991)
Route and Stop Spacing, Headway, and Fare	Maximize Profit, and Social Welfare	Grid	Elastic, Many-to-Many	Chien and Spasovic (2002)
Route and Station Spacing, Headway, and Fare,	Maximize Profit, and Social Welfare	Irregular grid	Elastic, Many-to-One	Spasovic, Boile, and Bladikas (1994)
Fare Structure	Minimize User Cost	Line	Elastic	Lam and Zhou (1999)
Fare, Passenger Route Choice	Maximize Revenues	Line	Elastic	Lam and Zhou (2000)
Fare, Number of Passengers	Maximize Profit, and Minimize Generalized Cost	Line	Elastic	Lee and Tsai (2004)
Temporal Headway, and Differentiated Fare	Maximize Profit	Line	Time Dependent, Elastic	Chien and Tsai (2006)
Headway, and Differentiated Fare	Maximum Profit	Line	Elastic, Many-to-Many	Tsai, Chien, and Spasovic (2007)

2.3 Optimization Algorithms and Heuristics

The studied differentiated fare optimization problem is a large combinatorial optimization problem in which decision variables include the ranges of travel distance, service frequency, and fare. In spite of the importance of the zone/distance-based fare design problem, few studies developed algorithms to optimize differentiated transit fares.

Some of the recent studies focused on both fare optimization and zone design (e.g., optimize number of zones) used operations research models. Hamacher and Schobel (2004) developed a model to count zone fares by minimizing the deviation between distance-based and zone-based fares. Later, a study was conducted by Schobel (2006) about the zone design problem with an arbitrary fare. The algorithm was developed based on the clustering theory, particularly in the sequential agglomerative hierarchical non-overlapping (SAHN) algorithm. The optimal fare problem was solved by a closed form solutions with respect to a given zone partition and three heuristic algorithms were proposed to solve the zone design problem. Babel and Kellerer (2003) presented theoretical results for local public transportation networks based on the same model developed by Hamacher and Schobel (2006). A Tabu Search (TS) method was implemented to solve the general transportation network problem.

Pratelli (2004) developed a bi-level model to optimize zone-based fare under various zone partitions. The objective of the model was to minimize an aggregated cost function mainly related to both the budget required for transit operations and the fare charged to patrons. The optimal zone partitions were obtained by a heuristic iterative procedure based on simulated annealing (SA), which randomly searches for an optimal zone configuration reflecting a given fare policy.

A robust searching algorithm, such as the Genetic Algorithm (GA) and other intelligent optimization techniques, are desirable to be developed to find a near optimum solution efficiently in the enormous solution space. Many techniques have been developed to approximate optimal solutions for the basic and multiple-depot vehicle routing problems. These include ant algorithms (Bullnheimer et al. 1999), the tabu search method (Cordeau et al. 1997), evolutionary algorithms (Machado et al. 2002), and GA (Chien et al. 2001).

GA, introduced by Holland (1975) in his seminal work, is commonly used as an adaptive approach that provides a randomized, parallel, and global search method based on the mechanics of natural selection and genetics to find solutions of a problem. GA is different from normal optimization and search procedures in four ways (Herrera et al. 1994): (a) GA works with a coded parameter set, not the parameters themselves, (b) GA searches from random selected points, not from a single point, (c) GA uses objective function information, and (d) GA uses probabilistic transition rules, not deterministic ones.

Although there are many possible variants of genetic algorithms (Ho et al. 1999) and (Tang et al. 1998), the fundamental is based on the Simple Genetic Algorithm (SGA) (Holland, 1992). In general, GA starts with some randomly selected genes, the first generation, called population. Each individual in the population corresponding to a solution in the problem domain is called chromosome. An objective, or fitness function, is used to evaluate the quality of each chromosome. The chromosomes with high quality will survive and form the population of the next generation. By using three operators, reproduction, crossover, and mutation, a new generation is recombined to find the best

solution. The process will iterate many times until a predefined condition is satisfied, or a pre-specified number of iterations is reached.

Chien et al. (2001) developed a GA to search for the optimal bus route using two major operations: Route Generator and Genetic Operator. The GA starts with an initial population size and street pattern of a service area. The developed GA algorithm consists of three genetic operators (e.g., reproduction, crossover, and mutation), which incorporate the ideas of survival of the fittest and genetic selection. The function of the crossover operator is to generate new routes based on the existing routes. Since certain segments of different routes may be desirable for optimal operation and therefore by combining these desirable segments, a better route can be obtained. The function of the mutation operator is to introduce random variations into the population so that it would not be saturated with a single route and lead to premature convergence.

The literature revealed that each algorithm has its own advantage in solving particular types of optimization problems. It was found that GA outperforms SA and TS in solving traveling salesman problems (Pham and Karaboga, 2000). However, a comparative study of SA, TS and GA was conducted in solving machine-grouping problems by Zolfaghari and Liang (2002), and the results indicated that SA outperforms both GA and TS for large-scale problems, while GA is slightly better than TS for comprehensive grouping problems.

GA is heuristic in nature, involving algorithmic parameters that may have a critical impact on their performance, but must be chosen empirically. This empirical nature of the approach makes it even more important to synthesize applications in past studies (Fu, 2004). It was found that GA can solve almost any types of objective function

(e.g., linear, nonlinear, integer, mix-integer, logical, or discontinuous) subject to a set of constraints (Dandy and Engelhardt, 2001). The studied fare optimization problem under flexible RTD in this study has a nonlinear, mix-integer objective function, which is solved by the GA developed in Chapter 4.

2.4 Transit Demand

Most previous studies (Baumol 1965, Henderson and Quandt 1985) have been focused on developing stochastic disaggregate and deterministic aggregate demand prediction functions. Stochastic disaggregate demand models were used to predict the behavior of a single consumer and explore the models used for predicting responses of different consumers in various situations. It is assumed that consumers formulate their preferences explicitly, identify the alternatives and their consequences, evaluate the alternatives, and choose the best one among them using a well-defined decision. For practical predictions of the impacts of transportation strategies, however, it is important to predict the behavior of groups of consumers (e.g., several individuals, households). Therefore, an aggregate demand function is well fit to predict the behavior of a group of consumers in response to changes in future conditions.

Historically, transportation demand analysis has been focused on aggregate demand functions, which predicts the behavior of a potential volume and composition of flow between two (or more) points as a function of the service attributes for a particular social, economic, and other characteristics activity system. The activity system variables describe the characteristics of the consumers whose behavior is represented by the

demand function that influences their choices (Manheim, 1979). The general form of the demand functions is shown in Equation 2.1

$$V = D(A, S) \quad (2.1)$$

where **D** is the aggregate demand function, **V** is the vector of volumes or numbers of consumers making particular choices, **A** represents the social, economic, and other characteristics of the activity system and of the individuals in the group, and **S** represents the service attributes that characterize the transportation choices open to prospective travelers.

In Equation 2.1, various choices can be made to decide what activity system and service variables are explicitly included in the demand function. The activity system may be described in terms of variables, such as population, market segment (e.g., income or household), and employment. The service attributes of the transportation system include travel time (e.g., in-vehicle time, access time, transfer time), service schedule, and fare that have been the primary service variables used to predict traveler behavior in urban transportation, especially for conventional transportation. The relationships might simply be described by Manheim (1979) that as transit travel time, wait time, and fare decrease, more consumers will find the transit mode more attractive.

There are many different forms of demand functions that can be represented by basic algebraic forms, such as linear, product, exponential, and logistic, as shown in Equations 4.2 to 4.5 by Manheim (1979).

Linear demand function:

$$V = \alpha + \beta X \quad (4.2)$$

Product demand function:

$$V = \alpha X^\beta \quad (4.3)$$

Exponential demand function:

$$V = \alpha e^{\beta X} \quad (4.4)$$

Logistic demand function:

$$V = \frac{\alpha}{1 + \beta X} \quad (4.5)$$

where X represents a single service attribute or activity system variable, and α , β represent the elasticity parameters of different curves which express the preferences of the consumer. For the linear demand function, the ratio of the two parameters represents the value of time to the consumer.

These functions are commonly used because of simplicity, and are particularly suitable for calibration by standard statistical techniques. For example, linear regression techniques can be used to estimate the parameters of the linear form of the demand model directly from observed (X, V) . To estimate the coefficients of the product and exponential forms, logarithms are taken to transform the equation into a linear form, and then regression techniques are used on this transformed equation.

Some major historical streams of aggregate demand functions were focused on the intercity passenger demand models, gravity models, and the urban transportation model system. Intercity passenger travel models were first developed for the Northeast Corridor project by the U.S. Department of Transportation (Kraft, 1963). The models were used to predict the level of travel demand between any pair of cities and the split among the competing modes. The gravity model by Isard (1960) is the classic transportation demand model to predict to which destination people will travel. The most commonly used models for urban transportation planning typically predict travel flows in

four steps. This breaks the demand model into four submodels, but also involves some significant assumptions and approximations in the way the submodels are used to compute equilibrium. The submodels are trip generation, trip distribution, mode split, and trip assignment.

Three similar intercity transportation demand models were developed, which are the Kraft-SARC model by Kraft (1963), the Quandt and Baumol model (1966), and the McLynn model by McLynn and Woronka (1969). These models considered time and cost as service variables, and assumed only one path connecting each O-D pair of zones. Later, a model developed by Lave (1972) included time series demand models, which focused on estimating demand for a single mode; and cross section models, which assumed that the prospective traveler would focus on the speed of the fastest mode, fare of the cheapest mode, and the frequency of schedule. A generalized model was developed having relevant demand functions without constant elasticities over the entire travel range, but having constant elasticities only within a limited range. It is worth noting that the conventional approach to estimate the demand for a mode contains a fundamental defect in that no attempt is made to separate direct elasticities from cross elasticities. One possible method to separate direct from cross elasticities is to formulate a simultaneous equation framework, where the demand for all modes is estimated simultaneously by taking account of interactions between cross and direct elasticities.

One approach to empirically test decision structure hypotheses as well as to provide an alternative decision structure between single level choice and sequential structures choice is presented as the nested decision structure by McFadden (1979). In a nested mode, decisions are made sequentially with higher-level decisions (e.g., one

makes decision early) including the calculated expectations concerning subsequent lower-level decisions (e.g., one makes decision later). In particular, the expected maximum utility associated with the next stage in the decision process is included in the current stage's utility function.

The choice of an algebraic form (e.g., linear, product, exponential, and logistic) for a demand function is determined based on the different assumptions on how consumers will respond to changes in the choices available. In this study, the demand function can be represented as the potential demand justified by a function of variables, including service frequency and fare.

2.5 Fare Elasticities

Transit ridership is a function of fare and service characteristics of a product. Fare elasticities are used to estimate the effects of fare changes on ridership. The industry standard for fare elasticity is called the Simpson-Curtin's rule (1968), which indicates that a decrease of three percent in ridership for every ten percent increase in fares has proved to be accurate in overall forecasts of ridership response to fare changes. This rate of demand decline corresponding to a fare elasticity of -0.33. The Simpson-Curtin's rule is based on a study of 77 cases of transit fare increases occurring over a twenty year period. The rule can be used for preliminary analysis and is too simple and generic for detail planning and modeling of transit service.

Studies examining particular groups of riders have revealed significant differences in fare elasticities (Mayworm, 1980, Fleishman, 1996). These studies concluded that regular commuters, riders with long trips, and peak-period riders are less

sensitive to fare changes than non-work riders, riders making short trips, and off-peak riders. A review of past behavioral research on transit pricing was conducted by Cervero (1990) with emphasis on rider's response to changes in transit fare levels and structures. Analyses were refined by studying ridership responses among sub-markets, which is broken down by user groups (e.g., age, gender), trip characteristics (e.g., purpose, length), and service types (e.g., express vs. local, peak vs. off-peak, bus vs. rail). The purpose of dividing riders and service types into subgroups was to study homogeneous groups that are fairly similar in their response to fare changes and differences between groups.

Previous studies (Thomson, 1967; Schmenner, 1976) showed that for passengers making short trips, fares are relatively elastic because the option of walking is readily available and the fare component constitutes a significant share of total generalized cost, the sum of fare and travel time cost. A study conducted by Ministry of Transport (1968) found that bus trips less than one mile had higher fare elasticity (-0.55) than trips between one to three miles (-0.29). Another study done in Germany by Baum (1973) indicated a similar result about fare elasticities for short trips (-0.32) and longer ones (-0.12). Research has also shown that fare elasticity varies due to different transit operating environments. Users are less sensitive to fare increase when trips are: radial vs. cross-town; intra-city vs. inter-city; rail vs. bus; and express vs. local (Mayworm et al. 1980; Cummings et al. 1989). Particularly, the intra-CBD trips have proven to be highly fare sensitive.

Three different time series scenarios were selected to estimate the fare elasticity by Guenther and Jea (1985). The evaluation of distance-based fares for each express bus service route was based on its length, where the fare elasticities for short to long travel

distance ranged from -0.37 to -0.74 based on 95 percent confidence interval. It was found that revenue increased without reducing ridership when a small increment of distance-based fare was implemented. The demand elasticity with respect to fare change can be predicted for new ridership.

Issues dealing with how fare and quality of transport services relate to travel distance were discussed by Jorgensen (2004). It was found that the relationship between ordinary fares and trip length is a linear function for buses, ferries, and planes. However, the relationship for trains is weakly concave. This means that the impact of travel distances on fares is diminished as the distance increases, which confirms the finding of Meyer (1965) and Daskin et al. (1998) that if the elasticity of demand is strongly dependent on distance, then the differentiated fares can maximize total revenue.

McFadden (1974) studied a rail transit system in the San Francisco Bay Area. The individual passenger travel behavior was investigated by using a conditional logit model and it was found that the ridership is elastic to fare changes. Voith (1991, 1997) conducted studies on demand elasticity with respect to the change in fare policy and demographic factors from a 13 year panel data, and found that in the long-run the demand elasticity is approximately twice as much as that of the short-run.

Ling (1998) found that the optimal fare was significantly affected by the elasticity of demand. The revenue, ridership, passenger-mile travel, and consumer surplus of a transit system under differential and flat fare structures were analyzed. A numerical example of a distance-based fare system was considered in which there are only two available destinations from a given origin (e.g., short trip and long trip). A sensitivity analysis was performed by varying the number of short trips and the fare elasticity of

short trip while the long trip elasticity was fixed. It was found that promoting a differentiated fare system may be viable to increase revenue, if the short distance trip elasticity is greater than that for long trips or the number of long trips is greater than that of short trips.

Chien and Spasovic (2001) considered realistic demand distributions and shapes of service areas to optimize public transit facilities (e.g., route and station spacing), operating headway, and fare. Sensitivity analyses were conducted for various pairs of important variables and parameters. It was found that if demand and fare elasticity increased, the optimal fare increased as well.

2.6 Summary

In summary, when designing a public transportation system, the service provider must decide what level of service to provide (e.g., how frequently vehicles will be dispatched) and what fare to charge. To maintain good financial health and provide adequate service quality, the service provider has a challenging objective of maximizing profit. In this study, the profit is defined as the total fare-box revenue minus the operator's cost, and the variables considered here include service headway and fare corresponding to ranges of travel distance.

The demand function in this study can be assumed to be linear for the development of the transit system optimization model. The ridership can be represented as the potential demand justified by a function of variables, such as service frequency and fare. The fare elasticity considered in this study estimates the changes in ridership. It is important for a transit company to have a good understanding of the nature of passenger

demand, to develop differential fares that are both based on the operator's average cost (e.g., cost per mile) and travel distance, while considering the travelers' willingness to pay. This approach can help service providers quantify how much better off, in terms of additional revenue and profit, they can be compared to the case of charging pure distance-based rates.

In this study, the developed methodologies are to optimize distance-based fares and service headway that will account for the sensitivity among the travelers traveling different distances. Four different models are developed in Chapter 3 by considering both given and variable ranges of travel distance for single and multiple time periods.

CHAPTER 3

METHODOLOGY

In this chapter, the objective functions for the four scenarios discussed in Chapter 1 are formulated. The total profit objective considered in this research is the revenue minus operator's cost, which is a function of fare and service frequency.

A set of system assumptions are made to formulate the research problem for each scenario and associated constraints, which are discussed in Sections 3.1 through 3.4 for Scenarios I through IV, respectively. The models are developed on a basis of the same transit network configuration. However, the model parameters, such as elasticity of fare, vary over the scenarios. The optimal solutions for each scenario are obtained considering the joint impact of elasticity parameters as well as the distribution of spatial and temporal demand for the studied intercity transit system.

3.1 Fixed RTD and Single Time Period – Scenario I

The base model formulated in Scenario I optimizes distance-based fare and service headway for a single time period with a given RTD. To formulate the model, the system assumptions, model formulation, constraints, and optimization problem are discussed in the following sections.

3.1.1 System Assumptions

To formulate a mathematical model for optimizing an intercity transit system, the following assumptions on system configuration (e.g., network configuration, station

spacing between stops), supply relations (e.g., service pattern, transit travel time, headway), demand characteristics (e.g., O-D demand, passengers' waiting time), and distance-based fare are made.

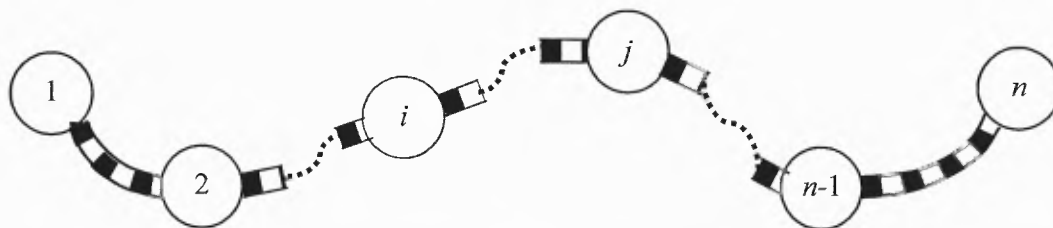
1. A transit route with n stations and a matrix of station-to-station distances L_{ij} from station i to j as shown in Figure 3.1 is given. The RTD may be mandatorily classified into three categories, such as short, medium and long travel distance.
2. All vehicles serve passengers boarding and alighting at every station in a designated service route, and the station-to-station travel time is independent of fare and service headway. The average speed is equal to the round trip route length divided by round trip travel time, excluding terminal time. The round trip travel time consists of operating time for the two directions between terminals, denoted as T_V , and terminal time, denoted as T_T . Note that the dwell time at each station between the terminals is included in T_V . Thus,

$$T_R = T_V + T_T \quad (3.1)$$

3. Assume that the long distance trips are less elastic with respect to fare than short distance trips. A weight factor is introduced to adjust unit fare per mile for different RTD (See Figure 3.1). The weight factor of unit fare, denoted as $\gamma_{z_{ij}}$, is a constant but may vary with RTD. Note that z represents the index of RTD. Thus, the weight factor of unit fare for short range of travel distance is denoted as γ_s , and medium and long RTD are denoted as γ_m and γ_l , respectively.
4. The distance-based fare for a passenger traveling from station i to j , denoted as F_{ij} , is the product of unit fare (δ), the weight factor of unit fare ($\gamma_{z_{ij}}$), and the travel distance between stations i and j (L_{ij}). Note that $\gamma_{z_{ij}}$ for each corresponding RTD decreases as the index of RTD (z_{ij}) increases from a short to long distance range. Thus,

$$F_{ij} = \delta \gamma_{z_{ij}} L_{ij} \quad i, j \in \{1, 2, \dots, n\}; z_{ij} \in \{s, m, l\} \quad (3.2)$$

where i represents the departing station; j represents the destination station.



D O	1	2	<i>i</i>	...	<i>j</i>	<i>n-1</i>	<i>n</i>
1		L_{12}	L_{1i}	...	L_{1j}	$L_{1(n-1)}$	L_{1n}
2	L_{21}		L_{2i}	...	L_{2j}	$L_{2(n-1)}$	L_{2n}
⋮	⋮	⋮	⋮	⋮	⋮	⋮
⋮	⋮	⋮	⋮	⋮	⋮	⋮
<i>i</i>	L_{i1}	L_{i2}	⋮	⋮		...	L_{ij}	$L_{i(n-1)}$	L_{in}
⋮	⋮	⋮	⋮	⋮	⋮	⋮	⋮	⋮	⋮	⋮	⋮
<i>j</i>	L_{j1}	L_{j2}	⋮	⋮	L_{ji}	⋮		$L_{j(n-1)}$	L_{jn}
⋮	⋮	⋮	⋮	⋮	⋮	⋮	⋮		...	⋮	⋮
⋮	⋮	⋮	⋮	⋮	⋮	⋮	⋮	⋮		⋮	⋮
<i>n-1</i>	⋮	⋮	⋮	⋮	$L_{(n-1)i}$	⋮	$L_{(n-1)j}$	⋮	⋮		$L_{(n-1)n}$
<i>n</i>	⋮	⋮	⋮	⋮	L_{ni}	⋮	L_{nj}	⋮	⋮	$L_{n(n-1)}$	

Legend: A. L_{ij} = distance from station *i* to station *j*

B. Given ranges of travel distance: : $\gamma_{z_{ij}} = \gamma_s$; : $\gamma_{z_{ij}} = \gamma_m$; : $\gamma_{z_{ij}} = \gamma_l$

Figure 3.1 Studied transit route configuration and station-to-station distance.

5. The average passenger wait time, denoted as t_w , is assumed to be a fraction of headway. Most intercity transportation systems, and especially trains, will dispatch vehicles according to a posted schedule. Newell (1971) discussed that the passenger arrival rate should follow a hypothetical smooth curve because the probability of passenger arrival times are dependent on two adjacent vehicle departure times, or headway denoted as H . The headway considered here is fixed for the study time period, and the average passenger wait time can be formulated as

$$t_w = \beta H \quad (3.3)$$

where β , the ratio of average wait time to the headway, can be determined by service frequency, the actual passenger travel behavior and terminal/station required processing time for each passenger.

6. The ridership (i.e., actual demand) from station i to j during the study time period, denoted as Q_{ij} , can be estimated from a demand function formulated as Equation 3.4. The potential hourly O-D demand for the study time period, denoted as Y_{ij} , is sensitive to fare and level of service (e.g., the travel time of passengers). Note that the elasticity parameter of fare, denoted as $E_{F_{z_{ij}}}$, is constant within the same index of RTD, z .

$$Q_{ij} = Y_{ij} (1 - E_w t_w - E_I t_{I_{ij}} - E_{F_{z_{ij}}} F_{ij}) \quad i, j \in \{1, 2, \dots, n\}; z_{ij} \in \{s, m, l\} \quad (3.4)$$

The average in-vehicle time from station i to j during the study time period, denoted as $t_{I_{ij}}$, can be referred to the operating schedule. The elasticity parameters of wait time, denoted as E_w , and in-vehicle time, denoted as E_I , are constant. Note that the elasticity parameters are not actual elasticities. The ratio between the elasticity parameter for wait time and fare determines the implied value of wait time. Similarly, the ratio between the elasticity parameter for in-vehicle time and fare determines the implied value of in-vehicle time.

3.1.2 Model Formulation

The objective profit function defines a range of possible combinations of fare, travel demand, and service quality that are achievable by various conditions. The total profit function, denoted as P , is defined as the total fare box revenue, denoted as R , minus the operators' cost, denoted as C . Thus,

$$P = R - C \quad (3.5)$$

Since the potential demand and all model parameters are fixed within the studied time period in the model of Scenario I, the hourly revenue and operator's cost are formulated on a hourly basis for estimating the profit. The revenue is the product of actual hourly demand, denoted as Q_{ij} and obtainable from Equation 3.4, multiplied by the fare, denoted as F_{ij} for all O-D pairs of i and j , where $i, j \in \{1, 2, \dots, n\}$. Thus,

$$R = \sum_{i=1}^n \sum_{j=1}^n Q_{ij} F_{ij} \quad (3.6)$$

The operator's cost, denoted as C , is defined as the cost of operating a transit system, which is affected by the service frequency (or headway) and the costs of maintaining the rail line and stations of the studied network. The hourly vehicle operating cost, denoted as c_o , reflects the cost to maintain and repair vehicles (e.g., rolling stock for train operation), and other administrative expenses associated with running vehicles on the route. As formulated in Equation 3.7, the vehicle operating cost, denoted as C_o , is equal to the fleet size multiplied by the operating cost per vehicle-hour:

$$C_o = Nc_o \quad (3.7)$$

where N is given as the round trip vehicle travel time, denoted as T_R , divided by the headway, denoted as H . The fleet size is defined as the number of vehicles (or trains in this study) needed for maintaining the desired service, which is an integer, and $[]^+$ indicates that the fleet size, if not integer already, is rounded up. Thus,

$$N = \left[\frac{T_R}{H} \right]^+ \quad (3.8)$$

The unit transit line cost, denoted as c_L , is related to the length of transit line and includes maintenance of roadway, signal equipment, and administrative costs. The transit line cost, denoted as C_L , equals to the route length (L) multiplied by c_L . Thus,

$$C_L = Lc_L \quad (3.9)$$

Similarly, the station cost, denoted as C_S , accounts for station maintenance operation and costs, which is the number of stations multiply by the unit station cost, denoted as c_S . Thus,

$$C_S = nc_S \quad (3.10)$$

Finally, the operator's cost, denoted as C , is the sum of C_O , C_L , and C_S . Note that the transit line and station costs considered in this study are given (the costs of station and route length are known), while the operator's cost varies with headway. Thus,

$$C = Nc_o + Lc_L + nc_S \quad (3.11)$$

The revenue can be formulated by substituting the distance-based fare structure of Equation 3.2 into Equation 3.6. Therefore, the hourly profit function can be derived by substituting Equations 3.6 and 3.11 into Equation 3.5. Thus,

$$P = \sum_{i=1}^n \sum_{j=1}^n Q_{ij} (\delta\gamma_{z_{ij}} L_{ij}) - (Nc_o + Lc_L + nc_S) \quad z_{ij} \in \{s, m, l\} \quad (3.12)$$

3.1.3 Constraints

Two practical constraints are considered in Scenario I. The first constraint, called capacity constraint, ensures that the transit service operates at a sufficient capacity to accommodate the design ridership. The second constraint, called fleet size constraint, establishes the maximum capacity, i.e., it calculates the minimum headway that can be

maintained given the route characteristics, such as round trip travel time and the available fleet size. Therefore, bounds are placed on the optimal headway. It must not exceed the headway at which the capacity accommodates the design ridership; meanwhile, it can not be smaller than the minimum headway that can be attained.

Capacity Constraint

The capacity constraint is designed to ensure sufficient service capacity to accommodate demand. The hourly capacity in each link is the maximum number of passengers that can be loaded in a vehicle divided by the vehicle headway. To satisfy the capacity constraint, the maximum design headway equals the hourly capacity divided by the maximum demand through flow in link g . To this end, the optimized headway must not exceed the maximum headway, denoted as H_{\max} . Thus,

$$H_{\max} = \frac{B}{Q_{\max}} \quad (3.13)$$

where B is train capacity. Note that the product of B and the inverse of H_{\max} (called minimum frequency) is equal to the maximum demand to be served.

In general, the demand from station i to j , the outbound (e.g., from 1 to n) demand and inbound (e.g., from n to 1) demand of link g can be represented by Q_{ij} , O_g , and I_g , respectively. Note that g , the index of links, varies between 1 and $(n-1)$. With Equation 3.14, the maximum demand can be identified by calculating the number of inbound and outbound trips on all links of the studied route.

$$Q_{\max} = \text{Max}[O_g, I_g] = \text{Max} \left[\sum_{i=1}^g \sum_{j=g+1}^n Q_{ij}, \sum_{i=g+1}^n \sum_{j=1}^g Q_{ij} \right] \quad \forall g \quad (3.14)$$

Figures 3.2 and 3.3 illustrate the example of the outbound and inbound demand for all O-D trips that travel through link m , denoted as O_m and I_m , which can be calculated by Equations 3.15 and 3.16, respectively. A link with the highest demand can be identified from the outbound and inbound demand for any link g as discussed below.

Outbound demand of link m (O_m):

$$O_m = \sum_{i=1}^m \sum_{j=m+1}^n Q_{ij} \quad (3.15)$$

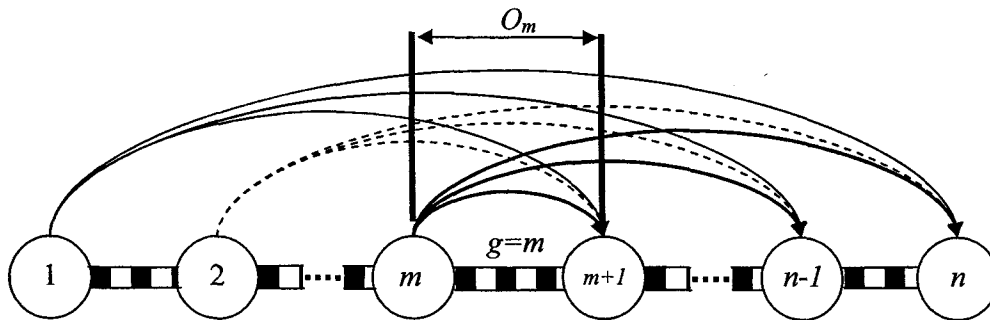


Figure 3.2 Configuration of outbound travel demand at link m .

Inbound demand of link m (I_m):

$$I_m = \sum_{i=m+1}^n \sum_{j=1}^m Q_{ij} \quad (3.16)$$

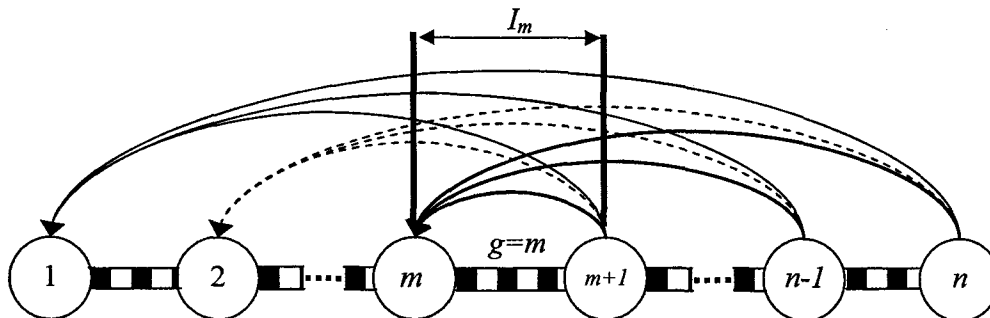


Figure 3.3 Configuration of inbound travel demand at link m .

Fleet Size Constraint

The minimum headway during the study time period, denoted as H_{\min} , equals the round trip travel time divided by the maximum operable fleet size, denoted as N' . Thus,

$$H_{\min} = \frac{T_R}{N'} \quad (3.17)$$

The optimal headway, denoted as H^* , is governed by the maximum and minimum headways formulated in Equations 3.13 and 3.17, respectively. Thus,

$$H_{\min} \leq H^* \leq H_{\max} \quad (3.18)$$

3.1.4 Optimization Problem

Based on the discussion from Sections 3.1.1 through 3.1.3, the studied fare and service headway optimization problem that maximizes the hourly profit of transit service under the condition of given RTD subject to the capacity and fleet size constraints is thus formulated as follows:

$$\left. \begin{array}{l} \text{Maximize} \\ P = \sum_{i=1}^n \sum_{j=1}^n Q_{ij} \delta \gamma_{z_{ij}} L_{ij} - \left(\frac{T_R}{H} c_O + Lc_L + nc_S \right) \quad z_{ij} \in \{s, m, l\} \\ \text{st.} \\ H \leq \frac{B}{\text{Max} \left[\left(\sum_{i=1}^g \sum_{j=g+1}^n Q_{ij}, \sum_{i=g+1}^n \sum_{j=1}^g Q_{ij} \right) \quad \forall g \right]} \\ \frac{T_R}{N'} \leq H \\ H, \delta, \text{ and } \gamma_{z_{ij}} \geq 0 \quad z_{ij} \in \{s, m, l\} \end{array} \right\} (P1)$$

Note that the objective function of P1 is given by Equation 3.12, while the constraint is derived from Equations 3.13 and 3.17. Q_{\max} in Equation 3.13 is replaced by Equation

3.14.

The optimal service design consists of the fixed optimal headway and fare. The optimal service design problem, structured as P1, is a constrained non-linear optimization problem. Assuming that the optimal headway will fall within the acceptable headway range, the constraints can be relaxed; therefore, P1 can be solved as an un-constrained optimization problem.

This is accomplished by first deriving formulae for the optimal headway and fare structure. These are obtained by taking the partial derivatives of the profit function (Equation 3.12) with respect to headway, unit fare and weight factor of unit fare, and setting them equal to zero. By solving these equations with respect to the decision variables yields a set of optimal solutions that maximize profit. The optimal headway, unit fare, and weight factor of unit fare can be derived as follows:

$$H^* = \sqrt{\frac{T_R C_o}{E_w \beta \delta \sum_{i=1}^n \sum_{j=1}^n Y_{ij} \gamma_{z_{ij}} L_{ij}}} \quad z_{ij} \in \{s, m, l\} \quad (3.19)$$

$$\delta^* = \frac{\sum_{i=1}^n \sum_{j=1}^n Y_{ij} (1 - E_w \beta H - E_t t_{i,j}) \gamma_{z_{ij}} L_{ij}}{2 \sum_{i=1}^n \sum_{j=1}^n E_{F_{z_{ij}}} Y_{ij} \gamma_{z_{ij}} L_{ij}^2} \quad z_{ij} \in \{s, m, l\} \quad (3.20)$$

$$\gamma_{z_{ij}}^* = \frac{\sum_{i=1}^n \sum_{j=1}^n Y_{ij} (1 - E_w \beta H - E_t t_{i,j}) L_{ij}}{2 \delta \sum_{i=1}^n \sum_{j=1}^n E_{F_{z_{ij}}} Y_{ij} L_{ij}^2} \quad z_{ij} \in \{s, m, l\} \quad (3.21)$$

If H^* fulfils the constraints discussed in Equation 3.18, the solution is optimal.

Figure 3.4 shows that the optimal headway that maximizes profit is dependent on its relationship vis-à-vis H_{min} and H_{max} . Figure 3.4a shows that H^* is within the feasible

range; therefore, the optimal headway can be calculated using Equation 3.19. However, in Figure 3.4b, the optimal headway is limited by H_{\max} and is calculated by Equation 3.13. Figure 3.4c, shows that the optimal headway is governed by H_{\min} that is achievable on the route and is thus calculated using Equation 3.17. The solution algorithm to solve P1 is discussed in Section 4.1.

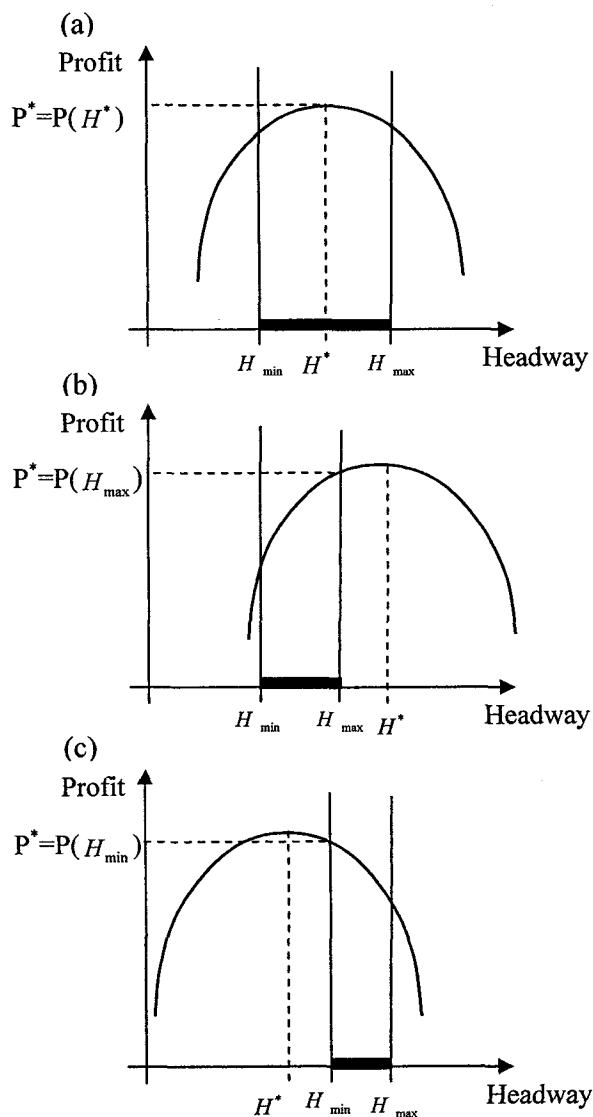


Figure 3.4 Optimal headway for various feasible conditions (Single time period)

3.2 Variable RTD and Single Time Period – Scenario II

The optimization model developed in Scenario II enhances Scenario I and optimizes RTD, distance-based fare and service frequency. Similar to Scenario I, a single time period is considered in Scenario II, in which each O-D demand is uniformly distributed within the studied time period. The optimized RTD, including the number of ranges and the distance of each range, can be determined by maximizing the objective hourly profit function.

The optimization problem considering variable RTD, service headways, and fare for the study time period is a large combinatorial problem. It is a challenging task to optimize all possible combinations of the numbers and RTD that best satisfy the given objectives and constraints. A solution algorithm, called Genetic Algorithm, is developed in Chapter 4 to search for the optimal solution. To formulate the optimization model, the system assumptions, model formulation, constraints, and optimization problem are discussed in the following sections.

3.2.1 System Assumptions

The model in Scenario II is developed mostly based on the assumptions discussed for Scenario I, except that assumption of given RTD is released. Therefore, the formulation of fare and demand are based on variable RTD. Thus, fare, service frequency, and RTD can be optimized simultaneously. The assumptions of Scenario II are:

1. The transit route is referred to 3.1.1 item 1. The maximum number of RTD, denoted as q , is based on the number of stations, denoted as n , which is equal to $\binom{n}{2}$. The travel distance at range z is between $d_{z_{ij}-1}$ and $d_{z_{ij}}$ as shown in Table 3.1. Note that z_{ij} is the index of RTD, which varies from 1 to q .
2. The round trip travel time is the same as in Assumption 2 discussed in Section 3.1.1

3. A more general classification of the weight factor of unit fare during the study time period, denoted as $\gamma_{z_{ij}}$, is shown in Table 3.1.
4. The distance-based fare is the product of unit fare (δ), the weight factor of unit fare ($\gamma_{z_{ij}}$), and the travel distance between stations i and j (L_{ij}). Note that $\gamma_{z_{ij}}$ for each corresponding RTD decreases as the index of RTD (z_{ij}) increases from short to long distance range. Thus,

$$F_{ij} = \delta \gamma_{z_{ij}} L_{ij} \quad i, j \in \{1, 2, \dots, n\}; z_{ij} \in \{1, 2, \dots, q\}; L_{ij} \in \{d_{z_{ij}-1}, d_{z_{ij}}\} \quad (3.22)$$

5. The average wait time is the same as Assumption 5 discussed in Section 3.1.1.
6. The fare elasticity parameter from station i to j , denoted as $E_{F_{ij}}$, varies by each O-D pair. The hourly ridership (i.e., actual demand) can be estimated by using a demand function as

$$Q_{ij} = Y_{ij} (1 - E_w t_w - E_I t_{I_{ij}} - E_{F_{ij}} F_{ij}) \quad i, j \in \{1, 2, \dots, n\} \quad (3.23)$$

where the potential hourly O-D demand for the study time period, denoted as Y_{ij} , is sensitive to fare and level of service (e.g., the travel time of passengers). The average in-vehicle time from station i to j during the study time period, denoted as $t_{I_{ij}}$, can be obtained from the operating schedule. Elasticity parameters of wait time, denoted as E_w , and in-vehicle time, denoted as E_I , are constant.

Table 3.1 Weight Factors of Unit Fare by Different RTD (Single Time Period)

Ranges of Travel Distance (RTD)	Index of RTD (z_{ij})	Weight Factors of Unit Fare ($\gamma_{z_{ij}}$)
$0 < L_{ij} \leq d_1$ miles	1	γ_1
$d_1 < L_{ij} \leq d_2$ miles	2	γ_2
⋮	⋮	⋮
$d_{z_{ij}-1} < L_{ij} \leq d_{z_{ij}}$ miles	z_{ij}	$\gamma_{z_{ij}}$
⋮	⋮	⋮
$d_{q-1} < L_{ij} \leq L$ miles	q	γ_q

3.2.2 Model Formulation

The total profit function for Scenario II can be obtained from Equation 3.5 in Scenario I. The hourly revenue and operator's cost are formulated to calculate the hourly profit. The revenue is the product of hourly demand multiplied by fare which can be formulated by substituting the distance-based fare of Equation 3.22 into Equation 3.6. Furthermore, the hourly operator's cost has been formulated in Scenario I as the sum of vehicle operating cost, transit line cost, and station cost as Equation 3.11. Therefore, the hourly profit function can then be derived by substituting Equations 3.6 and 3.11 into Equation 3.5. Thus,

$$P = \sum_{i=1}^n \sum_{j=1}^n Q_{ij} (\delta \gamma_{z_{ij}} L_{ij}) - (Nc_o + Lc_L + nc_S) \quad z_{ij} \in \{1, 2, \dots, q\}; L_{ij} \in \{d_{z_{ij}-1}, d_{z_{ij}}\} \quad (3.24)$$

Note that the ridership and fare varies with the optimized number of RTD, denoted as q^* , corresponding with the weight factor of unit fare for each RTD, which yields the maximum total profit.

3.2.3 Constraints

The capacity and fleet size constraints considered in Scenario I are both used in Scenario II. Since the weight factor of unit fare is determined based on the optimized RTD, the estimation of hourly demand can be calculated by Equation 3.23. Meanwhile, the capacity and fleet size constraints can be determined by Equations 3.13 and 3.17, respectively. The optimal headway during the studied time period is governed by the minimum and maximum headways as shown in Equation 3.18.

3.2.4 Optimization Problem

Based on the discussion from Section 3.2.1 through 3.2.3, the studied fare and service headway optimization problem that maximizes the hourly profit of transit service under the optimized numbers and RTD subject to the capacity and fleet size constraints is formulated as follows:

$$\begin{aligned}
 & \text{Maximize} \\
 & P = \sum_{i=1}^n \sum_{j=1}^n Q_{ij} \delta \gamma_{z_{ij}} L_{ij} - \left(\frac{T_R}{H} c_O + L c_L + n c_S \right) \quad z_{ij} \in \{1, 2, \dots, q\} \\
 & \text{st.} \\
 & H \leq \frac{B}{\text{Max} \left[\left(\sum_{i=1}^g \sum_{j=g+1}^n Q_{ij}, \sum_{i=g+1}^n \sum_{j=1}^g Q_{ij} \right) \quad \forall g \right]} \\
 & \frac{T_R}{N'} \leq H \\
 & H, \delta, \text{ and } \gamma_{z_{ij}} \geq 0 \quad z_{ij} \in \{1, 2, \dots, q\}
 \end{aligned} \quad \left. \vphantom{\begin{aligned} & \text{Maximize} \\ & P = \sum_{i=1}^n \sum_{j=1}^n Q_{ij} \delta \gamma_{z_{ij}} L_{ij} - \left(\frac{T_R}{H} c_O + L c_L + n c_S \right) \quad z_{ij} \in \{1, 2, \dots, q\} \\ & \text{st.} \\ & H \leq \frac{B}{\text{Max} \left[\left(\sum_{i=1}^g \sum_{j=g+1}^n Q_{ij}, \sum_{i=g+1}^n \sum_{j=1}^g Q_{ij} \right) \quad \forall g \right]} \\ & \frac{T_R}{N'} \leq H \\ & H, \delta, \text{ and } \gamma_{z_{ij}} \geq 0 \quad z_{ij} \in \{1, 2, \dots, q\} \right.} (P2)
 \end{aligned}$$

Note that the objective function of P2 is given by Equation 3.24, while the constraint is derived from Equations 3.13 and 3.17. F_{ij} and Q_{ij} are calculated by Equations 3.22 and 3.23 based on the optimized RTD.

Optimizing the number of RTD, denoted as q^* to yield the maximum profit operation while considering the joint impact of fare and service frequency, is a large combinatorial problem. A GA is used to solve P2 as discussed in Chapter 4.

The general procedure to solve P2 is an iterative process, which first determines the feasible RTD, and therefore, the decision variables (e.g., headway, fare) can be optimized by taking the partial derivatives of the profit function (Equation 3.24) with respect to headway, unit fare and the weight factor of unit fare, and setting them equal to zero. To solve these equations with respect to the decision variables yields a set of

optimal solutions that maximize profit. The optimal headway, unit fare, and weight factor of unit fare can be derived as follows:

$$H^* = \sqrt{\frac{T_R c_o}{E_w \beta \delta \sum_{i=1}^n \sum_{j=1}^n Y_{ij} \gamma_{z_{ij}} L_{ij}}} \quad z_{ij} \in \{1, 2, \dots, q\} \quad (3.25)$$

$$\delta^* = \frac{\sum_{i=1}^n \sum_{j=1}^n Y_{ij} (1 - E_w \beta H - E_1 t_{1_{ij}}) \gamma_{z_{ij}} L_{ij}}{2 \sum_{i=1}^n \sum_{j=1}^n E_{F_{z_{ij}}} Y_{ij} \gamma_{z_{ij}} L_{ij}^2} \quad z_{ij} \in \{1, 2, \dots, q\} \quad (3.26)$$

$$\gamma_{z_{ij}}^* = \frac{\sum_{i=1}^n \sum_{j=1}^n Y_{ij} (1 - E_w \beta H - E_1 t_{1_{ij}}) L_{ij}}{2 \delta \sum_{i=1}^n \sum_{j=1}^n E_{F_{z_{ij}}} Y_{ij} L_{ij}^2} \quad z_{ij} \in \{1, 2, \dots, q\} \quad (3.27)$$

If H^* fulfils the constraints discussed in Equation 3.18, the solution is optimal.

The solution algorithm for P2 is discussed in Section 4.2.

3.3 Fixed RTD for Multiple Time Periods – Scenario III

The model developed in Scenario III considers temporal distance-based fare and service headway with given RTD. It enhances Scenario I by considering that the daily operation is sensitive to temporal demand in peak and off-peak hours. The system assumptions, model formulation, constraints, and optimization problem for daily operation are discussed next.

3.3.1 System Assumptions

The Scenario III model considers temporal O-D demand, waiting time, and fare with given RTD. The assumptions made for formulating the model are discussed below:

1. The transit route and corresponding RTD is the same as in Assumption 1 discussed in Section 3.1.1.
2. The round trip travel time is the same as in Assumption 2 discussed in Section 3.1.1.
3. The weight factor of unit fare, denoted as $\gamma_{z_{ij}}^t$, is a constant but may vary with RTD and time periods (e.g., peak and off-peak). While considering the differentiated fare for peak and off-peak periods, the weight factors of unit fare for short, median, and long range of travel distance during time periods t are denoted as γ_s^t , γ_m^t , and γ_l^t , respectively.
4. The temporal distance-based fare for passengers traveling from stations i to j during the study time periods, denoted as F_{ij}^t , is the product of the time differential unit fare (δ^t) and weight factor of unit fare ($\gamma_{z_{ij}}^t$). Note that $\gamma_{z_{ij}}^t$ for each corresponding RTD decreases as the index of RTD (z_{ij}) increases from short to long distance range. Thus,

$$F_{ij}^t = \delta^t \gamma_{z_{ij}}^t L_{ij} \quad i, j \in \{1, 2, \dots, n\}; z_{ij} \in \{s, m, l\}; t \in \{P, OP\} \quad (3.28)$$

5. The average passenger wait time is determined by the temporal headway. Thus, the average wait time can be formulated as

$$t_w^t = \beta H^t \quad t \in \{P, OP\} \quad (3.29)$$

where β , the ratio of average wait time to headway, can be determined by service frequency, the actual passenger travel behavior and terminal/station required processing time for each passenger. H^t denotes the temporal headway.

6. The hourly ridership (i.e., actual demand) and potential O-D travel demand from station i to j during multiple time periods, denoted as Y_{ij}^t and Q_{ij}^t , can be estimated from a demand function formulated in Equation 3.30. Thus,

$$Q_{ij}^t = Y_{ij}^t (1 - E_w t_w^t - E_I t_{I_{ij}} - E_{F_{z_{ij}}} F_{ij}^t) \quad i, j \in \{1, 2, \dots, n\}; z_{ij} \in \{s, m, l\}; t \in \{P, OP\} \quad (3.30)$$

where the average in-vehicle time from station i to j during the study time period, denoted as $t_{I_{ij}}$, can be obtained from the operating schedule. The elasticity parameters of wait time, denoted as E_w , and in-vehicle time, denoted as E_I , are constant.

3.3.2 Model Formulation

The objective total profit function for Scenario III is obtained from a modified Equation 3.5 discussed in Scenario I by considering daily revenue and operator's cost due to temporal demand. The daily revenue is the product of operation hours (e.g., peak and off-peak periods) multiplied by hourly ridership, denoted as Q_{ij}^t and obtained from Equation 3.30, and temporal fare, denoted as F_{ij}^t for all O-D pairs of i and j , where $i, j \in \{1, 2, \dots, n\}$.

Thus,

$$R = \sum_{t \in \{P, OP\}} \sum_{i=1}^n \sum_{j=1}^n D^t Q_{ij}^t F_{ij}^t \quad (3.31)$$

where D^t is the number of operation hours during period t , and n represents the number of stations on the route.

The daily vehicle operating cost is the product of fleet size, denoted as N^t , multiplied by the number of operation hours (e.g., peak and off-peak periods), denoted as D^t , and hourly vehicle operating cost, denoted as c_o , for peak and off-peak hours. The daily operating cost and fleet size are respectively formulated as Equations 3.32 and 3.33:

$$C_o = \sum_{t \in \{P, OP\}} N^t D^t c_o \quad (3.32)$$

$$N^t = \left[\frac{T_R}{H^t} \right]^+ \quad t \in \{P, OP\} \quad (3.33)$$

where N^t is fleet size and equal to the round trip vehicle travel time, denoted as T_R , divided by the headway, denoted as H^t . The fleet size is integer and $[]^+$ indicates that the fleet size, if not integer already, is rounded up.

The unit transit line cost, denoted as c_L , and the unit station cost, denoted as c_S , considered in this study are fixed in different time periods. Thus, the daily transit line cost and station cost are shown in Equations 3.34 and 3.35, respectively.

$$C_L = \sum_{t \in \{P, OP\}} LD^t c_L \quad (3.34)$$

$$C_S = \sum_{t \in \{P, OP\}} nD^t c_S \quad (3.35)$$

Finally, the operator's cost, denoted as C , is the sum of C_O , C_L , and C_S . Thus, the daily operator's cost is shown in Equation 3.36.

$$C = \sum_{t \in \{P, OP\}} (N^t c_o + Lc_L + nc_S) D^t \quad (3.36)$$

The revenue can be formulated by substituting temporal distance-based fare (e.g., Equation 3.28) into Equation 3.31. Therefore, the daily profit function can then be derived by substituting Equations 3.31 and 3.36 into Equation 3.5. Thus,

$$P = \sum_{t \in \{P, OP\}} \sum_{i=1}^n \sum_{j=1}^n [Q_{ij}^t \delta^t \gamma_{z_{ij}}^t L_{ij} - (N^t c_o + Lc_L + nc_S)] D^t \quad z_{ij} \in \{s, m, l\} \quad (3.37)$$

3.3.3 Constraints

The capacity and fleet size constraints considered in Scenario I are used in Scenario III. However, the capacity constraints are dominated by temporal demand. Note that the operable fleet size is fixed in any time period of the day.

Capacity Constraint

The maximum design headway during time periods t , denoted as H'_{\max} , ensures that the capacity is greater than or equal to the maximum demand. The hourly capacity, denoted as p^t , equals to the train capacity, denoted as B , divided by temporal headway:

$$p^t = \frac{B}{H^t} \quad t \in \{P, OP\} \quad (3.38)$$

To satisfy the capacity constraint, p^t must be greater than or equal to the maximum demand through flow in link g , denoted as Q'_{\max} . Thus, from Equation 3.39, the maximum headway, denoted as H'_{\max} , is derived as:

$$H'_{\max} = \frac{B}{Q'_{\max}} \quad t \in \{P, OP\} \quad (3.39)$$

In general, the demand from station i to j , the outbound (e.g., from 1 to n) demand and inbound (e.g., from n to 1) demand of link g can be represented by Q'_{ij} and O'_g , and I'_g , respectively. Note that g , the index of links, varies between 1 and $(n-1)$. With Equation 3.40, the maximum demand can be identified by calculating the number of inbound and outbound trips on all links of the studied route for the study time period.

$$Q'_{\max} = \text{Max}[O'_g, I'_g] = \text{Max} \left[\sum_{i=1}^g \sum_{j=g+1}^n Q'_{ij}, \sum_{i=g+1}^n \sum_{j=1}^g Q'_{ij} \right] \quad \forall g; t \in \{P, OP\} \quad (3.40)$$

Fleet Size Constraint

Since the operable fleet sizes are constant for peak and off-peak periods, the minimum headway, denoted as H'_{\min} , can be obtained from the same equation as Scenario I. Thus,

$$H'_{\min} = \frac{T_R}{N} \quad (3.41)$$

The optimal headways for the multiple time periods, denoted as H'^* , are governed by the maximum and minimum temporal headways as shown in Equation 3.42.

$$H'_{\min} \leq H'^* \leq H'_{\max} \quad (3.42)$$

3.3.4 Optimization Problem

Based on the discussion from Section 3.3.1 through 3.3.3, the studied temporal fare and headway optimization problem that maximizes the daily profit of transit service under the condition of given RTD subject to the capacity and fleet size constraints is thus formulated as follows:

$$\begin{aligned}
 & \text{Maximize} \\
 & P = \sum_{t \in \{P, OP\}} \sum_{i=1}^n \sum_{j=1}^n D^t Q_{ij}^t \delta^t \gamma_{z_{ij}}^t L_{ij} - \left[\left(\frac{1}{H^P} D^P + \frac{1}{H^{OP}} D^{OP} \right) T_R c_O + (D^P + D^{OP})(Lc_L + nc_S) \right] \quad z_{ij} \in \{s, m, l\} \\
 & \text{st.} \\
 & H^t \leq \frac{B}{\text{Max} \left[\left(\sum_{i=1}^g \sum_{j=g+1}^n Q_{ij}^t, \sum_{i=g+1}^n \sum_{j=1}^g Q_{ij}^t \right) \quad \forall g \quad t \in \{P, OP\} \right]} \\
 & \frac{T_R}{N^t} \leq H^t \quad t \in \{P, OP\} \\
 & H^t, \delta^t, \text{ and } \gamma_{z_{ij}}^t \geq 0 \quad z_{ij} \in \{s, m, l\} \quad t \in \{P, OP\}
 \end{aligned} \tag{P3}$$

Note that the objective function of P3 is formulated in Equation 3.37, while the constraints are derived in Equations 3.39 and 3.41. Q'_{\max} in Equation 3.39 is replaced by Equation 3.40.

The optimal service design consists of the temporal optimal headway and fare. The optimal service design problem, structured as P3, is a constrained non-linear optimization problem. Assuming that the optimal headway will fall within the acceptable headway range, the constraints can be relaxed; therefore, P3 can be solved as unconstrained optimization problems.

This is accomplished by first deriving formulae for the optimal headway and fare structure. These are obtained by taking the partial derivatives of the profit function (Equation 3.37) with respect to headway, unit fare and the weight factor of unit fare, and setting them equal to zero. By solving these equations with respect to the decision

variables yields a set of optimal solutions that maximize profit. The optimal temporal headway, unit fare, and weight factor of unit fare can be derived as follows:

$$H^{P*} = \sqrt{\frac{T_R c_o}{E_W \alpha \delta^P D^P \sum_{i=1}^n \sum_{j=1}^n Y_{ij}^P \gamma_{z_{ij}}^P L_{ij}}} \quad z_{ij} \in \{s, m, l\} \quad (3.43)$$

$$H^{OP*} = \sqrt{\frac{T_R c_o}{E_W \alpha \delta^{OP} \sum_{i=1}^n \sum_{j=1}^n Y_{ij}^{OP} \gamma_{z_{ij}}^{OP} L_{ij}}} \quad z_{ij} \in \{s, m, l\} \quad (3.44)$$

$$\delta^{t*} = \frac{\sum_{i=1}^n \sum_{j=1}^n Y_{ij}^t (1 - E_W \alpha H^t - E_t t_{ij}) \gamma_{z_{ij}}^t L_{ij}}{2 \sum_{i=1}^n \sum_{j=1}^n E_{F_{z_{ij}}} Y_{ij}^t \gamma_{z_{ij}}^t L_{ij}^2} \quad t \in \{P, OP\}; z_{ij} \in \{s, m, l\} \quad (3.45)$$

$$\gamma_{z_{ij}}^{t*} = \frac{\sum_{i=1}^n \sum_{j=1}^n Y_{ij}^t (1 - E_W \alpha H^t - E_t t_{ij}) L_{ij}}{2 \delta^{t*} \sum_{i=1}^n \sum_{j=1}^n E_{F_{z_{ij}}} Y_{ij}^t L_{ij}^2} \quad t \in \{P, OP\}; z_{ij} \in \{s, m, l\} \quad (3.46)$$

If H^{t*} fulfils the constraints discussed in Equation 3.42, the solution is optimal.

Figure 3.5 shows that the optimal headway that maximizes profit is dependent on its relationship vis-à-vis H'_{\min} and H'_{\max} . Figure 3.5a shows that H^{t*} is within the feasible range; therefore, the optimal headway can be calculated using Equations 3.43 and 3.44. However, in Figure 3.5b, the optimal headway is limited by H'_{\max} and is calculated by Equation 3.39. Figure 3.5c, shows that the optimal headway is governed by the H'_{\min} that is achievable on the route and is thus calculated using Equation 3.41. The solution algorithm to solve P3 is discussed in Section 4.1.

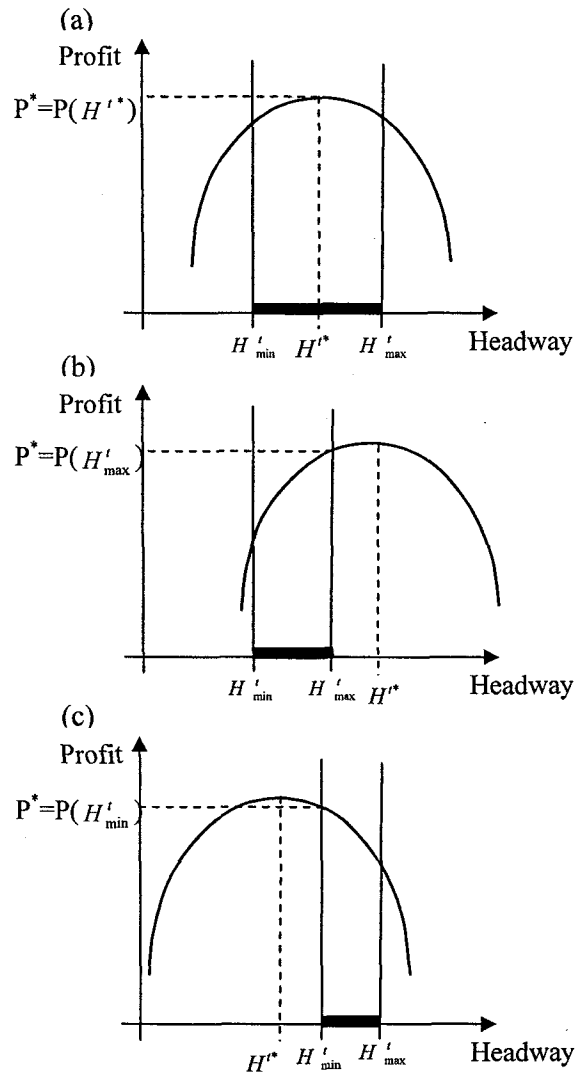


Figure 3.5 Optimal headway for various feasible conditions (Multiple time periods).

3.4 Variable RTD for Multiple Time Periods – Scenario IV

The optimization model developed in Scenario IV enhances Scenario III and optimizes RTD, temporal distance-based fare and headway. Similar to Scenario III, the daily operation hours including peak and off-peak periods are considered in the optimization model. The optimized RTD, including the number of ranges and the distance of each

range, can be determined by maximizing the objective daily profit function. The developed model is to find all possible combinations of RTD that best satisfy the given objectives and constraints, which can be used for the operator's decision making. To formulate the optimization model, the system assumptions, model formulation, constraints, and optimization problem are discussed in the following sections.

3.4.1 System Assumptions

The model in Scenario IV is developed mostly based on the assumptions discussed in Scenario III, except that the assumption of given RTD is relaxed. Therefore, the formulation of fare and demand are based on variable RTD during peak and off-peak periods. The assumptions of Scenario IV are:

1. The transit route and corresponding RTD is the same as in Assumption 1 discussed in Section 3.2.1.
2. The round trip travel time is the same as in Assumption 2 discussed in Section 3.1.1.
3. A more general classification of the weight factor of unit fare for the study time periods, denoted as $\gamma'_{z_{ij}}$, is shown in Table 3.2.
4. The temporal distance-based fare for the study time periods, denoted as F'_{ij} , is formulated as the product of time differential unit fare (δ') and weight factor of unit fare ($\gamma'_{z_{ij}}$). Note that $\gamma'_{z_{ij}}$ for each corresponding RTD decreases as the index of RTD (z_{ij}) increases from short to long distance range. Thus,

$$F'_{ij} = \delta' \gamma'_{z_{ij}} L_{ij} \quad i, j \in \{1, 2, \dots, n\}; z_{ij} \in \{1, 2, \dots, q\}; t \in \{P, OP\} \quad (3.47)$$

5. The average wait time is the same as in Assumption 5 discussed in Section 3.3.1.
6. The elasticity parameter of fare from station i to j , denoted as $E_{F_{ij}}$, varies by each O-D trip. Thus, the hourly ridership (i.e., actual demand) during multiple time periods can be estimated through an assumed demand function shown in Equation 3.48.

$$Q'_{ij} = Y'_{ij}(1 - E_w t'_w - E_I t'_{I_{ij}} - E_{F_{ij}} F'_{ij}) \quad i, j \in \{1, 2, \dots, n\}; t \in \{P, OP\} \quad (3.48)$$

where the average in-vehicle time from station i to j during the study time period, denoted as $t'_{I_{ij}}$, can be referred to the operating schedule. Elasticity parameters of wait time, denoted as E_w , and in-vehicle time, denoted as E_I , are constant.

Table 3.2 Weight Factors of Unit Fare for Different RTD (Multiple Time Periods)

Ranges of Travel Distance (RTD)	Index of RTD (z_{ij})	Weight Factors of Unit Fare ($\gamma'_{z_{ij}}$) $t \in \{P, OP\}$
$0 < L_{ij} \leq d_1$ miles	1	γ'_1
$d_1 < L_{ij} \leq d_2$ miles	2	γ'_2
⋮	⋮	⋮
$d_{z_{ij}-1} < L_{ij} \leq d_{z_{ij}}$ miles	z_{ij}	$\gamma'_{z_{ij}}$
⋮	⋮	⋮
$d_{q-1} < L_{ij} \leq L$ miles	q	γ'_q

3.4.2 Model Formulation

The total profit function for Scenario IV is the same as defined in Equation 3.5 for Scenario I. The daily revenue and operator's cost are calculated to formulate the daily profit. The daily revenue is the product of daily operation hours multiplied by hourly demand fare which can be formulated by substituting the temporal distance-based fare of Equation 3.47 into Equation 3.31. The daily operator's cost is defined the same way as in Scenario III by calculating the summation of vehicle operating cost, transit line cost, and station cost in Equation 3.36. Therefore, the daily profit function can then be derived by substituting Equations 3.31 and 3.36 into Equation 3.5. Thus,

$$P = \sum_{t \in \{P, OP\}} \sum_{i=1}^n \sum_{j=1}^n [Q'_{ij} \delta^t \gamma'_{z_{ij}} L_{ij} - (N^t c_o + Lc_L + nc_S)] D^t \quad z_{ij} \in \{1, 2, \dots, q\} \quad (3.49)$$

3.4.3 Constraints

The capacity and fleet size constraints considered in Scenario II are both used in Scenario IV. Since the weight factor of unit fare is determined based on the optimized RTD by different time periods, the ridership during peak and off-peak periods can be calculated by using Equation 3.48. Meanwhile, the capacity and fleet size constraints can be determined by using Equations 3.39 and 3.41, respectively. The optimal headways during the multiple time periods are governed by the minimum and maximum headways as shown in Equation 3.42.

3.4.4 Optimization Problem

Based on the discussion from Sections 3.4.1 through 3.4.3, the studied fare and headway optimization problem that maximizes the daily profit of transit service under the condition of optimized RTD subject to the capacity and fleet size constraints is formulated as follows:

$$\left. \begin{aligned}
 & \text{Maximize} \\
 & P = \sum_{t \in \{P, OP\}} \sum_{i=1}^n \sum_{j=1}^n D^t Q'_{ij} \delta^t \gamma'_{zy} L_{ij} - \left[\left(\frac{D^P}{H^P} + \frac{D^{OP}}{H^{OP}} \right) T_R c_O + (D^P + D^{OP})(Lc_L + nc_S) \right] \quad z_{ij} \in \{1, 2, \dots, q\} \\
 & \text{st.} \\
 & H^t \leq \frac{B}{\text{Max} \left[\left(\sum_{i=1}^g \sum_{j=g+1}^n Q'_{ij}, \sum_{i=g+1}^n \sum_{j=1}^g Q'_{ij} \right) \quad \forall g \quad t \in \{P, OP\} \right]} \\
 & \frac{T_R}{N^t} \leq H^t \quad t \in \{P, OP\} \\
 & H^t, \delta^t, \text{ and } \gamma'_{zy} \geq 0 \quad z_{ij} \in \{1, 2, \dots, q\} \quad t \in \{P, OP\}
 \end{aligned} \right\} (P4)$$

Note that the objective function of P4 is given by Equation 3.49, while the constraint is derived from Equations 3.39 and 3.41. F'_{ij} and Q'_{ij} are calculated by Equations 3.47 and 3.48 based on the optimized RTD.

Optimizing the number of RTD, denoted as q^* to yield the maximum daily profit operation, while considering the joint impact of temporal fare and headway, is a large combinatorial problem. This research uses a GA to solve P4, which is discussed in Chapter 4.

The general procedure to solve this problem is an iterative process, which first determines a feasible RTD and therefore, the decision variables of temporal headway and fare can be optimized by taking the partial derivatives of the profit function (Equation 3.49) with respect to headway, unit fare and the weight factor of unit fare, and setting them equal to zero. By solving these equations with respect to the decision variables yields a set of optimal solutions that maximize profit. The optimal temporal headway, unit fare, and weight factor of unit fare can be derived as follows:

$$H^{P*} = \sqrt{\frac{T_R C_O}{E_W \alpha \delta^P D^P \sum_{i=1}^n \sum_{j=1}^n Y_{ij}^P \gamma_{z_{ij}}^P L_{ij}}} \quad z_{ij} \in \{1, 2, \dots, q\} \quad (3.50)$$

$$H^{OP*} = \sqrt{\frac{T_R C_O}{E_W \alpha \delta^{OP} \sum_{i=1}^n \sum_{j=1}^n Y_{ij}^{OP} \gamma_{z_{ij}}^{OP} L_{ij}}} \quad z_{ij} \in \{1, 2, \dots, q\} \quad (3.51)$$

$$\delta^{t*} = \frac{\sum_{i=1}^n \sum_{j=1}^n Y_{ij}^t (1 - E_W \alpha H^t - E_I t_{I_{ij}}) \gamma_{z_{ij}}^t L_{ij}}{2 \sum_{i=1}^n \sum_{j=1}^n E_{F_{z_{ij}}} Y_{ij}^t \gamma_{z_{ij}}^t L_{ij}^2} \quad t \in \{P, OP\}; z_{ij} \in \{1, 2, \dots, q\} \quad (3.52)$$

$$\gamma_{z_{ij}}^{t*} = \frac{\sum_{i=1}^n \sum_{j=1}^n Y_{ij}^t (1 - E_W \alpha H^t - E_I t_{I_{ij}}) L_{ij}}{2 \delta^{t*} \sum_{i=1}^n \sum_{j=1}^n E_{F_{z_{ij}}} Y_{ij}^t L_{ij}^2} \quad t \in \{P, OP\}; z_{ij} \in \{1, 2, \dots, q\} \quad (3.53)$$

If H^{t*} fulfils the constraints discussed in Equation 3.41, the solution is optimal.

The solution algorithm to solve P4 is discussed in Section 4.2.

3.5 Summary

In this chapter, the objective total profit functions and sets of constraints for Scenarios I through IV were formulated. The developed models are based on the assumptions and constraints summarized in Table 3.3; and the decision variables used in each model include unit fare (e.g., δ in Scenarios I and II, and δ' in Scenarios III and IV), service headway (e.g., H in Scenarios I and II, and H' in Scenarios III and IV), weight factor of unit fare (e.g., $\gamma_{z_{ij}}$ in Scenarios I and II, and $\gamma'_{z_{ij}}$ in Scenarios III and IV), the number of RTD (e.g., given in Scenarios I and II, and q^* to be optimized in Scenarios II and IV), and the index of travel distance at range z_{ij} ($d_{z_{ij}}$, where $z=1, 2, \dots, q$) are summarized in Table 3.4. Note that the index of travel distance range (z_{ij}) is determined based on the optimized number of RTD (q^*).

While considering the given RTD in Scenarios I and III, the optimization model can be solved by using the modified Gauss-Southwell method to optimize differentiated fares and headways. However, the combination and interdependent relations among the decision variables in Scenarios II and IV has an enormous number of decision variables to be optimized. By employing the Genetic Algorithm developed in Chapter 4, the combinatorial optimization problem of fare and headway with variable RTD can be solved.

Table 3.3 Characteristics of Models for Scenarios I through IV

	Scenario I	Scenario II	Scenario III	Scenario IV
<i>System Assumptions:</i>				
Geometric configuration	Given	Given	Given	Given
Service pattern	Serve every stop	Serve every stop	Serve every stop	Serve every stop
Elasticity parameter of fare	Fixed in each RTD	Vary with O-D	Fixed in each RTD	Vary with O-D
O-D demand	Peak	Peak	Temporal	Temporal
Waiting time	Peak	Peak	Temporal	Temporal
<i>Constraints:</i>				
Capacity	Peak	Peak	Temporal	Temporal
Operable fleet size	Given	Given	Given	Given

Table 3.4 Decision Variables in the Models for Scenarios I through IV

Decision Variables	Scenario I	Scenario II	Scenario III	Scenario IV
Number of RTD	-	q^*	-	q^*
Travel distance range	-	$d_{z_{ij}}$ $z \in \{1, \dots, q^*\}$	-	$d_{z_{ij}}$ $z \in \{1, \dots, q^*\}$
Unit fare	δ	δ	δ^t $t \in \{P, OP\}$	δ^t $t \in \{P, OP\}$
Weight factors of unit fare	$\gamma_{z_{ij}}$ $z_{ij} \in \{s, m, l\}$	$\gamma_{z_{ij}}$ $z_{ij} \in \{1, \dots, q^*\}$	$\gamma'_{z_{ij}}$ $z_{ij} \in \{s, m, l\}$	$\gamma'_{z_{ij}}$ $z_{ij} \in \{1, \dots, q^*\}$
Headway	H	H	H^t $t \in \{P, OP\}$	H^t $t \in \{P, OP\}$

CHAPTER 4

SOLUTION ALGORITHMS

As discussed previously in this dissertation, the objective of this study is to develop models, discussed in Chapter 3, which maximize the total profit functions for Scenarios I through IV. The decision variables of the developed models include fare, service headway, and RTD. Due to the various combinations and interdependent relation among these decision variables summarized in Section 3.5, the studied optimization problem has an enormous number of decision variables to be optimized.

This chapter presents a successive substitution method (i.e., modified Gauss-Southwell method) to optimize differentiated fares and service headways for solving fixed RTD problems discussed in Scenarios I and III. The RTD is treated as a decision variable in Scenarios II and IV, making the models combinatorial optimization problems due to the combination and interdependent relationships among the decision variables. A solution algorithm, called Genetic Algorithm (GA), is also developed in this chapter to search for the optimal solution.

The successive substitution method for Scenarios I and III is discussed in Section 4.1, and the developed GA for Scenarios II and IV is discussed in Section 4.2.

4.1 Fixed RTD in Scenarios I and III

4.1.1 Successive Substitution Method

The objective function of the profit maximization problem formulated in Chapter 3.1 is a multi-dimensional function for a single time period. Several purely numerical algorithms are available to solve such a multi-dimensional optimization problem, including variations of the Conjugate Gradient method (Hestenes and Stiefel, 1952), Powell's method (Powell, 1964), and Variable Metric methods (Press et al. 1992). However, a more efficient optimization method has been used in this study using ideas similar to the Gauss Southwell (1989), and Powell methods. The basic concept of the optimization method is to derive, for each decision variable, the gradient vector by setting the first derivative of the objective function with respect to each decision variable equal to zero and solving it.

In the Gauss Southwell method, changes in a single decision variable are allowed in seeking a new gradient vector. Unlike the Gauss Southwell method, the method used here is a modified Gauss Southwell (1989) method, also called the successive substitution method by Chien and Schonfeld (1997). The successive substitution method used here allows changes in all decision variables within each iteration. The method provides an efficient way to find an ascent direction in searching for optimal solutions by computing the components in the gradient vector sequentially and iteratively.

A numerical successive substitution method is used to optimize differentiated fare and headway for the given RTD. Since RTD are fixed in Scenarios I and III, the decision variables of fare and headway can be optimized by maximizing the total profit with

successive substitutions through numerous iterations. Meanwhile, the concavity of the objective function must be verified to guarantee that the optimized solution is unique.

The successive substitution method is employed to search for the optimal solution for fixed RTD problems, which is described below and shown in Figure 4.1.

Step 1: Select a set of initial solutions for all decision variables (e.g., unit fare (δ), the weight factor of unit fare ($\gamma_{z_{ij}}$), service headway (H)) and give a solution tolerance limit (ε).

Step 2: Start the iteration counter (k).

Step 3: Calculate the optimal decision variables by using Equations 3.17 through 3.19; and compute the actual ridership with Equation 3.4.

Step 4: Check the optimal headway. If it falls within the range specified by Equations 3.14 and 3.15, then set H^* as the optimal service headway. If not, H^* is obtained from one of the governing bounds as indicated in Figure 3.2.

Step 5: Determine the required fleet size (N) with Equation 3.8 and re-calculate all decision variables and the objective value.

Step 6: Record the values of all decision variables and the objective function.

Step 7: Compare the objective solution. If it is sufficiently close, stop. The optimal solution has been reached. Otherwise, go to Step 2 and advance the iteration counter.

Step 8: Check the Hessian matrix. If all nonzero principal minors have the same sign as $(-1)^h$, where h is the order of partial derivatives, a global solution of maximum profit is reached. Otherwise, a local maximum is obtained.

Step 9: Report the optimal solution and stop.

First, create an initial set of non-negative initial values for the decision variables. Secondly, the sequence for calculating the optimal solution is developed according to the relative importance of each variable in influencing the objective function with capacity constraints. The provisional solutions are obtained by the sequence of headway, unit fare, and weight factor of unit fare. Corresponding to the initial values from Step 1 or a provisional set of values from the previous iteration, an updated provisional set of optimal decision variables can be calculated by means of the derivative equations developed in Step 3. The optimal headway should be located within the bounded headway in Step 4, and the corresponding required fleet size is obtained in Step 5. After all decision variables have been calculated, the entire process is repeated until adequate convergence has been attained in Steps 6 and 7. The optimality test is implemented by calculating the Hessian matrix of the total profit function to verify whether the maximum solution is obtained.

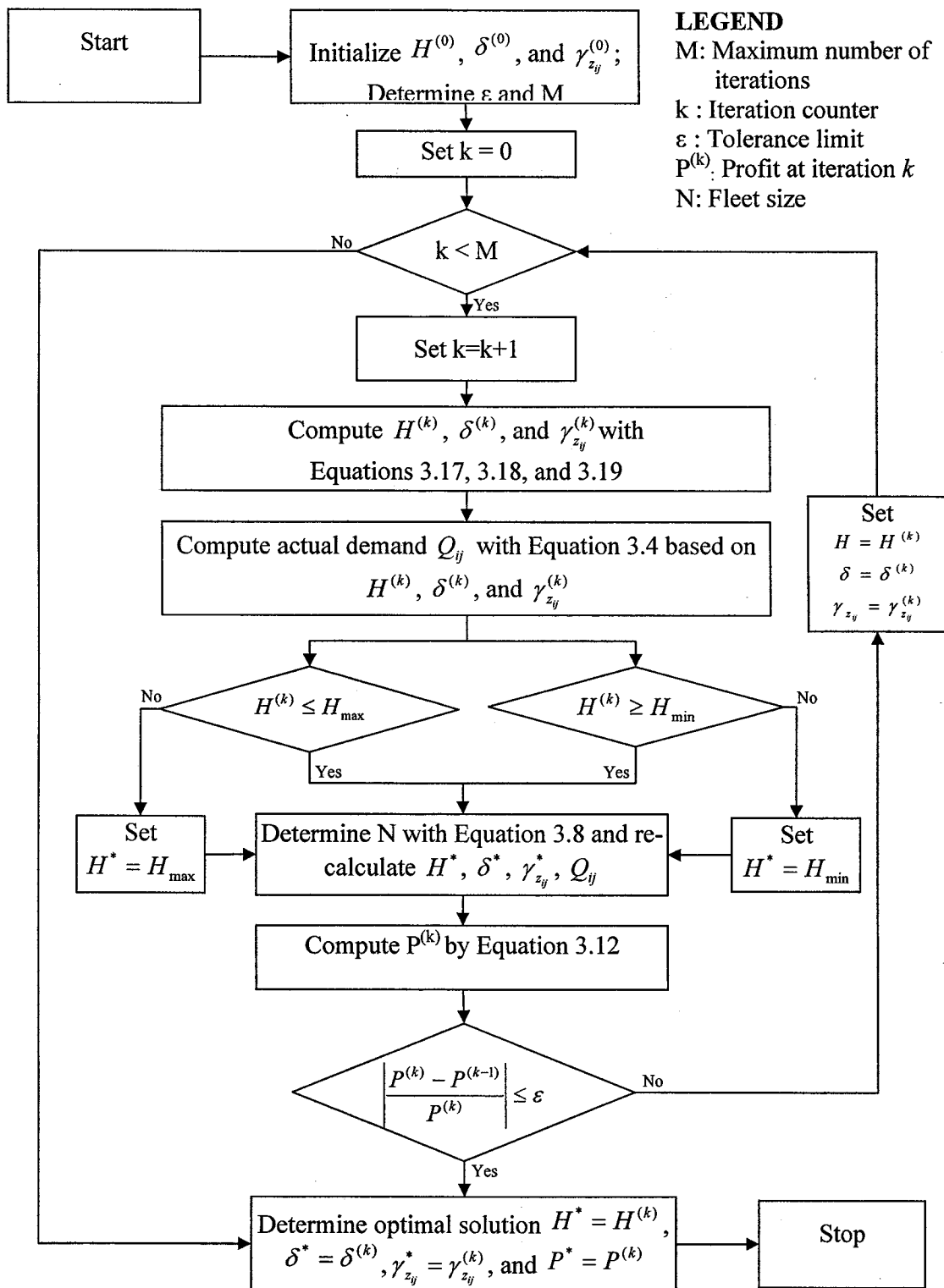


Figure 4.1 Flow chart of the modified Gauss-Southwell method.

4.1.2 The Hessian Matrix

To determine the convexity of an objection function, evaluating the values of the second derivative of the objective function to each decision variable is required. The square matrix of second-order partial derivatives of the objective function is known as the Hessian matrix. The objective function is a concave function if and only if all nonzero principal minors have the same sign as $(-1)^h$, where h is the order of partial derivatives based on the number of variables. Assume that the objective function of profit maximization has continuous second-order partial derivatives for all decision variables [e.g., unit fare (δ), service headway (H), and the weight factor of unit fare (γ_{z_i})]. The necessary and sufficient conditions for a maximum result are that the Hessian determinants are all satisfied within the range of interest for the design variables.

The example below indicates an objective function, denoted as P , with three decision variables [e.g., unit fare (δ), service headway (H), and the weight factor of unit fare (γ)]. Thus, the Hessian matrix, denoted as H_x , is expressed by

$$H_x = \begin{bmatrix} \frac{\partial^2 P}{\partial \delta^2} & \frac{\partial^2 P}{\partial \delta \partial H} & \frac{\partial^2 P}{\partial \delta \partial \gamma} \\ \frac{\partial^2 P}{\partial H \partial \delta} & \frac{\partial^2 P}{\partial H^2} & \frac{\partial^2 P}{\partial H \partial \gamma} \\ \frac{\partial^2 P}{\partial \gamma \partial \delta} & \frac{\partial^2 P}{\partial \gamma \partial H} & \frac{\partial^2 P}{\partial \gamma^2} \end{bmatrix} \quad (4.1)$$

The total of seven principal minors of H_x is obtained by Equations 4.2 through

4.8. The three diagonal entries of H_x (e.g., $\frac{\partial^2 P}{\partial \delta^2}$, $\frac{\partial^2 P}{\partial H^2}$, $\frac{\partial^2 P}{\partial \gamma^2}$) are represented as first-

order principal minors shown in Equations 4.2 through 4.4, while the three second-order

principal minors are calculated by deleting corresponding rows and columns for each variable shown in Equations 4.5 through 4.7. The third-order principal minor is the determinant of H_x as shown in Equation 4.8. To determine the concavity of the profit function, the determinant of first- and third-order principal minors in Equations 4.2 through 4.4 and Equation 4.8 should be definite negative; and the second-order principle minors in Equations 4.5 through 4.7 should be positive definite. If the principal minors violate one of the checking criteria for any point, the objective function is neither concave nor convex. Therefore, the optimal solution obtained for the profit maximization problem is a local optimum. Each of the Hessian determinants can be calculated using Equations 4.2 through 4.8.

By deleting rows and columns 2 and 3 of the Hessian matrix, the first-order principal minor is derived as

$$H_1 = \frac{\partial^2 P}{\partial \delta^2} < 0 \quad (4.2)$$

Similarly, by deleting rows and columns 1 and 3 (and 1 and 2) of the Hessian matrix, the first-order principal minors are derived as Equation 4.3 (and 4.4) respectively.

$$H_2 = \frac{\partial^2 P}{\partial H^2} < 0 \quad (4.3)$$

$$H_3 = \frac{\partial^2 P}{\partial \gamma^2} < 0 \quad (4.4)$$

By deleting row 1 and column 1 of the Hessian matrix, the second-order principal minor is derived as

$$H_4 = \det \begin{bmatrix} \frac{\partial^2 P}{\partial H^2} & \frac{\partial^2 P}{\partial H \partial \gamma} \\ \frac{\partial^2 P}{\partial \gamma \partial H} & \frac{\partial^2 P}{\partial \gamma^2} \end{bmatrix} > 0 \quad (4.6)$$

By deleting row 2 and column 2 of the Hessian matrix, the second-order principal minor is derived as

$$H_5 = \det \begin{bmatrix} \frac{\partial^2 P}{\partial \delta^2} & \frac{\partial^2 P}{\partial \delta \partial \gamma} \\ \frac{\partial^2 P}{\partial \gamma \partial \delta} & \frac{\partial^2 P}{\partial \gamma^2} \end{bmatrix} > 0 \quad (4.7)$$

By deleting row 3 and column 3 of the Hessian matrix, the second-order principal minor is derived as

$$H_6 = \det \begin{bmatrix} \frac{\partial^2 P}{\partial \delta^2} & \frac{\partial^2 P}{\partial \delta \partial H} \\ \frac{\partial^2 P}{\partial H \partial \delta} & \frac{\partial^2 P}{\partial H^2} \end{bmatrix} > 0 \quad (4.5)$$

The third-order principal minor is simply the determinant of the Hessian itself.

Expanding by row 1 of the cofactors, the third-order principal minor is derived as

$$H_7 = \left\{ \frac{\partial^2 P}{\partial \delta^2} \det \begin{bmatrix} \frac{\partial^2 P}{\partial H^2} & \frac{\partial^2 P}{\partial H \partial \gamma} \\ \frac{\partial^2 P}{\partial \gamma \partial H} & \frac{\partial^2 P}{\partial \gamma^2} \end{bmatrix} + \frac{\partial^2 P}{\partial H \partial \delta} \det \begin{bmatrix} \frac{\partial^2 P}{\partial \delta \partial H} & \frac{\partial^2 P}{\partial \delta \partial \gamma} \\ \frac{\partial^2 P}{\partial \gamma \partial H} & \frac{\partial^2 P}{\partial \gamma^2} \end{bmatrix} + \frac{\partial^2 P}{\partial \gamma \partial \delta} \det \begin{bmatrix} \frac{\partial^2 P}{\partial \delta \partial H} & \frac{\partial^2 P}{\partial \delta \partial \gamma} \\ \frac{\partial^2 P}{\partial H^2} & \frac{\partial^2 P}{\partial H \partial \gamma} \end{bmatrix} \right\} < 0 \quad (4.8)$$

In general, suppose $f(x_1, x_2, \dots, x_m)$ has continuous second-order partial derivatives for each point $x = (x_1, x_2, \dots, x_m) \in S$. Then $f(x_1, x_2, \dots, x_m)$ is a concave function on S , if and only if, for each $x \in S$ and $k = 1, 2, \dots, m$, all nonzero principal

minors have the same sign as $(-1)^k$. The total numbers of principal minors for a $m \times m$ Hessian matrix are calculated by

$$\binom{m}{1} + \binom{m}{2} + \dots + \binom{m}{m} = 2^m - 1 \quad (4.9)$$

Table 4.1 indicates that the total number of principle minors increase dramatically when the number of decision variable increases, especially in solving the variable RTD in Scenarios II and IV. The optimality test of the Hessian matrix in calculating the principal minors becomes an encumbrance of the solution method. Therefore, GA is used to maximize the total profit achieved by the optimal RTD in Scenarios II and IV.

Table 4.1 Number of Decision Variables and Principal Minors

Number of decision variables (m)	2	3	4	...	m-1	m
Number of principle minors	3	7	15	...	$2^{(m-1)} - 1$	$2^m - 1$

4.2 Variable RTD in Scenarios II and IV

4.2.1 Genetic Algorithm

The objective function of profit maximization problem formulated in Scenarios II and IV are enhanced from models developed for Scenarios I and III respectively, by treating RTD as a decision variable. This enhancement results in the studied problem become combinatorial optimization problems. In Scenarios II, the decision variables are determined by the unit fare (δ), service headway (H), weight factor of unit fare ($\gamma_{z_{ij}}$),

number of RTD (q^*), and the index of travel distance range z_{ij} ($d_{z_{ij}}$), where z_{ij} varies from 1 to q^* . Therefore, the total number of decision variables in Scenario II are

$\left\{ \binom{n}{q^*} - 1 \right\} \times (2q^* + 3)$. However, considering temporal unit fare (δ^t), service headway

(H^t), weight factor of unit fare ($\gamma'_{z_{ij}}$), number of RTD (q^*), and the index of travel

distance range z_{ij} (d_z) in Scenario IV, the total number of decision variables increases to

$\left\{ \binom{n}{q^*} - 1 \right\} \times (3q^* + 5)$.

The developed GA is used to search for the maximum total profit for various combinations of RTD. Assuming that the service line with n stations consists of $\binom{n}{2}$ pairs of unique O-D travel distance (L_{ij}), the total number of decision variables for three RTD in Scenarios II and IV can be derived by Equations 4.10 and 4.11, respectively.

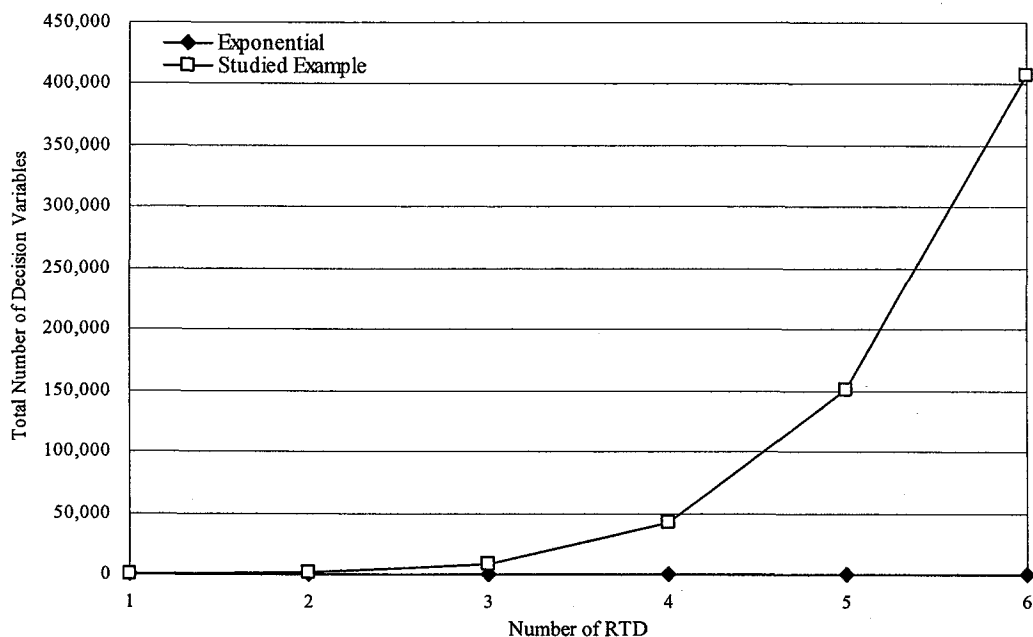
$$\frac{\{[\binom{n}{2} - 1][\binom{n}{2} - 2]\}}{2} \times (2q^* + 3) \quad (4.10)$$

$$\frac{\{[\binom{n}{2} - 1][\binom{n}{2} - 2]\}}{2} \times (3q^* + 5) \quad (4.11)$$

The number of decision variables for each RTD in Scenarios II and IV can be estimated based on equations summarized in Table 4.2, which increases more than exponentially as the number of RTD increases. Figure 4.3 indicates that more than 100,000 decision variables, consisting of the combinations of RTD and corresponding variables, need to be generated when the number of RTD is 5 and greater.

Table 4.2 Number of Decision Variables for Different RTD

Number of RTD (q^*)	Number of decision variables	
	Scenario II	Scenario IV
1	5	8
2	$\binom{n}{1}-1 \times (7)$	$\binom{n}{1}-1 \times (11)$
3	$\binom{n}{2}-1 \times (9)$	$\binom{n}{2}-1 \times (14)$
\vdots	\vdots	\vdots
$q-1$	$\binom{n}{q-2}-1 \times (2q+1)$	$\binom{n}{q-2}-1 \times (3q+2)$
q	$\binom{n}{q-1}-1 \times (2q+3)$	$\binom{n}{q-1}-1 \times (3q+5)$

**Figure 4.2** Total number of decision variables vs. RTD of Scenario II.

The GA procedure developed is different from a successive substitution method in three ways: (a) GA works with a coded variable set, not the variables themselves, (b) GA uses the objective profit function to determine the optimized RTD, and (c) GA uses probabilistic transition rules, not deterministic ones.

The successive substitution method discussed in the Section 4.1 is very costly to use to optimize RTD and other decision variables because Scenarios II and IV are combinatory optimization problems. Therefore, GA with the mechanics of natural selection and natural genetics is developed and used to search for the optimal solutions which yield maximum total profit. Note that the studied profit maximization problem is a mixed-integer, non-linear, and constrained optimization problem.

As discussed in the literature review, GA is a stochastic algorithm which mimics the natural phenomena of genetic inheritance and Darwinian strife for survival (Michalewicz, 1999) to search for the optimal solution. Although there are many possible variants of GA, the fundamental concept is based on the Simple Genetic Algorithm (SGA) by Holland (1992). The seminal work introduced by Holland was commonly used as an adaptive approach that provides a randomized, parallel, and global search based on the mechanics of natural selection and genetics to find solutions of a problem. Generally, within a GA operation four major components are involved as discussed below:

1. A criterion for evaluating the performance of a solution. In this study, the maximum total profit is the criterion to determine the optimal RTD.
2. A genetic representation for encoding feasible solutions. An efficient genetic representation needs to accommodate all decision variables and reduce the difficulties of encoding a solution, which is a key component of GA. An efficient data structure can also facilitate the processes of generating new valid solutions and reducing computation time. In this study, the developed integer string is designed to transform the problem of optimizing RTD concerning a distanced-base fare to a GA, which is discussed in Section 4.2.2.

3. A reproduction process to produce offspring solutions. Crossover and mutation operations corresponding to the genetic representations were developed to generate new solutions in the potential solution space, which are discussed in Sections 4.2.3.
4. A constraint checking method to direct the search of feasible solution space is needed to verify the constraints defined in Section 4.2.4.

In general, GA starts with some randomly selected genes as the first generation, called population. Each individual in the population corresponding to a solution in the problem domain is called chromosome. The criterion of an objective function, called fitness function, is used to evaluate the performance of a solution (e.g., total profit) of each chromosome. The chromosomes with higher profit will survive and form the new population of the next generation. Therefore, the equality of the new generation, in terms of profit, is always superior to the one generated in the previous iteration. To recombine a new generation to find the best solution, three operators: reproduction, crossover, and mutation were used. The process is repeated until a predefined condition is satisfied or a constant number of iterations are reached. The predefined condition in this study is the situation when we can eventually reach the maximum total profit.

The developed GA in this study for searching the optimal RTD includes two major operations: RTD generation and genetic operation. To generate all feasible travel distance ranges, each pair of O-D travel distance (L_{ij}) of the service route is selected and sorted in an ascending order. Note that the duplicated O-D travel distances will be eliminated and only a unique O-D travel distance is considered as a feasible boundary.

The developed GA consists of three genetic operators (e.g., reproduction, crossover, and mutation), which incorporate the ideas of survival of the fittest and genetic selection processes, which begins with defining the objective function, numbers of genes,

sizes of population (e.g., population pool), crossover rate, critical value and mutation rate. Then, a step procedure for implementing the genetic operation is performed, which is summarized below and shown in Figure 4.3.

Step 1: Generate a group of random feasible solutions (e.g., RTD, unit fare, and weight factor of unit fare). Then, the GA starts with the initial group of solutions as the first generation, called the population pool.

Step 2: Translate integers into real numbers for each corresponding chromosome. Then, calculate the service headway by using Equation 3.23.

Step 3: Calculate the objective value of total profit for each chromosome.

Step 4: Select the solutions with good performance to reproduce new solutions (i.e., offspring) in accordance with the elitist selection method discussed in Section 4.2.3.

Step 5: Obtain the new generation by recombining the preceding chromosomes (e.g., the solutions selected in Step 4) using crossover and mutation. Thus, a new population pool is formed for the next generation.

Step 6: Apply the constraints discussed in Section 4.2.3 to verify that each new solution satisfies the constraints.

Step 7: Terminate the GA processes and output the optimized solutions if the predefined stop-criteria (e.g., maximum iterations or maximum total profit) are reached. Otherwise terminate. Repeat Steps 1 to 6 until a predefined condition is satisfied, or a constant number of iterations is reached.

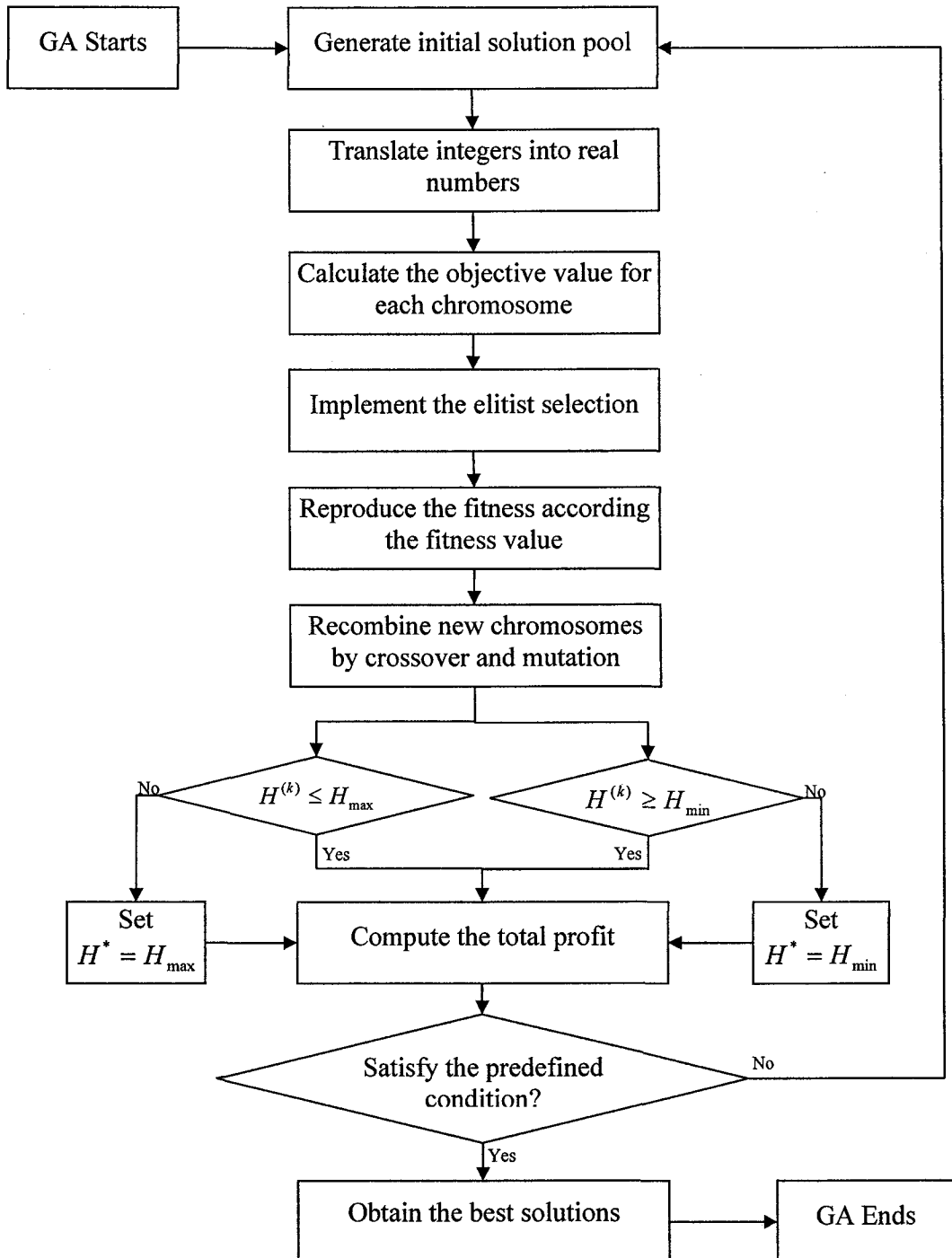


Figure 4.3 Flow chart of the developed Genetic Algorithm.

4.2.2 Encoding and Decoding Schemes

This section introduces the encoding and decoding scheme of the genetic representation. The procedures of reproduction, crossover and mutation as well as the constraint handling method are discussed in Sections 4.2.3 and 4.2.4, respectively. To apply GA to the studied profit maximization problems, a chromosome, denoted as G , consisting of three parts of genes is encoded as shown in Figure 4.4. An integer string consisting of a series of cells is designed to represent various travel distance ranges, denoted as Part 1, the corresponding unit fares, denoted as Part 2, and weight factors of unit fare, denoted as Part 3.

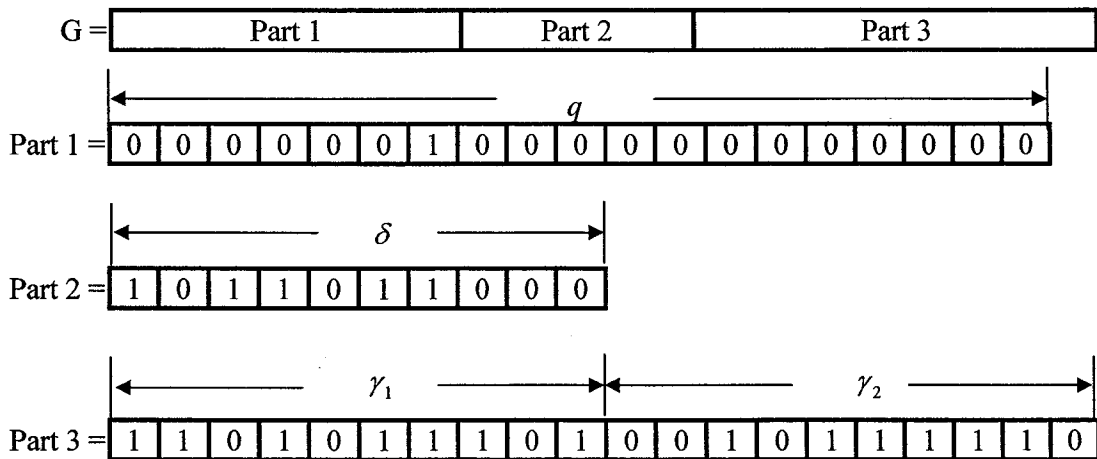


Figure 4.4 Encoding scheme of a chromosome representation.

In Part 1, an integer attribute is assigned to define the genes corresponding to each unique pair of O-D travel distance (L_{ij}) by ascending order, while “1” represents that the boundary of RTD is selected and “0” represents that it is not selected. An integer attribute,

denoted as g_k , is assigned to define the boundary of RTD is selected or not, as indicated in Equation 4.12.

$$g_k = \begin{cases} 1, & \text{the boundary of RTD is selected;} \\ 0, & \text{the boundary of RTD is not selected.} \end{cases} \quad (4.12)$$

The genes decoded in Parts 2 and 3 correspond to the value of unit fare (δ) and the weight factor of unit fare ($\gamma_{z_{ij}}$), respectively. Note that the unit fare is represented by a binary string with ten-digit genes in Part 2. In Part 3, each set of ten-digit genes corresponds to $\gamma_{z_{ij}}$ is also represented by the binary string, while z varies between 1 and the optimal number of RTD denoted as q^* . Therefore, the total number of genes in Part 3 is $(10 \times q)$. In Figure 4.4, the number of genes in Part 1 for single and multiple time periods are consistent, however, they are doubled in Parts 2 and 3 when both the peak and off-peak periods are considered.

For example, the studied transit route having seven stations and 19 unique O-D pairs of travel distance (e.g., excluding two duplicated pairs of travel distance) is illustrated in an ascending order in the first column of Table 4.3, while the gene is decoded as “1” or “0” in the second column with corresponding to each travel distance. The integer attribute ($g_k, k=1,2,\dots,19$) of this example is (0000000100000000000). Note that “1” represents that the boundary of RTD is selected and “0” represents that it is not selected. Therefore, the example indicated that the boundary of RTD locates at O-D travel distance of 58.8 mile, and two RTD between the range of $0 \leq L_{ij} \leq 58.8$ and $58.8 < L_{ij} \leq 211.9$ are assigned and shown in the third column of Table 4.3.

Table 4.3 Usage of the Genes in Part 1

Travel Distance Range (mile)	Genes	RTD
0	0	z = 1
18.8	0	
22.5	0	
39.5	0	
41.3	0	
53.8	0	
58.1	0	
58.8	1	
77.5	0	
93.1	0	
100.0	0	
111.9	0	
112.5	0	
131.3	0	
151.9	0	
153.8	0	
170.6	0	
189.4	0	
193.1	0	
211.9	0	

The unit fare (δ) is encoded in Part 2 of the chromosome as shown in Figure 4.4. The unit fare is defined as a real number in the range of (0~1), and it can be decoded based on the binary ten-digit genes illustrated in the first row of Table 4.4. The value (e.g., third row) represented in Table 4.4 is calculated by multiplying each binary gene, denoted as g_k , and factor, denoted as 2^{k-1} , where g_k is the value of k^{th} gene and $k=1,2,\dots,10$. For instance, the representation of the ten-digit genes (1011011000) can be translated into real numbers of unit fare by using Equation 4.13.

Table 4.4 Representation of the genes in Part 2

1	Genes (g_k)	1	0	1	1	0	1	1	0	0	0	Total
2	Factor (2^{k-1})	2^0	2^1	2^2	2^3	2^4	2^5	2^6	2^7	2^8	2^9	1023
3	Value ($g_k \times 2^{k-1}$)	1	0	4	8	0	32	64	0	0	0	110

$$\delta = \frac{\sum_{k=1}^{10} g_k \times 2^{(k-1)}}{\sum_{k=1}^{10} 2^{(k-1)}} \quad (4.13)$$

where g_k is the value of k^{th} gene and k varies from 1 to 10.

The weight factor of unit fare ($\gamma_{z_{ij}}$) is encoded in the Part 3 of the chromosome as shown in Figure 4.4. The maximum number of 19 possible boundaries is considered to determine the optimal RTD in this study. Therefore, a total number of 190 and 380 genes are designed to determine the value of weight factor for single (e.g., Scenario II) and multiple (e.g., Scenario IV) time periods, respectively. The $\gamma_{z_{ij}}$ for each RTD can be calculated based on the binary string of ten-digit genes and translate into real numbers. While considering that the elasticity parameter of fare ($E_{F_{ij}}$) varies with distance between an O-D pair, the maximum profit is reached by sorting the $\gamma_{z_{ij}}$ in a descending order with $\gamma_{z_{ij}} = 1$ in the longest travel distance.

$\gamma_{z_{ij}}$ is defined as a real number between 1 and 2, and it can be decoded based on the ten-digit genes illustrated in Table 4.5 for two RTD. The value of each travel distance range (z_{ij}) is calculated by multiplying each binary gene, denoted as $g_{k_{z_{ij}}}$, and factor, denoted as 2^{k-1} , where $g_{k_{z_{ij}}}$ is the value of the k^{th} gene at travel distance range (z_{ij}), and

k varies between 1 and 10. The calculated values for each z_{ij} are sorted by a descending order, and $\gamma_{z_{ij}}$ for each z_{ij} can be formulated in Equation 4.14. An example indicated in Table 4.5 represents two sets of genes, γ_1 (1101011101) and γ_2 (0010111111), which can be translated into real numbers by using Equation 4.14.

Table 4.5 Representation of the Genes in Part 3

z=1												
1	Genes ($g_{k_{z_{ij}}}$)	0	0	1	0	1	1	1	1	1	1	Total
2	Factor (2^{k-1})	2^0	2^1	2^2	2^3	2^4	2^5	2^6	2^7	2^8	2^9	1023
3	Value ($g_{k_{z_{ij}}} \times 2^{k-1}$)	0	0	4	0	16	32	64	128	256	512	1012
z=2												
1	Genes ($g_{k_{z_{ij}}}$)	1	1	0	1	0	1	1	1	0	1	Total
2	Factor (2^{k-1})	2^0	2^1	2^2	2^3	2^4	2^5	2^6	2^7	2^8	2^9	1023
3	Value ($g_{k_{z_{ij}}} \times 2^{k-1}$)	1	2	0	8	0	32	64	128	0	512	747

$$\gamma_{z_{ij}} = 1 + \frac{\sum_{k=1}^{10} g_{k_{z_{ij}}} \times 2^{k-1} - \min\{\sum_{k=1}^{10} g_{k_{z_{ij}}} \times 2^{k-1}\}}{1023 - \min\{\sum_{k=1}^{10} g_{k_{z_{ij}}} \times 2^{k-1}\}} \quad (4.14)$$

where $g_{k_{z_{ij}}}$ is the value of k^{th} gene at travel distance range (z_{ij}) and $k=1,2,\dots,10$. Note

that $\min\{\sum_{k=1}^{10} g_{k_{z_{ij}}} \times 2^{k-1}\}$ is retrieved from the minimum value of the descending order.

4.2.3 Reproduction, Crossover, and Mutation

The performance of each solution is evaluated by a fitness function (i.e., total profit). For profit maximization problems, the solution with a higher total profit is identified as a

better solution with greater probability to be selected to reproduce new solutions in the next generation. A straightforward GA selection method is used to insure that the new generation is produced based on the chromosomes having superior evaluation values in the current generation. Note that in each generation, the new population is generated by the operations of reproduction, crossover, and mutation. The size of the new population is the same as the size of the population in previous generations.

During the processes of reproduction, the classic genetic operators (i.e., crossover and mutation) are adopted to produce new solutions by altering their parent solutions (i.e., solution strings in a previous population pool). The top 12.5% reproduce excellent chromosomes from the population because of their high qualities (e.g., greater profit). Since GA is a stochastic algorithm, the probabilities of performing the crossover and mutation operations are defined as crossover and mutation ratios, which are pre-determined model parameters. In this study, there are 40 chromosomes in each generation, and the ratios of reproduction, crossover, and mutation are assumed as 0.125, 0.75, and 0.125, respectively. The procedures of crossover and mutation are illustrated in Tables 4.6 and 4.7 for the ten-digit genes of chromosome.

Let R_p , R_M , and R_C denote the ratios of production, mutation, and crossover, respectively. In the beginning, a small R_p and R_M and a large R_C were selected to enable the global search. After certain iterations, decreasing the value of R_C and increasing the values of R_M and R_p can shift the focus to local search if the current generation is better than the old one; otherwise, continuously increase R_C and decrease R_M and R_p to enlarge the range of global search. Note that this property must be satisfied: $R_p + R_M + R_C = 100\%$.

This operation generates chromosomes by exchanging genes from their parents. It is used to gestate better offspring by inheriting good genes (i.e., higher profit in the fitness evaluation) from their parents. The often-used crossovers are one-point, two-point, and multipoint crossovers shown in Table 4.6. The criteria of selecting a suitable crossover depend on the length and structure of chromosomes. In this study, the one and two-point crossovers were adopted in this study by selecting from each part of the chromosome.

Table 4.6 One-Point and Two-Point Crossovers

	One-Point	Point 1		Two-Point	Point1 Point2		
Before Crossover	Chromosome A	1011	010101	Chromosome A	111	010	0011
	Chromosome B	0010	111001	Chromosome B	011	111	1010
After Crossover	Chromosome A	1011	111001	Chromosome A	111	111	0011
	Chromosome B	0010	010101	Chromosome B	011	010	1010

The operation randomly selects a chromosome from the population and change the k^{th} bit. It is used to generate new chromosomes. The mutation is usually performed with a probability p ($0 < p < 1$), meaning that only a portion of the genes in a chromosome will be selected to be mutated. The one and two-point mutations are adopted in this study from each part of the chromosomes shown in Table 4.7.

Table 4.7 One-Point and Two-Point Mutations

	One-Point	Two-Point
Before Mutation	Chromosome A	1011010101
		▲
After Mutation	Chromosome A	1010010101
		▲

The service capacity and fleet size constraints are used to ensure that the route operates at a sufficient capacity to accommodate the design ridership and satisfy the operable fleet size. The optimal service headway calculated by the developed GA is examined by the bounds of maximum headway where the service capacity accommodates the design ridership. The optimal headway can not be smaller than the minimum headway that can be attained. The constraint indicates that if the optimal headway is within the feasible range, then the calculated headway has reached the optimal solution. Otherwise, the optimal headway is limited by the maximum and minimum headway.

4.3 Summary

In this chapter, two solution algorithms were developed to solve the optimization problems discussed in Chapter 3. The successive substitution method (i.e., modified Gauss-Southwell method) is used to optimize differentiated fares and service headways for given RTD in Scenarios I and III. However, a Genetic Algorithm is developed to search for optimal solutions of combinatorial optimization problems in Scenarios II and IV. To search for the optimal number of RTD, the developed GA can be used to calculate the maximum total profit for various combinations of RTD. To demonstrate that the developed solution algorithms are applicable in the studied optimization problems, a real-world example of the Taiwan High Speed Rail (THSR) system is discussed in Chapter 5.

CHAPTER 5

CASE STUDY

This chapter demonstrates the applicability of the developed models for various scenarios discussed in Chapter 3 and employs the solution algorithms developed in Chapter 4 to optimize the studied research problems. The system configuration and operation data of a real-world intercity transit system, The Taiwan High Speed Rail (THSR) system, are discussed in Sections 5.1, while the input parameters and optimal results, such as optimized solutions and performance measures for Scenarios I through IV are presented in Sections 5.2 through 5.5, respectively. The findings and comparisons are indicated in Section 5.6. Finally, the sensitive analyses conducted in Section 5.7 focuses on evaluating the impact of decision variables to various indicators, such as profit, revenue, and operator cost.

5.1 The Taiwan High Speed Rail System

The Taiwan High Speed Rail (THSR) is a 212-mile long rail line serving eight stations shown in Figure 5.1, which connects three major cities, Taipei, Taichung, and Kaohsiung, along the west coast of Taiwan. It provides a vital corridor for business and leisure trips. The initial construction of THSR began in March 2000, and the revenue operation commenced in January 2007. It is worth noting that Taipei and Banchiao stations are very close to each other, the demand at both stations is assumed to be concentrated in Taipei in this chapter.

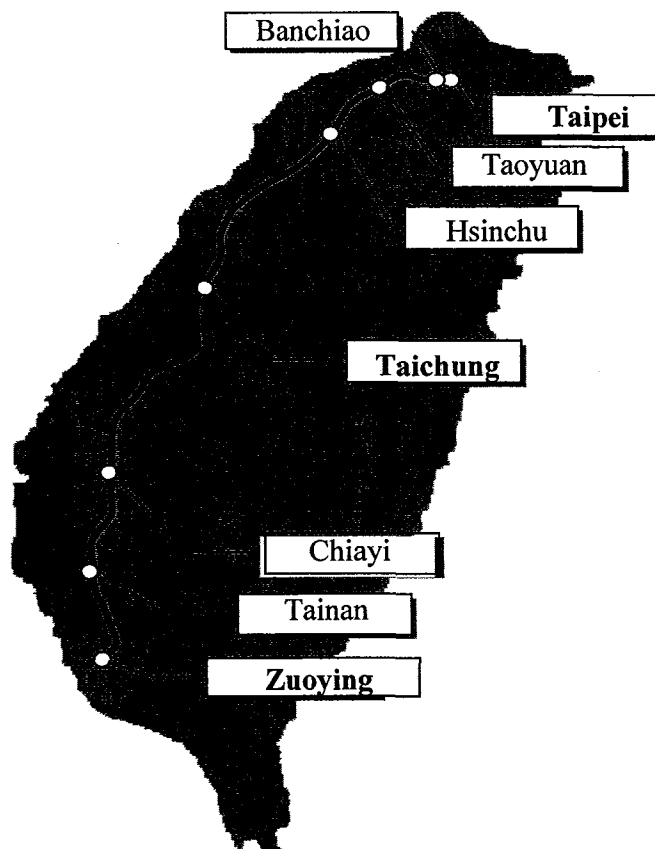


Figure 5.1 Configuration of the Taiwan High Speed Rail line.

The THSR offers better level of service to users, such as shorter travel time and a comfortable and quiet ride. As a public transportation mode, the THSR requires low land occupancy, generates low pollution, and results in drastic energy savings (Su et al. 2007), while carrying a high passenger volume. As indicated in an article published by The New York Times (Bradsher, 2007), one passenger traveling on a fully loaded train will use only one sixth of the energy and generate one-ninth of the carbon dioxide, compared to driving a car. By comparing with a bus ride, only half the energy and a quarter of the carbon

dioxide is used. Thus, the THSR service is welcome by many travelers who originally use automobiles, buses, conventional passenger trains, and air planes.

To demonstrate the applicability of the developed models, all THSR trains are assumed to depart from end terminals and serve every stop along the line. THSR uses the 700 series train (e.g., 700T locomotive), which adopted Japan's Shinkansen technology for the core system and is manufactured by Japanese company. The total THSR fleet includes thirty 12-car trains with capacity of 990 passengers per train. The vehicle operating cost, transit line cost and station cost were obtained from the statistics of six Japanese Rail (JR) passenger railway companies in fiscal year 2004 (Demery, 2006).

The THSR trains are operated at an average speed of 155 mph, whose maximum operating speed is 186 mph. Therefore, a round-trip between the end terminals takes about five hours. During the peak periods, the service frequency is five to six trains per hour with headway less than 12 minutes. The average waiting time is about a half of the headway (e.g., $\beta=0.5$). The station-to-station distance and travel time (including dwell time) between each pair of stations are shown in Table 5.1, in which the numbers at the upper right triangle represent station-to-station distances (in miles), and that at the lower left triangle represent travel times (in hours). The base line values of input parameters for all scenarios are summarized in Table 5.2, and are used to demonstrate the developed models.

Table 5.1 Station-to-Station Distances and Travel Times

D O	Taiepi (1)	Taoyuan (2)	Hsinchu (3)	Taichung (4)	Chiayi (5)	Tainan (6)	Zuoying (7)
Taiepi (1)		[22.5]	[41.3]	[100.0]	[153.8]	[193.1]	[211.9]
Taoyuan (2)	(0.40)		[18.8]	[77.5]	[131.3]	[170.6]	[189.4]
Hsinchu (3)	(0.63)	(0.23)		[58.8]	[112.5]	[151.9]	[170.6]
Taichung (4)	(1.08)	(0.68)	(0.45)		[53.8]	[93.1]	[111.9]
Chiayi (5)	(1.53)	(1.13)	(0.90)	(0.45)		[39.4]	[58.1]
Tainan (6)	(1.88)	(1.48)	(1.25)	(0.80)	(0.35)		[18.8]
Zuoying (7)	(2.17)	(1.77)	(1.53)	(1.08)	(0.63)	(0.28)	

Source: a. Taiwan High Speed Rail Website, 2006 (<http://www.thsrc.com.tw/>)

b. []: Station-to-station distance in miles; (): Travel time in hours

Table 5.2 Baseline Values of Input Parameters for All Scenarios

Variables	Descriptions	Baseline Values
B	Capacity of train includes seats	990 pass./train
c_o	Vehicle operating cost	420 \$/train-hour
c_L	Transit line cost	67 \$/mile-hour
c_s	Station operation cost	341 \$/station-hour
$d_{z_{ij}}$	Boundary distance between RTD z_{ij} and $z_{ij} + l$	To be determined
d_s	Boundary distance between RTD s and m	65 miles
d_m	Boundary distance between RTD m and l	155 miles
d_l	Boundary distance at RTD l	212 miles
D^P	Duration of peak period	6 hours
D^{OP}	Duration of off-peak period	9 hours
$E_{F_{ij}}$	Elasticity parameter of fare from station i to j	Table 5.5
E_{F_s}	Elasticity parameter of fare for short distance trip	0.033
E_{F_m}	Elasticity parameter of fare for medium distance trip	0.013
E_{F_l}	Elasticity parameter of fare for long distance trip	0.008
E_W	Elasticity parameter of wait time	0.200
E_I	Elasticity parameter of in-vehicle time	0.075
L	Length of the THSR line	212 miles
L_{ij}	Distance from station i to j	Miles (Table 5.1)
N'	Operable fleet size	30 vehicles
n	Number of stations	7 stations
$t_{I_{ij}}$	Average in-vehicle time from station i to j	Hours (Table 5.1)
T_R	Round-trip travel time considering terminal time	5.0 hours
T_V	Round-trip time	4.33 hours
T_T	Terminal time	0.67 hours
Y_{ij}	Potential demand from station i to j	pass./hour (Table 5.3)
Y_{ij}^P	Potential demand from station i to j for peak period	pass./hour (Table 5.15)
Y_{ij}^{OP}	Potential demand from station i to j for off-peak period	pass./hour (Table 5.16)
β	Ratio of average waiting time to headway	0.5

5.2 Fixed RTD and Single Time Period – Scenario I

The potential hourly O-D travel demand was predicted by MVA Hong Kong Ltd. in 2005, as shown in Table 5.3, considering the demand shifting from other competing transportation modes (e.g., airplanes, buses, conventional trains, automobiles, etc.) after the start of THSR's operations. The potential O-D demand matrix given in Table 5.3 is calculated based on the highest peak hour demand from outbound and inbound trips.

Table 5.3 Potential Demand in Passengers per Hour

O \ D	(1)	(2)	(3)	(4)	(5)	(6)	(7)	Total
(1)		997	863	1,476	938	579	968	5,821
(2)	596		141	140	42	26	37	981
(3)	1,378	300		475	215	123	170	2,661
(4)	2,306	397	771		506	271	647	4,897
(5)	1,008	150	236	798		233	500	2,925
(6)	619	90	135	441	366		700	2,351
(7)	1,038	127	171	699	787	424		3,247
Total	6,945	2,061	2,316	4,028	2,854	1,656	3,021	22,882

Source: Demand Forecast Report, MVA Hong Kong Ltd., 2005

The demand considered in this chapter is a function of fare and service quality (e.g., travel time and wait time). In Scenario I, the elasticity parameter of wait time, denoted as E_w , and elasticity parameter of in-vehicle time, denoted as E_t , are given as 0.20 and 0.075, respectively, while RTD is classified into three categories: short distance trips (0 ~ 65 miles and $z_{ij}=s$), medium distance trips (66 ~ 155 miles and $z_{ij}=m$), and long distance trips (156 ~ 212 miles and $z_{ij}=l$). The corresponding elasticity parameter of

fare, denoted as $E_{F_{xy}}$, for short, medium, and long distance travel is 0.033, 0.013 and 0.008, respectively.

With the baseline model parameters shown in Tables 5.2 and the potential O-D demand of THSR shown in Table 5.3, the distance-based fare and service headway are optimized for maximum total profit. It was found that the maximum hourly profit of \$254,586 is achieved when THSR is operated at a headway of 0.25 hours per train with a unit fare, δ , of \$0.260 per mile, while the optimal weight factors of unit fare for short, medium and long travel ranges, denoted as γ_s and γ_m , and γ_l , are 1.192, 1.117, and 1.000, respectively. Thus, the resulting optimal weighted unit fares for short, medium, and long trips are 0.310 (= 0.260*1.192) \$/mile, 0.290 (= 0.260*1.117) \$/mile, and 0.260 (=0.260*1.000) \$/mile, respectively.

As shown in Table 5.4, the RTD of THSR and corresponding weight factors are indicated with the optimal weighted unit fare and final fares (e.g., the product of the optimal weighted unit fare and associated travel distance) placed in the lower left and upper right triangles, respectively. For instance, the optimal fare of \$55.1 for a long travel range (e.g., between (1) and (7)) is equal to the distance of 211.9 miles multiplied by 0.26 \$/mile. Meanwhile, the optimal fare of \$44.6 and \$12.8 for medium (e.g., between (1) and (5)) and short trips (e.g., between (1) and (3)) are equal to the distance of 153.8 and 41.3 miles multiplied by 0.29 and 0.31 \$/mile, respectively.

Table 5.4 Optimized Fares and Weighted Unit Fares of Scenario I

O \ D	(1)	(2)	(3)	(4)	(5)	(6)	(7)
(1)		[7.0]	[12.8]	[29.0]	[44.6]	[50.2]	[55.1]
(2)	(0.310)		[5.8]	[22.5]	[38.1]	[44.4]	[49.2]
(3)	(0.310)	(0.310)		[18.2]	[32.6]	[44.0]	[44.4]
(4)	(0.290)	(0.290)	(0.310)		[16.7]	[27.0]	[32.4]
(5)	(0.290)	(0.290)	(0.290)	(0.310)		[12.2]	[18.0]
(6)	(0.260)	(0.260)	(0.290)	(0.290)	(0.310)		[5.8]
(7)	(0.290)	(0.290)	(0.260)	(0.290)	(0.310)	(0.310)	

Note: []: Optimal Fare (\$/trip); (): Optimal Weighted Unit Fare (\$/mile);

Legend:  : $z_{ij} = s$  : $z_{ij} = m$  : $z_{ij} = l$

The transit ridership under the optimal operation is shown in Table 5.5, where short, medium and long distance travel are presented. As shown in Table 5.6, the total hourly ridership for all O-D pairs is 11,241 pass./hour, consisting of 5,279 pass./hour (46.91%), 4,358 pass./hour (38.73%), and 1,616 pass./hour (14.36%) falling in the short, medium and long travel ranges, respectively. The resulting total revenue of 279,672 \$/hour was yield by 58,854 \$/hour (21.04%), 137,370 \$/hour (49.12 %) and 83,448 \$/hour (29.84%) for short, medium and long distance trips.

The Revenue per Passenger-Mile (RPM) and Revenue per Seat-Mile (RSM) are equal to the revenue divided by the total passenger-miles and seat-miles traveled for each RTD. The results indicate that the highest RPM and RSM are both achieved by short distance travelers (see Table 5.6), while the overall RPM and RSM are \$0.28 and \$0.17, respectively. Meanwhile, an overall Profit per Passenger-Mile (PPM) of \$0.26 and Profit per Seat-Mile (PPS) of \$0.15 as well as a Cost (from operator cost) per Passenger-Mile (CPM) of \$0.03 and a Cost per Seat-Mile (CSM) of \$0.01 are obtained.

Table 5.5 Ridership under Optimal Operation of Scenario I

O \ D	(1)	(2)	(3)	(4)	(5)	(6)	(7)	Total
(1)		725	447	780	273	257	371	2,853
(2)	433		109	90	17	13	17	680
(3)	713	233		167	107	39	88	1,347
(4)	1,218	255	271		204	156	313	2,417
(5)	294	61	117	322		130	172	1,096
(6)	275	47	43	254	204		542	1,365
(7)	398	59	89	338	271	329		1,483
Total	3,332	1,380	1,076	1,950	1,076	924	1,503	11,241

Note: Ridership in Passengers per Hour (pass./hour)

Legend: : $z_{ij} = s$: $z_{ij} = m$: $z_{ij} = l$

Table 5.6 Ridership and Revenue under Optimal Operation of Scenario I

	RTD			Overall
	Short Range	Medium Range	Long Range	
Ridership (pass./hour)	5,272	4,355	1,614	11,241
Revenue (\$/hour)	58,854	137,370	83,448	279,672
RPM (\$/pass-mi)	0.31	0.29	0.26	0.28
RSM (\$/pass-mi)	0.23	0.16	0.06	0.17

The travel direction from Taipei (1) to Zuoying (7) is defined as, the outbound direction, while the inbound direction is from Station (7) to (1). In Table 5.7, the link and average load factors for outbound and inbound services were calculated. It was found that the most congested segment occurs in the inbound direction from Station (3) to (2), whose load factor is 0.90, while the lowest occupancy segment is at the inbound direction from Station (7) to (6), whose load factor is 0.37. The average load factors for outbound and inbound trips are 0.51 and 0.66, respectively.

Table 5.7 Load Factor under Optimal Operation of Scenario I

	Station-to-Station Link						
	(1)-(2)	(2)-(3)	(3)-(4)	(4)-(5)	(5)-(6)	(6)-(7)	(1)-(7)
Load Factor (Outbound)	0.72	0.60	0.56	0.47	0.39	0.38	0.51
Load Factor (Inbound)	0.84	0.90	0.79	0.58	0.50	0.37	0.66

5.3 Variable RTD and Single Time Period – Scenario II

The potential O-D demand matrix used in Scenario II is taken from Table 5.3. The elasticity parameters of wait time (E_w) and in-vehicle time (E_I) are also the same as those used in Scenario I, but the elasticity parameters of fare (E_{F_y}) considered here are varying with O-D pairs. Assume that the elasticity parameter of fare is affected by trip length (See Table 5.8), E_{F_y} decreases as travel distance increases.

Table 5.8 Elasticity Parameter of Fare of Scenario II

O \ D	(1)	(2)	(3)	(4)	(5)	(6)	(7)
(1)		0.029	0.025	0.015	0.010	0.006	0.005
(2)	0.029		0.033	0.017	0.012	0.009	0.007
(3)	0.025	0.033		0.019	0.013	0.011	0.008
(4)	0.015	0.017	0.019		0.023	0.016	0.014
(5)	0.010	0.012	0.013	0.023		0.027	0.021
(6)	0.006	0.009	0.011	0.016	0.027		0.031
(7)	0.005	0.007	0.008	0.014	0.021	0.031	

The studied intercity transit line with seven stations results in different distances for 19 O-D pairs, which can be arranged in an ascending order, as discussed in Section

4.2.2. To maximize profit, the developed GA programmed in C language and compiled by the Borland C++ Builder 2002 Version 6.0 was used to search for the optimal RTD in the combinatorial problem. As discussed in Section 4.2.3, the GA parameters used were a population size of 40, a reproduction rate of 0.125, and ratios of two-point crossover and mutation of 0.75, and 0.125, respectively. The optimization process terminates as 50 generations are completed.

Figure 5.2 shows that the maximum profit varies with the number of RTD, while the greatest profit of 319,419 \$/hr is achieved by seven RTD with as optimized headway of 0.24 hours and unit fare (δ) of 0.31 \$/mile. The weight factors of unit fare (γ_{z_y}) are determined corresponding to the optimized RTD, while the optimized γ_{z_y} for the shortest RTD, denoted as γ_1 , through the longest RTD, denoted as γ_7 , are 1.366, 1.326, 1.216, 1.088, 1.016, 1.002, and 1, respectively. In Figure 5.2, the distance-based fare under one RTD is defined as the fare determined purely based on the distance traveled, while the weight factor of unit fare is equal to one. It was found that the maximum profit is relatively low when it is purely distance-based as opposed to using optimized RTD.

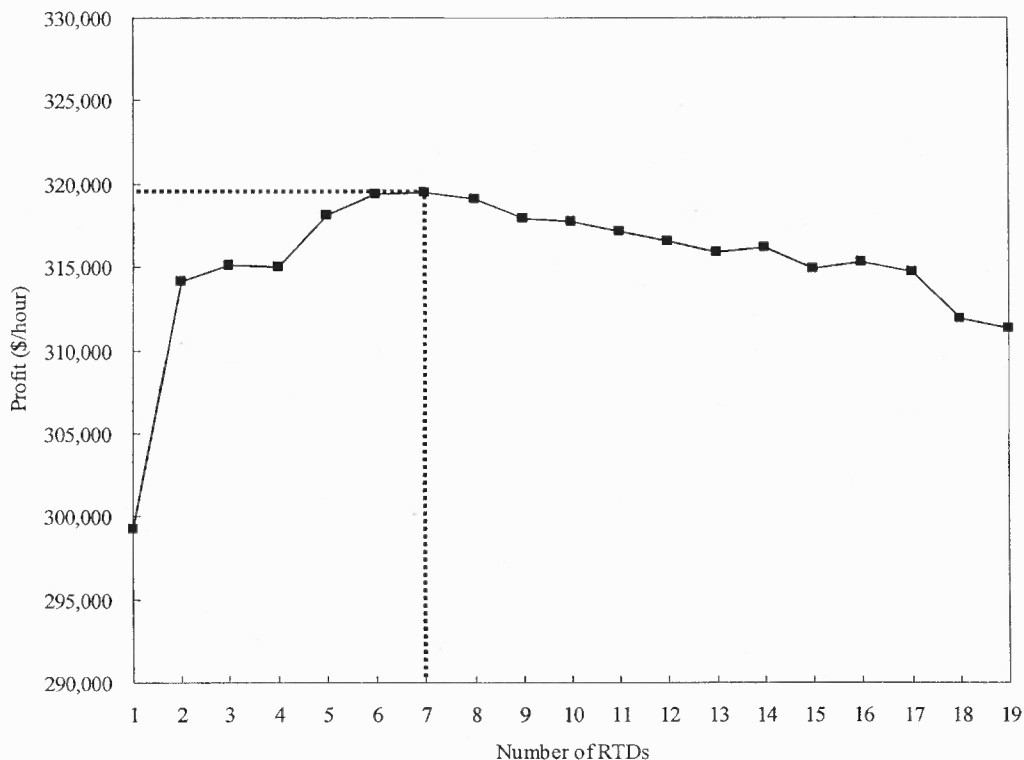


Figure 5.2 Maximum profit vs. number of RTD of Scenario II by GA.

The weighted unit fare is defined as the product of δ and γ_z where $z = 1, 2, \dots, q$. The optimal weighted unit fare and final fares (e.g., the product of the optimal weighted unit fare and associated travel distance) are indicated in the lower left and upper right triangles of Table 5.9, respectively. For instance, the fare between Taipei (1) and Zuoying (7), is the distance of 211.9 miles multiplied by 0.329 \$/mile, and equal to 69.7 \$/trip. The optimal fares in Table 5.9 illustrate that passengers starting from the same station are charged higher fares as the travel distance increases. The resulting ridership for all O-D pairs is shown in Table 5.10. Note that the optimized RTD are presented in Tables 5.9 and 5.10.

Table 5.9 Optimized Fares and Weighted Unit Fares of Scenario II

O \ D	(1)	(2)	(3)	(4)	(5)	(6)	(7)
(1)		[10.1]	[18.0]	[33.4]	[50.7]	[63.5]	[69.7]
(2)	(0.449)		[8.4]	[27.7]	[43.3]	[56.1]	[62.3]
(3)	(0.436)	(0.449)		[23.5]	[37.6]	[50.1]	[56.1]
(4)	(0.334)	(0.358)	(0.400)		[21.5]	[31.1]	[37.4]
(5)	(0.330)	(0.330)	(0.334)	(0.400)		[17.2]	[24.7]
(6)	(0.329)	(0.329)	(0.330)	(0.334)	(0.436)		[8.4]
(7)	(0.329)	(0.329)	(0.329)	(0.334)	(0.424)	(0.449)	

Note: []: Optimal Fare (\$/trip); (:): Optimal Weighted Unit Fare (\$/mile);

Legend: : $z_{ij} = 1$: $z_{ij} = 2$: $z_{ij} = 3$: $z_{ij} = 4$: $z_{ij} = 5$: $z_{ij} = 6$: $z_{ij} = 7$

Table 5.10 Ridership under Optimal Operation of Scenario II

O \ D	(1)	(2)	(3)	(4)	(5)	(6)	(7)	Total
(1)		535	424	600	344	270	462	2,635
(2)	320		80	65	16	10	16	507
(3)	677	171		241	93	42	72	1,296
(4)	937	185	392		233	117	249	2,113
(5)	370	58	102	367		116	227	1,240
(6)	289	34	46	190	182		414	1,155
(7)	496	53	73	269	357	251		1,499
Total	3,089	1,036	1,117	1,732	1,225	806	1,440	10,445

Note: Ridership in Passengers per Hour (pass./hour)

Legend: : $z_{ij} = 1$: $z_{ij} = 2$: $z_{ij} = 3$: $z_{ij} = 4$: $z_{ij} = 5$: $z_{ij} = 6$: $z_{ij} = 7$

The hourly ridership is 10,445 pass./hour, consisting of ridership from seven RTD summarized in Table 5.11, where the RPM and RSM are also indicated. It was found that the highest ridership of 1,775 pass./hour and revenue of 116,993 \$/hour are achieved by the longest RTD between 153.8 and 211.9 miles. However, the highest RPM and RSM

are achieved by the shortest RTD between 0 and 22.5 miles since a great percentage of ridership contributed significantly revenue within short travel distances. The overall RPM and RSM are \$0.35 and \$0.16, respectively. Meanwhile, an overall PPM of \$0.33 and PSM \$0.15 as well as a CPM (from operator cost) of \$0.03 and CSM of \$0.01 are obtained.

Table 5.11 Ridership and Revenue under Optimal Operation of Scenario II

Optimized RTD (mile)	Ridership (pass./hour)	Revenue (\$/hour)	RPM (\$/pass-mi)	RSM (\$/pass-mi)
z=1 (<22.5)	1,771	23,481	0.64	0.21
z=2 (22.6~41.3)	1,399	24,834	0.45	0.08
z=3 (41.4~58.8)	1,817	41,324	0.40	0.08
z=4 (58.9~77.5)	250	6,925	0.34	0.01
z=5 (77.6~112.5)	2,557	87,333	0.33	0.09
z=6 (112.6~153.8)	876	43,725	0.32	0.03
z=7 (153.9~211.9)	1,775	116,993	0.32	0.06
Overall	10,445	344,615	0.35	0.16

In Table 5.12, the link and average load factors for outbound and inbound services are calculated. The most congested segment occurs at the inbound direction from station (3) to (2), whose load factor is 0.66. However, the lowest occupancy segment is at the outbound direction from station (6) to (7), whose load factor is 0.29. The average load factors for the outbound and inbound directions are 0.41 and 0.52, respectively.

Table 5.12 Load Factor under Optimal Operation of Scenario II

	Station-to-Station Link						
	(1)-(2)	(2)-(3)	(3)-(4)	(4)-(5)	(5)-(6)	(6)-(7)	(1)-(7)
Load Factor (Outbound)	0.53	0.46	0.45	0.39	0.32	0.29	0.41
Load Factor (Inbound)	0.62	0.66	0.61	0.47	0.40	0.30	0.52

5.4 Fixed RTD and Multiple Time Periods – Scenario III

The model developed in Scenario III was used to maximize profit, considering multiple time periods of a day for a given RTD. The THSR operates 16 hours per day including 6-hour peak and 10-hour off-peak periods. The potential O-D demand matrix for each time period is shown in Tables 5.13 and 5.14, where the demand for peak periods were calculated by averaging potential demand during the morning peak (6AM to 9AM) and afternoon peak (4PM to 7PM) and the demand for off-peak period was calculated by averaging demand for the rest of the hours. Note that the elasticity parameters of fare (E_{F_z}), wait time (E_w) and in-vehicle time (E_l) have the same values discussed in Scenario I.

Table 5.13 Potential Demand in Passengers per Hour (Peak)

O \ D	(1)	(2)	(3)	(4)	(5)	(6)	(7)	Total
(1)		896	955	1,630	968	632	1,049	6,130
(2)	593		177	176	46	32	47	1,071
(3)	940	383		525	205	122	185	2,360
(4)	1,598	371	526		559	299	607	3,960
(5)	748	103	172	544		258	553	2,378
(6)	475	72	106	301	250		628	1,832
(7)	803	109	143	499	537	422		2,513
Total	5,157	1,934	2,079	3,675	2,565	1,765	3,069	20,244

Source: Demand Forecast Report, MVA Hong Kong Ltd., 2005

Table 5.14 Potential Demand in Passengers per Hour (Off-peak)

O \ D	(1)	(2)	(3)	(4)	(5)	(6)	(7)	Total
(1)		384	347	590	342	211	354	2,228
(2)	433		275	273	80	50	73	1,183
(3)	343	247		191	74	43	65	963
(4)	597	236	192		203	109	220	1,557
(5)	350	62	80	199		94	201	986
(6)	227	42	49	110	91		270	788
(7)	380	61	66	230	196	308		1,242
Total	2,330	1,034	1,009	1,593	986	815	1,182	8,948

Source: Demand Forecast Report, MVA Hong Kong Ltd., 2005

The model developed in Scenario III considers both temporal distance-based fare and service headway. It was found that the maximum profit of 2,410,523 \$/day is achieved by headways of 0.27 and 0.45 hours/train at the optimal unit fare of 0.265 and 0.244 \$/mile and temporal weight factors of unit fare for short and medium travel ranges of 1.36, 1.14 and 1.13, 1.04 for peak and off-peak periods, respectively. Note that γ'_i is equal to 1 in both periods to reduce the number of variables.

In Tables 5.15 and 5.16, the optimal RTD of THSR and the corresponding optimal weighted unit fares in the lower left triangle and optimal fares in the upper right triangle for peak and off-peak periods are indicated. For instance, the optimal peak (off-peak) fare between (1) and (7) of \$56.1 (\$51.6) is equal to the distance of 211.9 miles multiplied by 0.265 (0.244) \$/mile, respectively. Meanwhile, the optimal peak (off-peak) fare for medium RTD (e.g., between (1) and (5)) of \$46.4 (\$39.0) is equal to the distance of 153.8 (41.3) miles multiplied by 0.302 (0.254) \$/mile. The optimal peak (off-peak)

fare for short RTD (e.g., between (1) and (3)) of \$14.9 (\$11.3) is equal to the distance of 41.3 miles multiplied by 0.360 and (0.276) \$/mile.

Table 5.15 Optimized Fares and Weighted Unit Fares of Scenario III (Peak)

O \ D	(1)	(2)	(3)	(4)	(5)	(6)	(7)
(1)		[8.1]	[14.9]	[30.1]	[46.4]	[51.1]	[56.1]
(2)	(0.360)		[6.7]	[23.3]	[39.6]	[45.2]	[50.2]
(3)	(0.360)	(0.360)		[21.2]	[33.9]	[45.0]	[45.8]
(4)	(0.302)	(0.302)	(0.360)		[19.4]	[28.0]	[33.7]
(5)	(0.302)	(0.302)	(0.302)	(0.360)		[14.2]	[21.0]
(6)	(0.265)	(0.265)	(0.302)	(0.302)	(0.360)		[6.7]
(7)	(0.265)	(0.265)	(0.265)	(0.302)	(0.360)	(0.360)	

Note: []: Optimal Fare (\$/trip); (): Optimal Weighted Unit Fare (\$/mile);

Legend: : $z_{ij} = s$: $z_{ij} = m$: $z_{ij} = l$

Table 5.16 Optimized Fares and Weighted Unit Fares of Scenario III (Off-peak)

O \ D	(1)	(2)	(3)	(4)	(5)	(6)	(7)
(1)		[6.1]	[11.3]	[25.3]	[39.0]	[47.0]	[51.6]
(2)	(0.276)		[5.1]	[19.6]	[33.3]	[41.5]	[46.1]
(3)	(0.276)	(0.276)		[16.1]	[28.5]	[38.5]	[41.5]
(4)	(0.254)	(0.254)	(0.276)		[14.7]	[23.6]	[28.4]
(5)	(0.254)	(0.254)	(0.254)	(0.276)		[10.8]	[15.9]
(6)	(0.244)	(0.244)	(0.254)	(0.254)	(0.276)		[5.1]
(7)	(0.244)	(0.244)	(0.244)	(0.254)	(0.276)	(0.276)	

Note: []: Optimal Fare (\$/trip); (): Optimal Weighted Unit Fare (\$/mile);

Legend: : $z_{ij} = s$: $z_{ij} = m$: $z_{ij} = l$

The optimized transit ridership under the optimal operation for peak and off-peak periods are shown in Tables 5.17 and 5.18, in which the hourly ridership for short, medium and long distance trips is indicated.

Table 5.17 Ridership under Optimal Operation of Scenario III (Peak Hour)

O \ D	(1)	(2)	(3)	(4)	(5)	(6)	(7)	Total
(1)		617	426	837	260	276	393	2,809
(2)	408		132	111	18	16	21	706
(3)	420	285		132	98	36	94	1,065
(4)	820	234	132		174	168	283	1,811
(5)	201	40	82	169		126	136	754
(6)	207	37	31	169	122		466	1,032
(7)	301	49	73	233	132	313		1,101
Total	2,357	1,262	876	1,651	804	935	1,393	9,278

Note: Ridership in Passengers per Hour (pass./hour)


Legend:  : $z_{ij} = s$  : $z_{ij} = m$  : $z_{ij} = l$

Table 5.18 Ridership under Optimal Operation of Scenario III (Off-peak Hour)

O \ D	(1)	(2)	(3)	(4)	(5)	(6)	(7)	Total
(1)		289	196	340	125	99	145	1,194
(2)	326		220	186	37	27	35	831
(3)	194	197		80	41	17	35	564
(4)	344	160	81		95	68	118	866
(5)	128	29	44	93		57	83	434
(6)	107	23	19	68	55		215	487
(7)	156	30	36	123	81	245		671
Total	1,255	728	596	890	434	513	631	5,047

Note: Ridership in Passengers per Hour (pass./hour)

Legend:  : $z_{ij} = s$  : $z_{ij} = m$  : $z_{ij} = l$

As shown in Table 5.19, the resulting daily ridership for all O-D pairs is 106,138 pass./day, consisting of 50,210 pass./day (46.7%), 40,196 pass./day (38.2%), and 15,732 pass./day (15.1%) in the short, medium and long travel ranges, respectively. In the meantime, the total revenue of 2,520,448 \$/day was generated by 519,971 \$/day (20.6%), 1,205,724 \$/day (47.9 %) and 794,725 \$/day (31.5%) from short, medium and long distance travelers. It was found that the highest RPM and RSM are both contributed by short distance travelers who constitute the greatest percentage of ridership. The overall RPM and RSM are \$0.28 and \$0.19, respectively. Meanwhile, an overall PPM of \$0.27 and PSM of \$0.19 as well as a CPM (from operator cost) of \$0.012 and CSM of \$0.008 are obtained.

Table 5.19 Ridership and Revenue under Optimal Operation of Scenario III

	RTD			Overall
	Short Range	Medium Range	Long Range	
Ridership (pass./day)	50,210	40,196	15,732	106,138
Revenue (\$/day)	519,971	1,205,724	794,725	2,520,448
RPM (\$/pass-mi)	0.32	0.28	0.26	0.28
RSM (\$/pass-mi)	0.26	0.18	0.07	0.19

In Table 5.20, the link and average load factors for outbound and inbound services are calculated. It was found that the most congested segment occurs at the outbound direction from stations (1) to (2) during the peak hour, whose load factor is 0.71. However, the lowest occupancy segment is at the outbound direction from stations (6) to (7) during the off-peak hour, whose load factor is 0.21. The average load factors for

the outbound direction are 0.51 and 0.33 and for the inbound direction during peak and off-peak periods are 0.47 and 0.33, respectively.

Table 5.20 Load Factor under Optimal Operation of Scenario III

		Station-to-Station Link						
		(1)-(2)	(2)-(3)	(3)-(4)	(4)-(5)	(5)-(6)	(6)-(7)	(1)-(7)
Peak	Load Factor (Outbound)	0.71	0.63	0.58	0.46	0.39	0.35	0.51
	Load Factor (Inbound)	0.60	0.66	0.56	0.40	0.34	0.28	0.47
Off-peak	Load Factor (Outbound)	0.40	0.47	0.39	0.28	0.23	0.21	0.33
	Load Factor (Inbound)	0.42	0.46	0.39	0.29	0.24	0.23	0.33

5.5 Variable RTD and Multiple Time Periods – Scenario IV

The potential O-D demand used for Scenario IV was presented in Tables 5.13 and 5.14. The same elasticity parameters of fare (E_{F_y}), wait time (E_w) and in-vehicle time (E_t) discussed in Scenario II are assumed. Figure 5.3 shows the maximum daily profit varying with the number of RTD. The optimal total profit of 2,979,787 \$/day is achieved by eight RTD. In Figure 5.3, the distance-based fare under one RTD is defined as the fare determined purely based on the distance traveled, while the weight factor of unit fare is equal to one. It was found that the maximum profit is relatively low when it is purely distance-based as opposed to using optimized RTD.

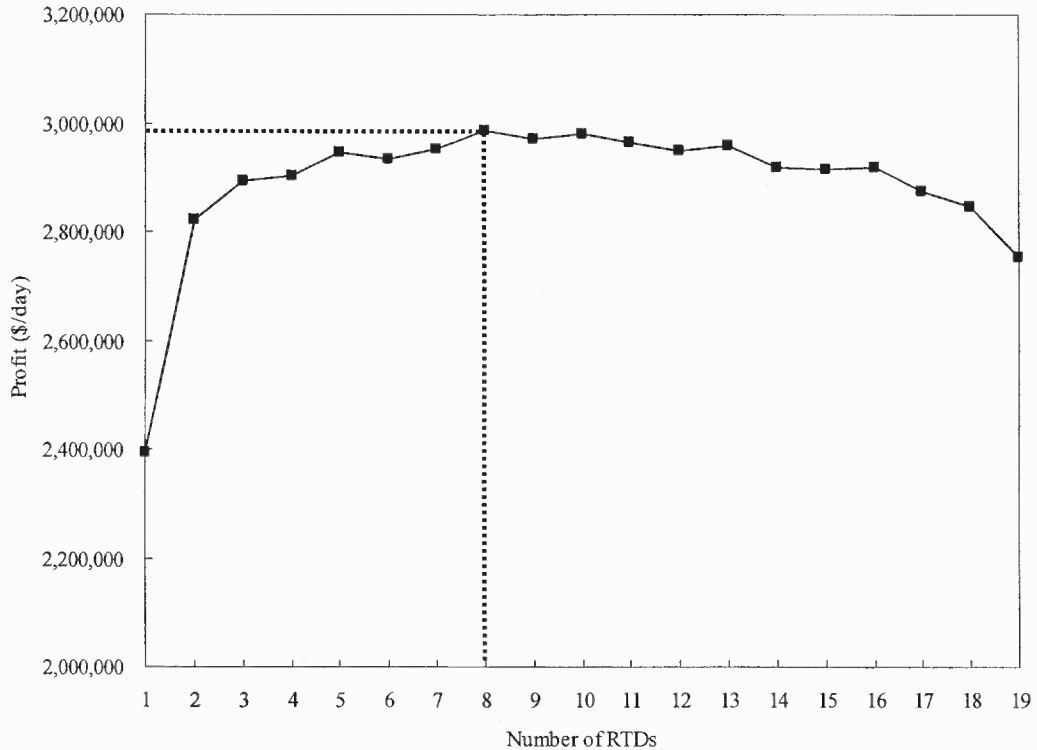


Figure 5.3 Maximum profit vs. number of RTD of Scenario IV by GA.

The maximum profit is achieved when the service is operated at headways of 0.25 and 0.39 hours/train corresponding to optimal unit fares of 0.33 and 0.30 \$/mile for peak and off-peak periods, respectively. The weighted unit fare is defined as the product of δ and γ_z where $z = 1, 2, \dots, q$. The optimized weight factors of unit fares of the optimized RTD are used to calculate the optimal weighted unit fares in the lower left triangle and final fares (e.g., the product of the optimal weighted unit fare and associated travel distance) in the upper right triangle of Tables 5.21 and 5.22 for peak and off-peak periods.

Table 5.21 Optimized Fares and Weighted Unit Fares of Scenario IV (Peak)

D O	(1)	(2)	(3)	(4)	(5)	(6)	(7)
(1)		[10.2]	[18.3]	[35.3]	[51.4]	[64.5]	[70.8]
(2)	(0.489)		[8.5]	[28.6]	[43.9]	[57.0]	[63.3]
(3)	(0.382)	(0.489)		[24.0]	[39.7]	[50.8]	[57.0]
(4)	(0.348)	(0.357)	(0.366)		[22.5]	[33.5]	[39.5]
(5)	(0.333)	(0.333)	(0.333)	(0.382)		[18.0]	[23.7]
(6)	(0.333)	(0.333)	(0.333)	(0.348)	(0.405)		[8.5]
(7)	(0.333)	(0.333)	(0.333)	(0.333)	(0.366)	(0.489)	

Note: []: Optimal Fare (\$/trip); (): Optimal Weighted Unit Fare (\$/mile);

Legend: : $z_{ij} = 1$: $z_{ij} = 2$: $z_{ij} = 3$: $z_{ij} = 4$: $z_{ij} = 5$: $z_{ij} = 6$: $z_{ij} = 7$: $z_{ij} = 8$

Table 5.22 Optimized Fares and Weighted Unit Fares of Scenario IV (Off-Peak)

D O	(1)	(2)	(3)	(4)	(5)	(6)	(7)
(1)		[8.8]	[15.7]	[31.3]	[46.9]	[58.9]	[64.6]
(2)	(0.439)		[7.4]	[26.3]	[40.0]	[52.0]	[57.8]
(3)	(0.384)	(0.439)		[21.1]	[35.2]	[46.3]	[52.0]
(4)	(0.328)	(0.334)	(0.339)		[20.1]	[29.3]	[35.1]
(5)	(0.305)	(0.307)	(0.307)	(0.384)		[15.5]	[20.9]
(6)	(0.305)	(0.305)	(0.305)	(0.328)	(0.351)		[7.4]
(7)	(0.305)	(0.305)	(0.305)	(0.307)	(0.339)	(0.439)	

Note: []: Optimal Fare (\$/trip); (): Optimal Weighted Unit Fare (\$/mile);

Legend: : $z_{ij} = 1$: $z_{ij} = 2$: $z_{ij} = 3$: $z_{ij} = 4$: $z_{ij} = 5$: $z_{ij} = 6$: $z_{ij} = 7$: $z_{ij} = 8$

The optimized transit ridership under optimal operation for peak and off-peak periods are shown in Tables 5.23 and 5.24, in which the daily ridership for various O-D with optimized RTD of index (z_{ij}) are indicated.

Table 5.23 Ridership under Optimal Operation of Scenario IV (Peak)

O \ D	(1)	(2)	(3)	(4)	(5)	(6)	(7)	Total
(1)		593	460	614	347	290	494	2,798
(2)	392		122	79	17	12	19	641
(3)	453	264		261	83	41	77	1,179
(4)	602	167	261		244	117	214	1,605
(5)	268	39	69	237		123	244	980
(6)	218	26	36	118	119		441	958
(7)	378	45	60	176	237	296		1,192
Total	2,311	1,134	1,008	1,485	1,047	879	1,489	9,353

Note: []: Optimal Fare (\$/trip); (): Optimal Weighted Unit Fare (\$/mile);

Legend: : $z_{ij} = 1$: $z_{ij} = 2$: $z_{ij} = 3$: $z_{ij} = 4$: $z_{ij} = 5$: $z_{ij} = 6$: $z_{ij} = 7$: $z_{ij} = 8$

Table 5.24 Ridership under Optimal Operation of Scenario IV (Off-peak)

O \ D	(1)	(2)	(3)	(4)	(5)	(6)	(7)	Total
(1)		269	189	257	138	104	178	1,135
(2)	303		200	133	34	20	33	723
(3)	187	179		105	34	17	30	552
(4)	260	115	106		100	50	91	722
(5)	141	26	37	98		51	101	454
(6)	112	17	19	50	49		199	446
(7)	191	27	30	96	98	227		669
Total	1,194	633	581	739	453	469	632	4,701

Note: []: Optimal Fare (\$/trip); (): Optimal Weighted Unit Fare (\$/mile);

Legend: : $z_{ij} = 1$: $z_{ij} = 2$: $z_{ij} = 3$: $z_{ij} = 4$: $z_{ij} = 5$: $z_{ij} = 6$: $z_{ij} = 7$: $z_{ij} = 8$

The daily ridership for all O-D pairs is 103,128 pass./hour, consisting of ridership from seven RTD summarized in Table 5.25, where the RPM and RSM are also indicated. It was found that the ridership within the shortest (e.g., < 22.5 mile) and longest (e.g.,

131.4~211.9 mile) travel ranges is relatively higher than that of others RTD. The highest revenue of 1,464,895 \$/day is achieved by the RTD between 131.4 and 211.9 miles. However, the highest RPM of \$0.44 and RSM of \$0.31 are achieved by RTD of less than 22.5 miles, while the overall RPM and RSM are \$0.34 and \$0.22, respectively. Meanwhile, an overall PPM of \$0.33 and PSM of \$0.21 as well as a CPM of \$0.013 and CSM of \$0.009 are obtained.

Table 5.25 Average Revenue under Optimal Operation of Scenario IV

Optimized RTD (mile)	Ridership (pass./day)	Revenue (\$/day)	RPM (\$/pass-mi)	RSM (\$/pass-mi)
z=1 (<22.5)	26,418	243,584	0.44	0.31
z=2 (22.6~39.5)	2,452	40,942	0.43	0.02
z=3 (39.6~53.8)	14,104	262,591	0.41	0.09
z=4 (53.9~58.8)	10,118	228,502	0.39	0.06
z=5 (58.9~77.5)	3,956	107,714	0.35	0.02
z=6 (77.6~100.0)	14,876	494,727	0.34	0.09
z=7 (100.1~131.3)	6,768	259,087	0.33	0.03
z=8 (131.4~211.9)	24,436	1,464,895	0.32	0.13
Overall	103,128	3,102,041	0.34	0.22

In Table 5.26, the link and average load factors for outbound and inbound services are calculated. It was found that the most congested segment occurs at the outbound direction from stations (1) to (2) during the peak hour, whose load factor is 0.72. However, the lowest occupancy segment is at the outbound direction from stations (6) to (7) during the off-peak hour, whose load factor is as 0.20. The average load factors for outbound trips during peak and off-peak periods are 0.54 and 0.29, and for inbound trips during peak and off-peak periods are 0.48 and 0.30.

Table 5.26 Load Factor under Optimal Operation of Scenario IV

		Station-to-Station Link						
		(1)-(2)	(2)-(3)	(3)-(4)	(4)-(5)	(5)-(6)	(6)-(7)	(1)-(7)
Peak	Load Factor (Outbound)	0.72	0.64	0.60	0.51	0.43	0.39	0.54
	Load Factor (Inbound)	0.60	0.64	0.56	0.44	0.37	0.31	0.48
Off-peak	Load Factor (Outbound)	0.36	0.40	0.34	0.26	0.22	0.20	0.29
	Load Factor (Inbound)	0.37	0.40	0.34	0.27	0.22	0.22	0.30

5.6 Optimal Results Comparison

The results of the optimization model such as profit, ridership, fare, and load factor obtained from previous sections for Scenarios I through IV are compared and discussed in this section. The optimized results generated from Scenarios I and II are shown in Table 5.27. The difference in Table 5.27 is the optimal values of Scenario II minus those of Scenario I. By comparing the profit for single time period with fixed and variable RTD respectively, the maximum hourly profit achieved by the optimized seven RTD of Scenario II is about 25% more than that with the fixed RTD of Scenario I, while the optimized service headway of Scenario II is shorter than that of Scenario I, but very close. However, the ridership under the optimized fare setting of Scenario II is 8% less than that of Scenario I because of higher fares. The comparison of the optimal fares for each O-D pair between Scenarios I and II is shown in Figure 5.4.

Table 5.27 Optimized Results of Scenarios I and II

Optimal Results \ Scenarios	Scenario I	Scenario II	Difference
Unit Fare (\$/mile)	0.26	0.33	0.07
Headway (hours)	0.25	0.23	-0.02
Ridership (pass./hour)	11,241	10,445	-796
Number of RTD	3	7	4
Revenue (\$/hour)	279,672	344,615	64,943
Operator Cost (\$/hour)	25,086	25,196	110
Profit (\$/hour)	254,586	319,419	64,833

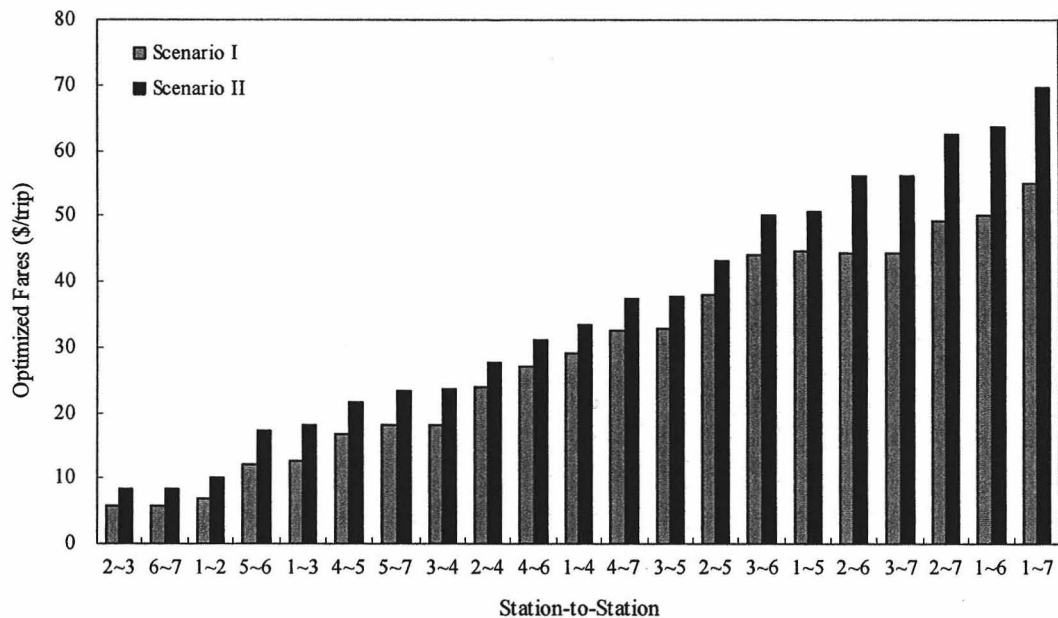


Figure 5.4 Optimized fares of Scenarios I and II.

The load factors for outbound and inbound services at each station link between Taiepi (1) and Zuoying (7) of Scenarios I and II are illustrated in the top and bottom of Figure 5.5, respectively. The load factors between the first four stations (e.g., (1)-(2), (2)-(3), (3)-(4)) for both outbound and inbound trips are all greater than the average load factors. It was also found that the load factors of Scenario I are greater than those of

Scenario II because that there are less fleet size (e.g., number of vehicles) and more ridership of Scenario I.

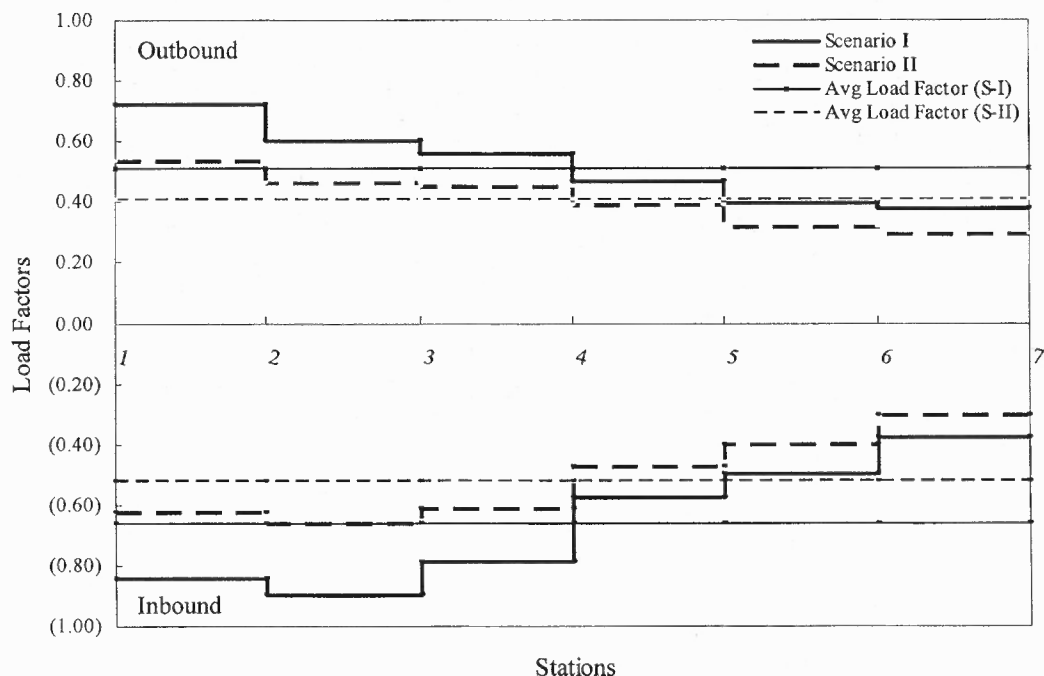


Figure 5.5 Load factor under optimal operation of Scenarios I and II.

The optimized results of the ridership, profit, temporal distance-based fare and service headway generated from Scenarios III and IV are shown in Table 5.28. The difference in Table 5.28 is the optimal values of Scenario IV minus those of Scenario III. By comparing the profit for multiple time periods with fixed and variable RTD, the maximum daily profit achieved of Scenario IV is about 24% more than that with the fixed RTD of Scenario III, while the optimized service headways during peak and off-peak periods of Scenario IV are both shorter than that of Scenario III. However, the ridership under the optimized fare setting of Scenario IV is only 3% less than that of Scenario III because of higher fares. The comparison of optimal differentiated fares in

each O-D pair is shown in Figure 5.6. It was found that optimal fares during peak and off-peak periods under optimized RTD are generally higher than those of Scenario III.

Table 5.28 Optimized Results of Scenarios III and IV

Optimal Results		Scenario III	Scenario IV	Difference
Headway (hours)	Peak	0.27	0.25	-0.02
	Off-peak	0.45	0.39	-0.06
Unit Fare (\$/mile)	Peak	0.27	0.33	0.06
	Off-peak	0.24	0.30	0.06
Ridership (pass./day)		106,138	103,128	-3,010
Number of RTD		3	8	5
Revenue (\$/day)		2,520,448	3,102,041	581,593
Operator Cost (\$/day)		109,925	122,254	12,329
Profit (\$/day)		2,410,523	2,979,787	569,264

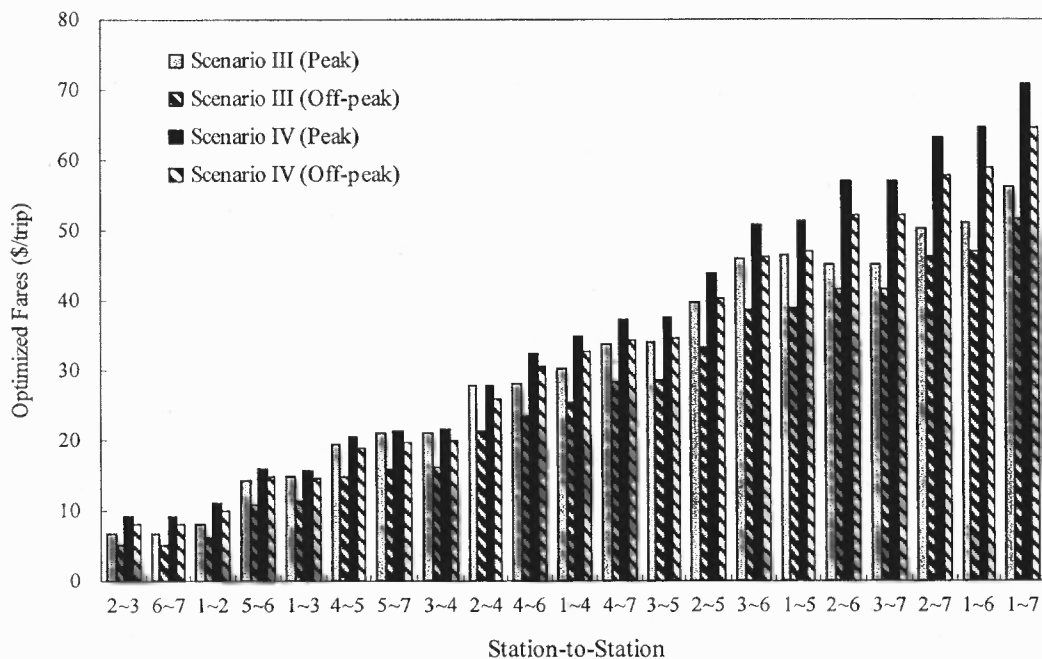


Figure 5.6 Optimized fares of Scenarios III and IV.

The load factors for outbound and inbound services at each station link between Taiepi (1) and Zuoying (7) of Scenarios III and IV are illustrated in the top and bottom of Figure 5.7, respectively. Similar to the result indicated for Scenarios I and II, the load factors between the first four stations (e.g., (1)-(2), (2)-(3), (3)-(4)) for both outbound and inbound trips are all greater than the average load factors. It was found that the load factors for outbound and inbound services between stations (2) and (3) have a relatively high ridership during the off-peak hour. As shown in Figure 5.7, the load factors for both outbound and inbound services are very close of Scenarios III and IV during the peak hour, which also implied that the distributions of ridership are very similar. Therefore, the distribution of ridership on each segment is not affected by the optimized RTD in this study.

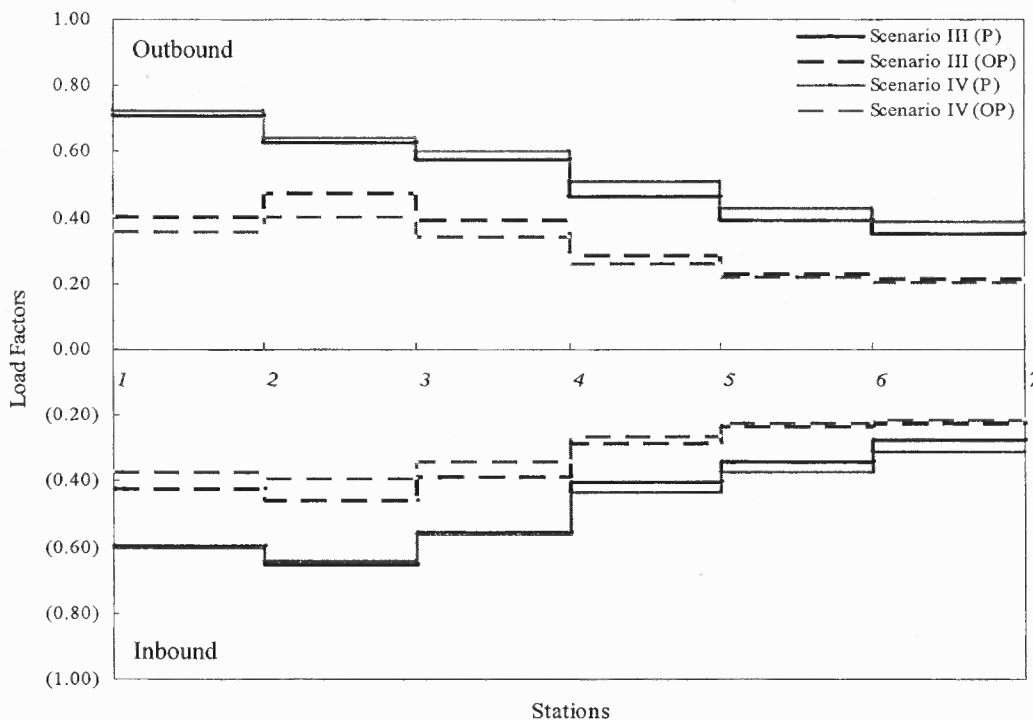


Figure 5.7 Load factor under optimal operation of Scenarios III and IV.

The optimal RTD for each scenario are identical in Figure 5.8. Note that the RTD are fixed in Scenarios I and III, and the optimal number of RTD for Scenarios II and IV are seven and eight, respectively. For example, the optimized RTD in Scenario II are classified into seven ranges, indicating $z = 1$ (0~22.5 miles), $z = 2$ (22.6~41.3 miles), $z = 3$ (41.4~58.8 miles), $z = 4$ (58.9~77.5 miles), $z = 5$ (77.6~112.5 miles), $z = 6$ (112.6~153.8 miles), and $z = 7$ (153.9~211.9 miles).

Travel Distance (miles)	Scenario I	Scenario II	Scenario III	Scenario IV		
$0 < L_{ij} \leq 18.8$	[Solid Black]	[Solid Black]	[Solid Black]	[Solid Black]		
$18.8 < L_{ij} \leq 22.5$						
$22.5 < L_{ij} \leq 39.4$						
$39.4 < L_{ij} \leq 41.3$		[Solid Black]		[Solid Black]		
$41.3 < L_{ij} \leq 53.8$						
$53.8 < L_{ij} \leq 58.1$		[Solid Black]		[Solid Black]	[Solid Black]	
$58.1 < L_{ij} \leq 58.8$						
$58.8 < L_{ij} \leq 77.5$		[Solid Black]		[Dark Gray]	[Light Gray]	
$77.5 < L_{ij} \leq 93.1$				[Medium Gray]	[White]	
$93.1 < L_{ij} \leq 100.0$		[Solid Black]		[Medium Gray]	[White]	[White]
$100.0 < L_{ij} \leq 111.9$						
$111.9 < L_{ij} \leq 112.5$		[Solid Black]		[Medium Gray]	[White]	[Diagonal Lines]
$112.5 < L_{ij} \leq 131.3$						
$131.3 < L_{ij} \leq 151.9$		[Solid Black]		[Medium Gray]	[White]	[Cross-hatch]
$151.9 < L_{ij} \leq 153.8$						
$153.8 < L_{ij} \leq 170.6$		[Solid Black]		[Diagonal Lines]	[Solid Black]	[Cross-hatch]
$170.6 < L_{ij} \leq 189.4$						
$189.4 < L_{ij} \leq 193.1$	[Solid Black]	[Diagonal Lines]	[Solid Black]	[Cross-hatch]		
$193.1 < L_{ij} \leq 211.9$						
Number of RTD	3	7*	3	8*		

* RTD is optimized

Figure 5.8 Optimized numbers and RTD of Scenarios I through IV.

In Scenario I, the model was tested by substituting various sets of nonzero initial values of the decision variables, and the same results were obtained. Therefore, the model has the flexibility and capability to achieve convergence of the decision variables to the same optimal values in a few iterations. Furthermore, the same optimal solution is reached when the decision variables are given any positive initial values that are very unreasonable (i.e., 20 hour initial headway, 30 \$/mile initial unit fare, etc.). Many sets of initial decision variables were used to test the optimality of the model. It was found that all sets of initial values achieve the same maximum total profit as shown in Figure 5.9. The concavity test of the total profit function was also conducted by evaluating the values of the 2nd derivative of the objective function with respect to each decision variable and the Hessian Matrix. It was found that the objective profit function is not strictly concave; therefore, the maximized profit from the optimal results may not be the global maximum.

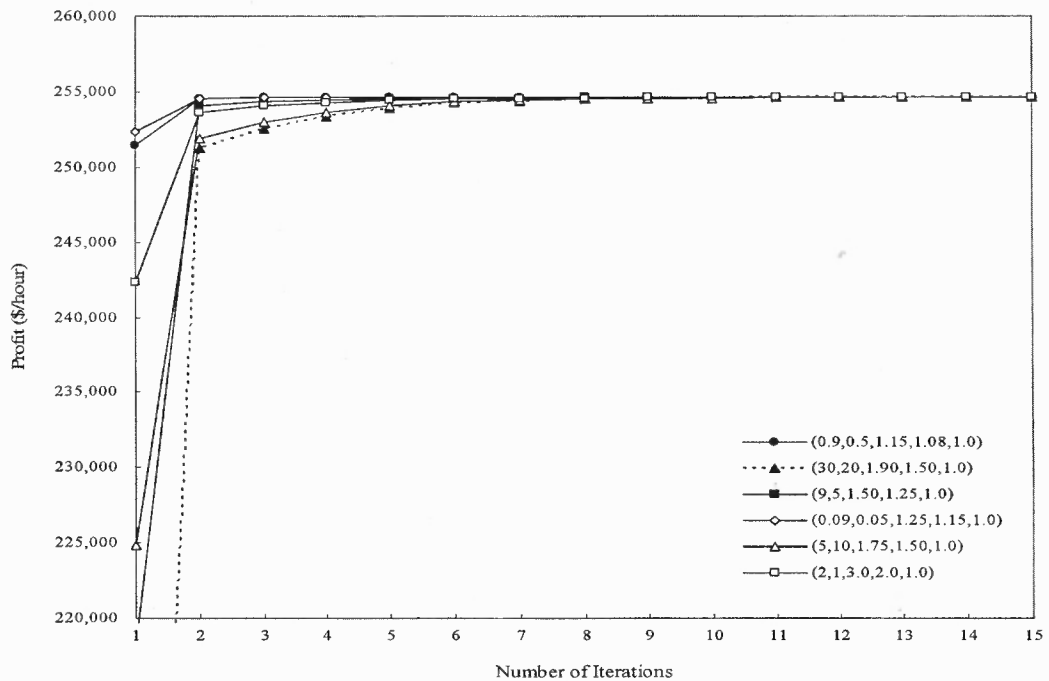


Figure 5.9 Profit achieved in each iteration of Scenario I.

To compare the results solved by the developed solution algorithms in Chapter 4, the comparison between profits, headways, unit fares, and weight factor of unit fare can be observed in Table 5.29, which shows that the maximum profit achieved by the heuristic GA is close to that from the successive substitution method. Therefore, the developed GA was used to confidently solve the combinatorial fare RTD optimization problem in Scenarios II and IV.

Table 5.29 Optimized Results of Scenario I by Various Solution Algorithms

Solution Algorithm	Total Profit (\$/hour)	Headway (hour)	Unit Fare (\$/mile)	Weight Factor of Unit Fare ($\gamma_s, \gamma_m, \gamma_l$)
Successive Substitution Method	254,586	0.25	0.26	(1.192, 1.117, 1.000)
Genetic Algorithm	254,520	0.26	0.27	(1.149, 1.086, 1.000)

5.7 Sensitivity Analysis

Previous sections discussed the optimized fares and service headway under various scenarios considering different peak/off-peak and fixed/variable RTD while utilizing the baseline values of input parameters shown in Table 5.2. Numerical results, including the optimized solutions and sensitivity analyses are presented. A sensitivity analysis was conducted to evaluate the differences in maximum profits obtained by changing headways, fares, unit weight factors of travel distance, elasticity parameters, and demand multipliers. Observations and solutions that could influence managerial decisions are discussed in the remainder of this chapter.

Figure 5.10 shows the impact on profit by varying headway from 0.10 to 0.37 hours/train while keeping the optimal fare and RTD fixed for Scenarios I and II. By

comparing the total profits in Figure 5.10, the maximum profits of 319,419 \$/hour is achieved by the optimized service headway of 0.23 hours/train of Scenario II. The total profits for Scenarios I and II are both shallow concave near the optimal profit for various headways. Similarly, Figure 5.11 shows the changes in profit by varying the unit fare (from \$0.15 to \$0.42), while the optimal headway, RTD and weight factors of unit fare are fixed. The maximum profit of 319,419 \$/hour is achieved by the optimized unit fare of 0.33 \$/mile of Scenario II.

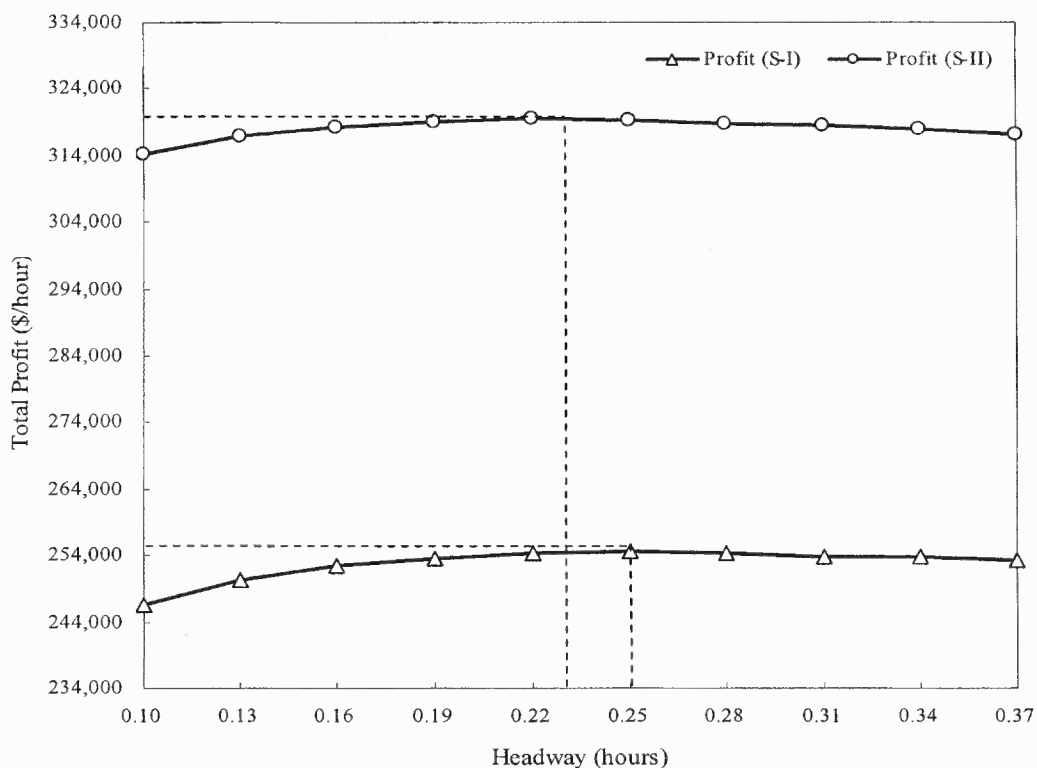


Figure 5.10 Profit vs. headway for Scenarios I and II.

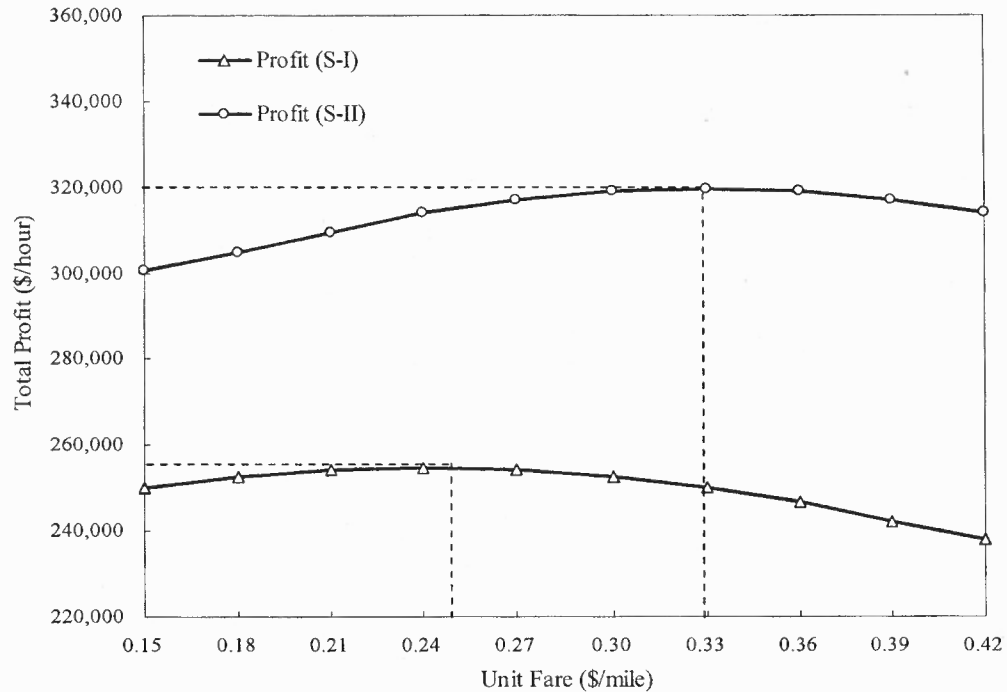


Figure 5.11 Profit vs. unit fare (δ) for Scenarios I and II.

Headway varies from 0.03 to 0.69 hours/train while keeping the optimal fare and RTD fixed for Scenarios III and IV in Figure 5.12. The maximum profits of 2,979,787 \$/day can be achieved by Scenario IV with an optimal headways of 0.25 and 0.39 hours/train for peak and off-peak periods, respectively. Note that for those profit curves (S-III, P) and profit (S-IV, P) in Figure 5.12 are derived by altering the headway for the peak hour, while fixing the optimal fare and headway for the off-peak hour. It was found that the total profit for Scenarios III and IV are both shallow concave near the optimal profit for various headways.

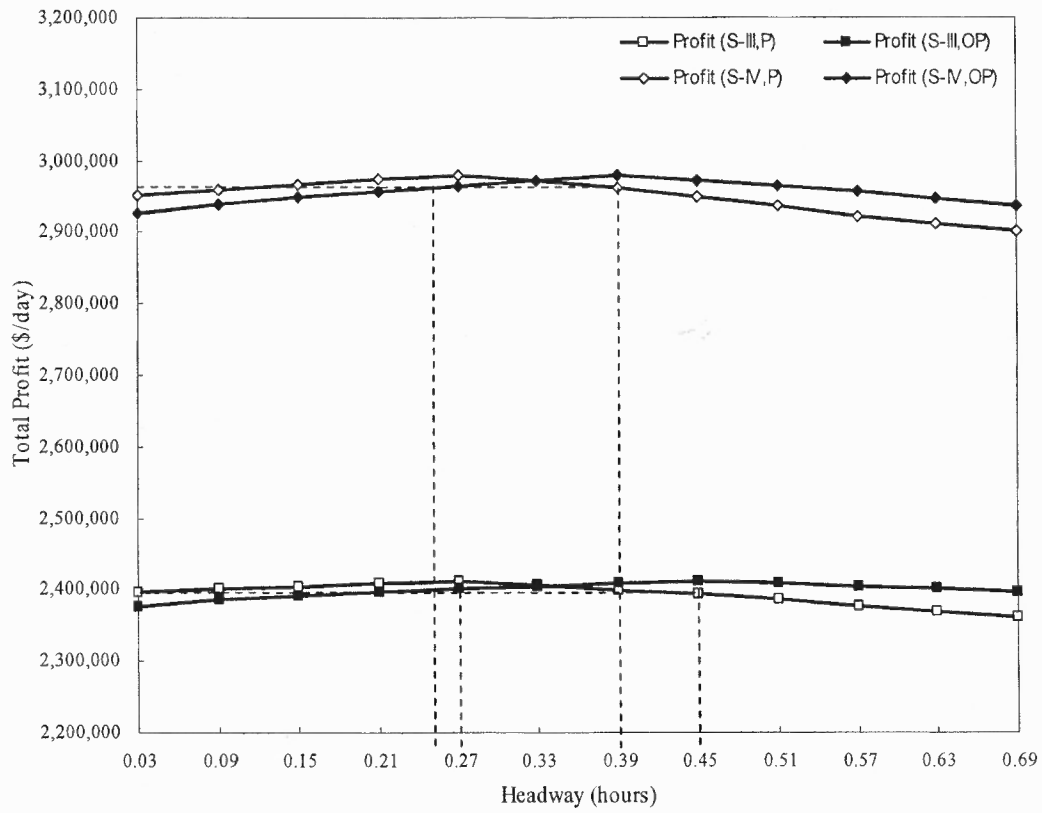


Figure 5.12 Profit vs. headway for Scenarios III and IV.

Similarly, Figures 5.13 and 5.14 show the changes in profit by varying the unit fare (from \$0.15 to \$0.42), while the optimal headway, RTD and weight factors of unit fare are fixed. The maximum profit of 2,979,787 \$/day is achieved by the optimized unit fare of 0.33 and 0.30 \$/mile for peak and off-peak periods in Scenario IV.

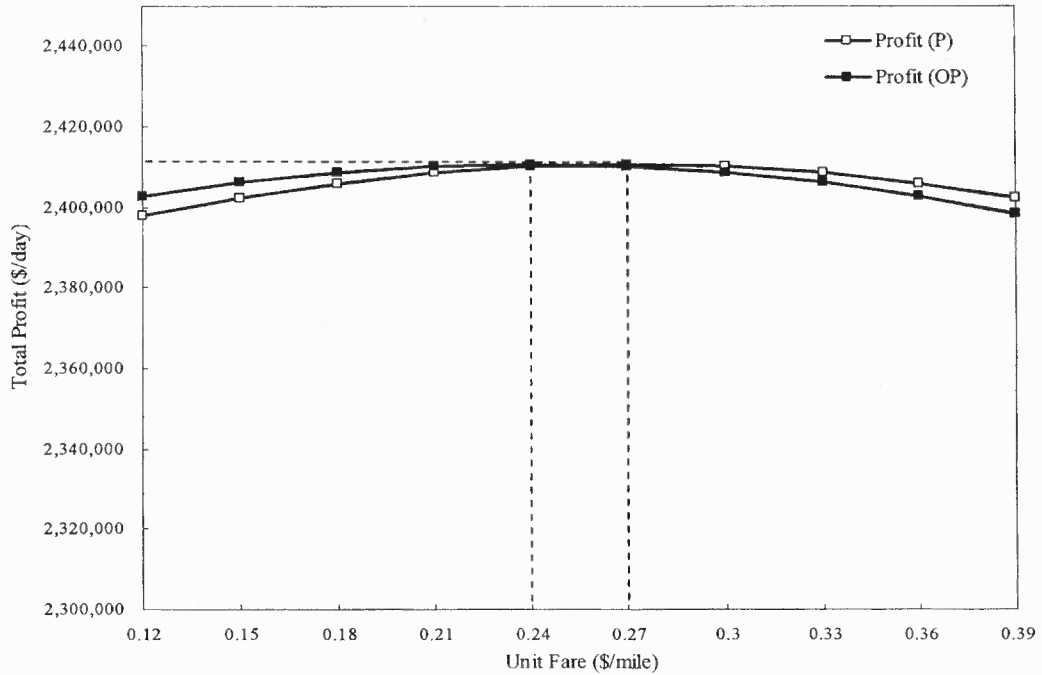


Figure 5.13 Profit vs. unit fare (δ') for Scenario III.

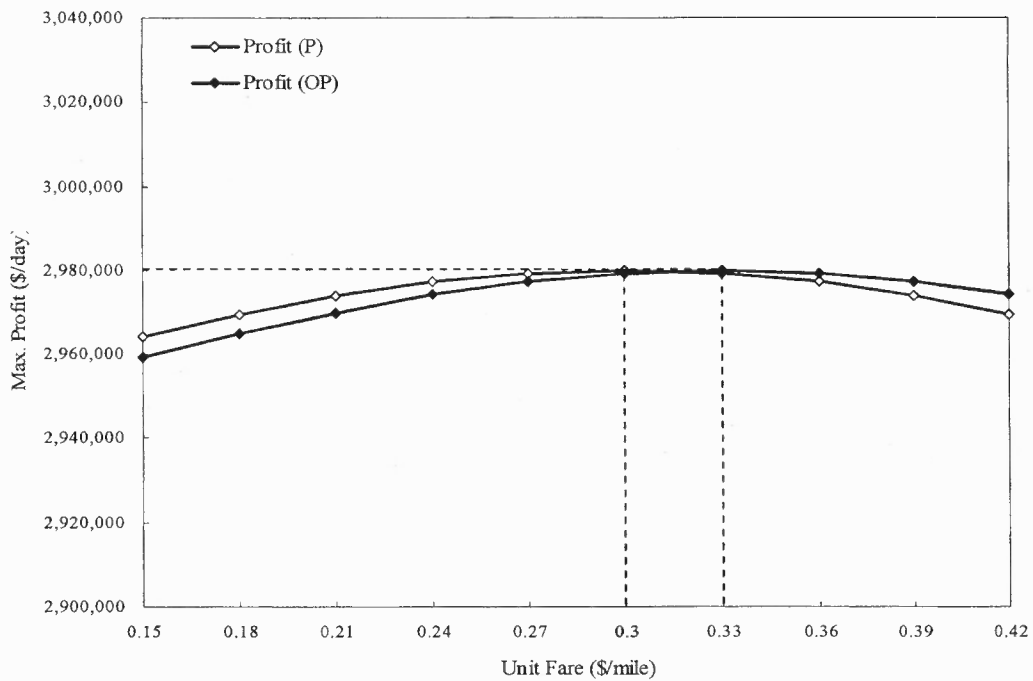


Figure 5.14 Profit vs. unit fare (δ') for Scenario IV.

Figure 5.15 demonstrates that the objective total profit function is concave by varying γ_s (from 1.16 to 1.22), and γ_m (from 1.09 to 1.15) while fixing the optimized headways, unit fare and RTD. From Figures 5.10 through 5.15, it is observed that the profit function is a shallow concave function at the optimum (i.e., the profit decreases rather slowly as one moves away from the optimum solution). The managerial implication is that many near-optimal solutions are available for the transit operator to adjust differentiated fare and service frequency without reducing the profit significantly. This is especially critical in setting the boundaries of RTD. The results also indicated that there are diminishing returns to increasing the fare differentiation, since much of the profit came from the initial attempt to reflect a differentiation principle and lesser profit improvements can be achieved from further fine tuning to obtain the exact optimum.

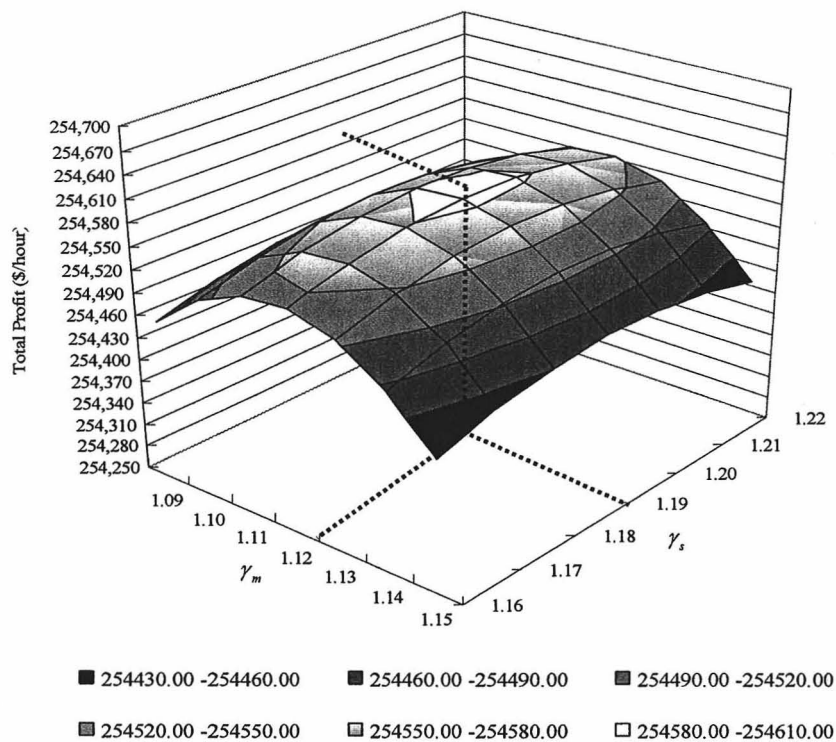


Figure 5.15 Profit vs. unit fares γ_s and γ_m for Scenario I.

Figures 5.16 and 5.17 show the impact of the fare elasticity parameter for a given RTD in Scenarios I and III (e.g., $E_{F_{z_{ij}}}$, where $z_{ij} = s, m, \text{ and } l$) on hourly and daily profits and ridership by comparing the results with and without re-optimized headway and weighted unit fare. The sensitivity of profit and ridership to E_{F_i} is calculated with fixed E_{F_m} and E_{F_l} . Without the re-optimization, the profit and ridership decrease as $E_{F_{z_{ij}}}$ increases for all RTD. However, the re-optimization achieves higher maximum profit because the ridership can be retained by using re-optimized headway, unit fare, and weight factor.

By comparing the reduction of ridership on different RTD (e.g., short, medium, and long) without the re-optimization for Scenarios I and III, the ridership significantly decreases due to passengers' sensitivity to fare. However, the ridership slightly decreases for long distance travel. Figures 5.16 and 5.17 also show that riders traveling long distances are less sensitive to the fare compared to those traveling short distances. In addition, the maximum profit is very sensitive to E_{F_i} especially when E_{F_i} approaches zero. The managerial implication of this is that riders traveling long distances are critical for the financial health of the route.

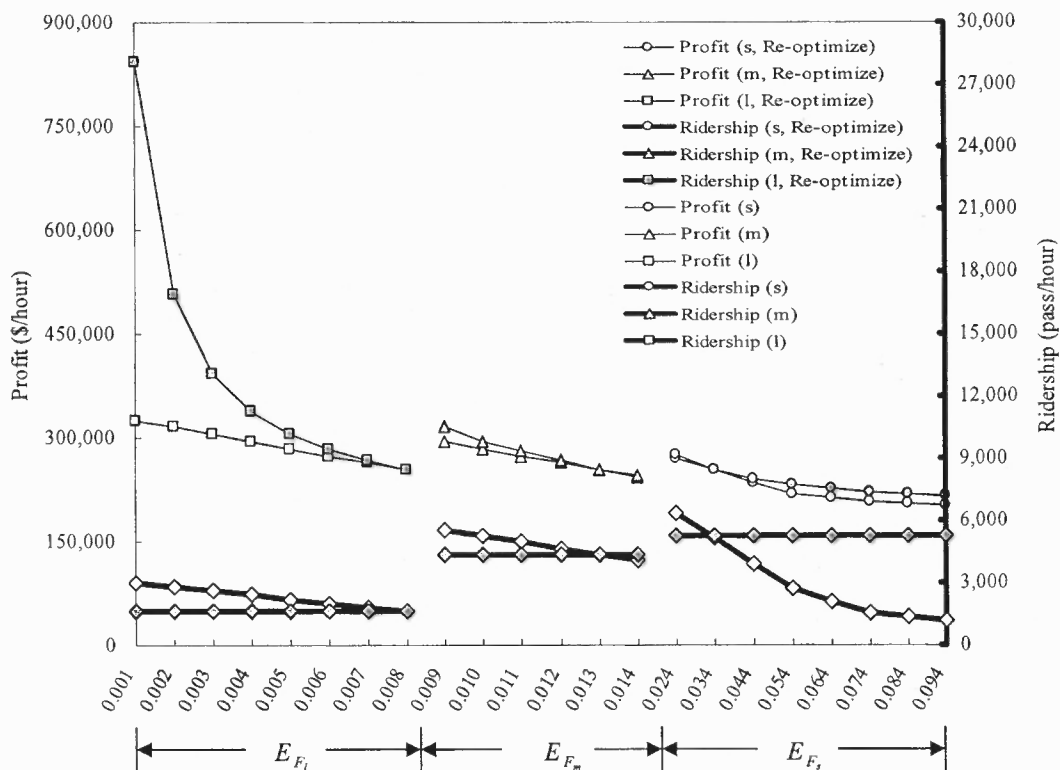


Figure 5.16 Profit and ridership vs. $E_{F_{z_{ij}}}$ in each RTD for Scenario I.

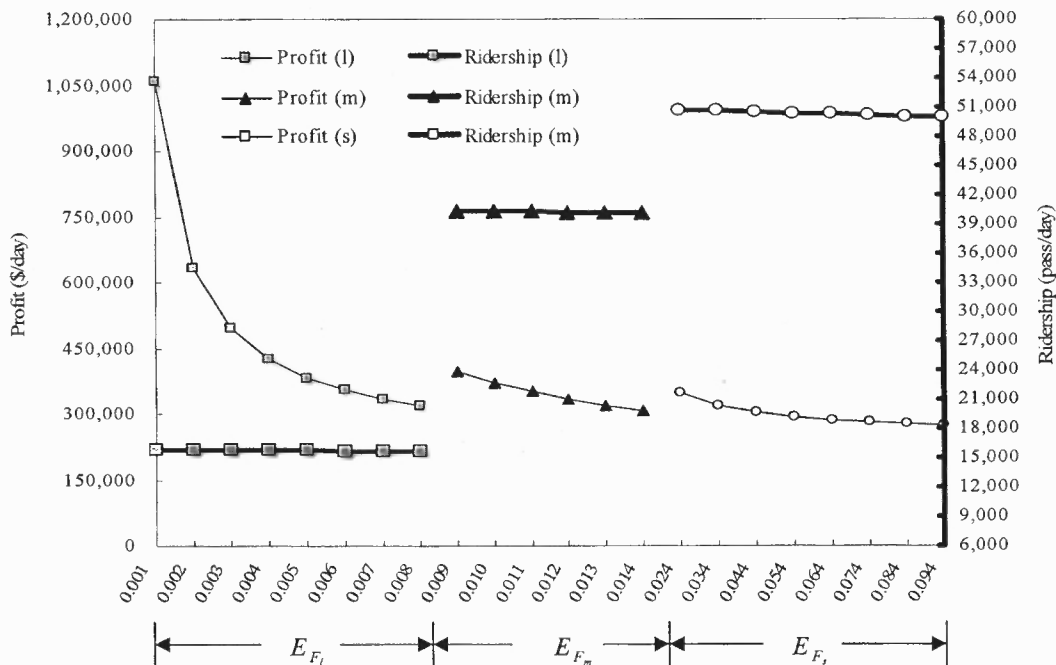


Figure 5.17 Profit and ridership vs. $E_{F_{z_{ij}}}$ in each RTD for Scenario III.

As shown in Figures 5.18 and 5.19, by increasing the elasticity parameter of fare ($E_{F_{ij}}$) for each O-D pair with a multiplier from 0.1 to 1.8, the profit and ridership decrease because passengers become more sensitive to fare. It was found that the profit is very sensitive especially when the $E_{F_{ij}}$ multiplier is less than 0.4, at which point the optimal profit increases quickly as $E_{F_{ij}}$ reduces. However, the decrease of the maximum profit is governed by the capacity constraint (e.g., maximum headway) when the multiplier of $E_{F_{ij}}$ increases more than 1.4 and 1.6 in Scenarios II and IV, respectively. At this headway, the train capacity accommodates the ridership.

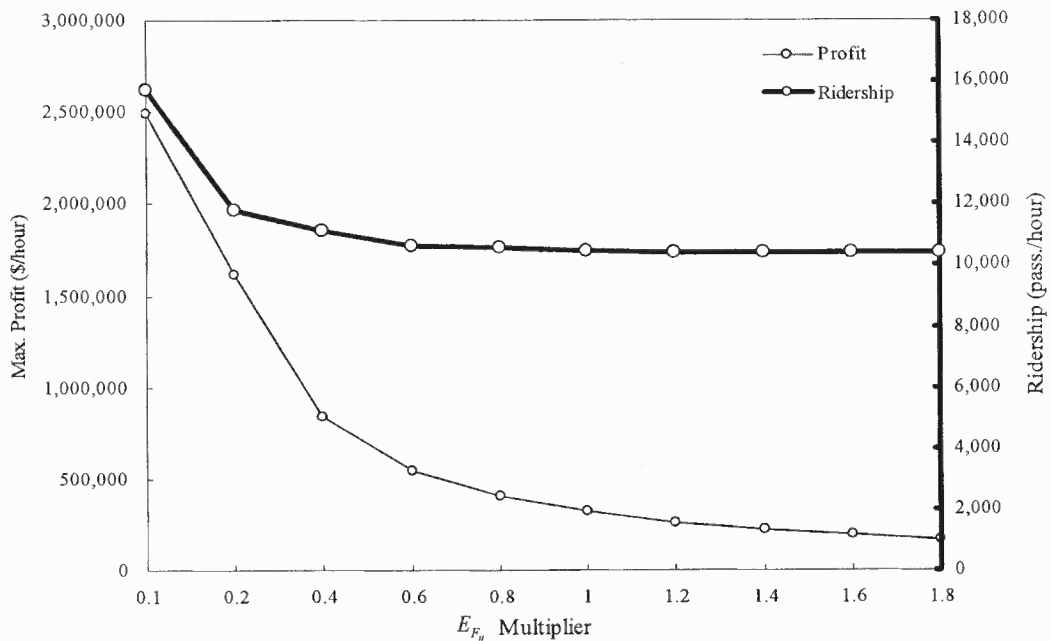


Figure 5.18 Maximized profit and ridership vs. $E_{F_{ij}}$ multiplier for Scenario II.

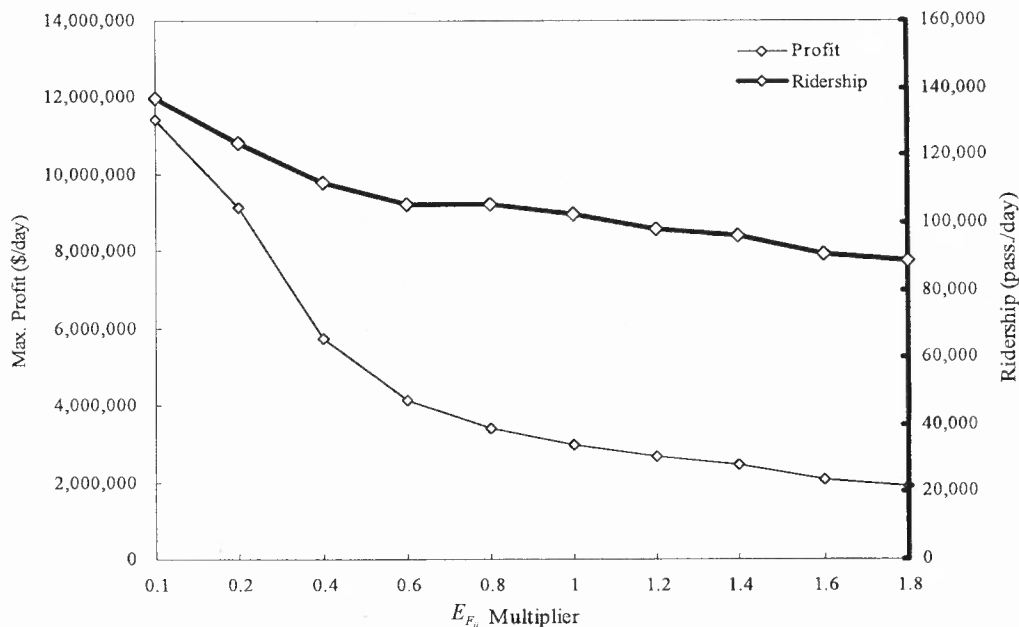


Figure 5.19 Maximized profit and ridership vs. $E_{F_{ij}}$ multiplier for Scenario IV.

Determining the number of RTD and the distance in each RTD for establishing distance-based fare is a critical step in the optimization process. It affects the unit fare, weight factors of unit fare and service headway for the designed service. The sensitive analysis in Figure 5.20 indicates that as the $E_{F_{ij}}$ multiplier increases from 0.1 to 1.8 for all RTD, indicating that the elasticity of demand with respect to fare increases from being inelastic to elastic, the optimal number of RTD tend to increase. Thus, the impact of fare on the demand of each RTD can be considered into the optimization process. However, the optimized unit fares decrease dramatically during the peak hour when the $E_{F_{ij}}$ multiplier is less than one because of the value of users' time (e.g., wait time and in-vehicle time) decreases.

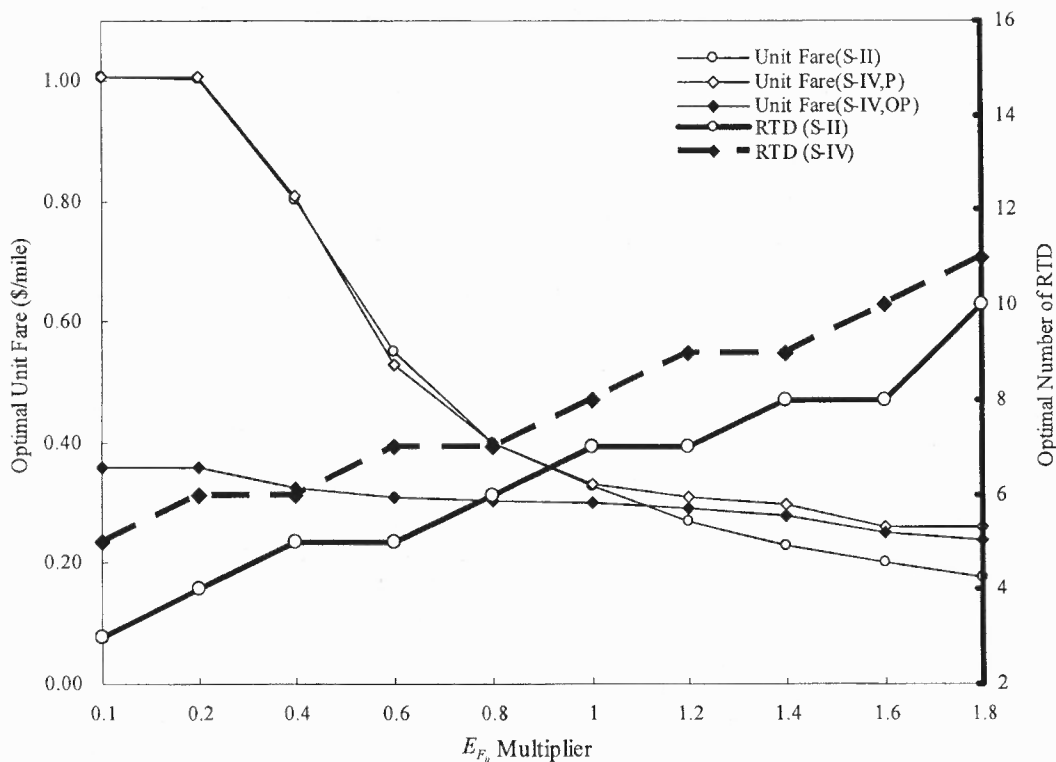


Figure 5.20 Optimal number of RTD vs. $E_{F_{ij}}$ multiplier for Scenarios II and IV.

The optimized RTD (e.g., optimal number of RTD and the distance of each RTD) are indicated in Figures 5.21 (Scenario II) and 5.22 (Scenario IV) for various elasticity parameter of fare ($E_{F_{ij}}$) multipliers. Because of demand and elasticity parameter heterogeneity, the optimized RTD generally increase as the $E_{F_{ij}}$ multiplier increases. It was also found that the boundaries of RTD are concentrated in the range of shorter travel distances (e.g., travel distance less than 100 miles), specifically as the $E_{F_{ij}}$ multiplier is greater than 1.4 and 1.2 for Scenarios II and IV, respectively.

Travel Distance (miles)	E_{F_y} Multiplier									
	0.1	0.2	0.4	0.6	0.8	1	1.2	1.4	1.6	1.8
$0 < L_{ij} \leq 18.8$										
$18.8 < L_{ij} \leq 22.5$										
$22.5 < L_{ij} \leq 39.4$										
$39.4 < L_{ij} \leq 41.3$										
$41.3 < L_{ij} \leq 53.8$										
$53.8 < L_{ij} \leq 58.1$										
$58.1 < L_{ij} \leq 58.8$										
$58.8 < L_{ij} \leq 77.5$										
$77.5 < L_{ij} \leq 93.1$										
$93.1 < L_{ij} \leq 100.0$										
$100.0 < L_{ij} \leq 111.9$										
$111.9 < L_{ij} \leq 112.5$										
$112.5 < L_{ij} \leq 131.3$										
$131.3 < L_{ij} \leq 151.9$										
$151.9 < L_{ij} \leq 153.8$										
$153.8 < L_{ij} \leq 170.6$										
$170.6 < L_{ij} \leq 189.4$										
$189.4 < L_{ij} \leq 193.1$										
$193.1 < L_{ij} \leq 211.9$										
Optimized No. of RTD with GA	3	4	5	5	6	7	7	8	8	10

Figure 5.21 Optimized RTD for various E_{F_y} multipliers for Scenario II.

Travel Distance (miles)	$E_{F_{ij}}$ Multiplier									
	0.1	0.2	0.4	0.6	0.8	1	1.2	1.4	1.6	1.8
$0 < L_{ij} \leq 18.8$										
$18.8 < L_{ij} \leq 22.5$										
$22.5 < L_{ij} \leq 39.4$										
$39.4 < L_{ij} \leq 41.3$										
$41.3 < L_{ij} \leq 53.8$										
$53.8 < L_{ij} \leq 58.1$										
$58.1 < L_{ij} \leq 58.8$										
$58.8 < L_{ij} \leq 77.5$										
$77.5 < L_{ij} \leq 93.1$										
$93.1 < L_{ij} \leq 100.0$										
$100.0 < L_{ij} \leq 111.9$										
$111.9 < L_{ij} \leq 112.5$										
$112.5 < L_{ij} \leq 131.3$										
$131.3 < L_{ij} \leq 151.9$										
$151.9 < L_{ij} \leq 153.8$										
$153.8 < L_{ij} \leq 170.6$										
$170.6 < L_{ij} \leq 189.4$										
$189.4 < L_{ij} \leq 193.1$										
$193.1 < L_{ij} \leq 211.9$										
Optimized No. of RTD with GA	5	6	6	7	7	8	9	9	10	11

Figure 5.22 Optimized RTD for various $E_{F_{ij}}$ multipliers for Scenario IV.

Results from the sensitivity analyses for the elasticity parameter of wait time (E_w) in Scenarios I through IV are respectively shown in Figures 5.23 and 5.24. It was found that the profit and re-optimized service headway decrease as (E_w) increases from 0.05 to 0.6. The increase of E_w indicates that the demand becomes more sensitive to wait time, which results in the reduction of service headway. Thus, the profit decreases due to increase of operation cost. However, as E_w continuously decreases to less than 0.1 and

0.15 in Scenarios I and II respectively, the maximum profit is governed by the operating cost at the maximum headway of 0.28 and 0.29 hours/trip. At these headways, the train capacity can accommodate the peak demand. Meanwhile, as E_w increases beyond 0.4 (0.5) in Scenario II (IV), the optimal headway is equal to the minimum headway to satisfy the constraint of operable fleet size.

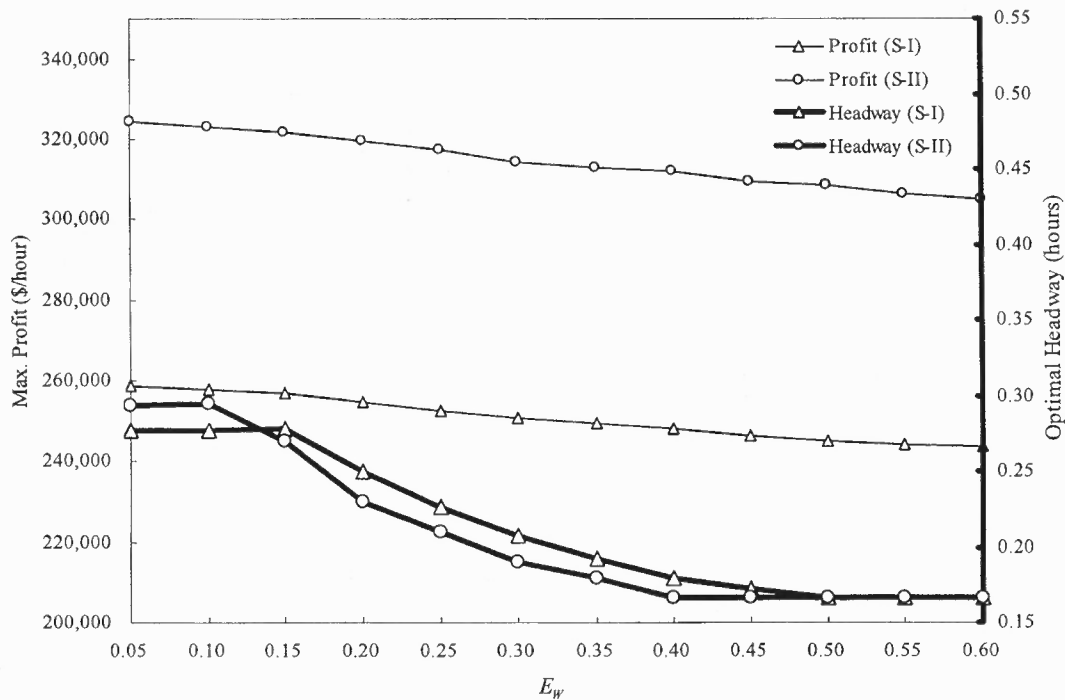


Figure 5.23 Maximized profit and optimal headway vs. E_w for Scenarios I and II.

Similar to Figure 5.23, the temporal headway and daily profit are re-optimized by varying E_w for Scenarios III and IV in Figure 5.24. It was found that as E_w increases, the optimal headway decreases resulting in a concurrent increase in the operator's cost. The combined effect of this change is the reduction in profit. Therefore, by doubling the value of the wait time (e.g., E_w from 0.2 to 0.4), the maximum profit decreases five

percent (from 2,965,860 \$/day to 2,805,116 \$/day). As a result, the transit operator will reduce the service frequency to cut the cost of running the service and offset the lost revenue. The service headway during the off-peak hour drops dramatically when E_w is less than 0.15, however, it is dominated by the capacity constraint during the peak period when E_w is less than 0.1.

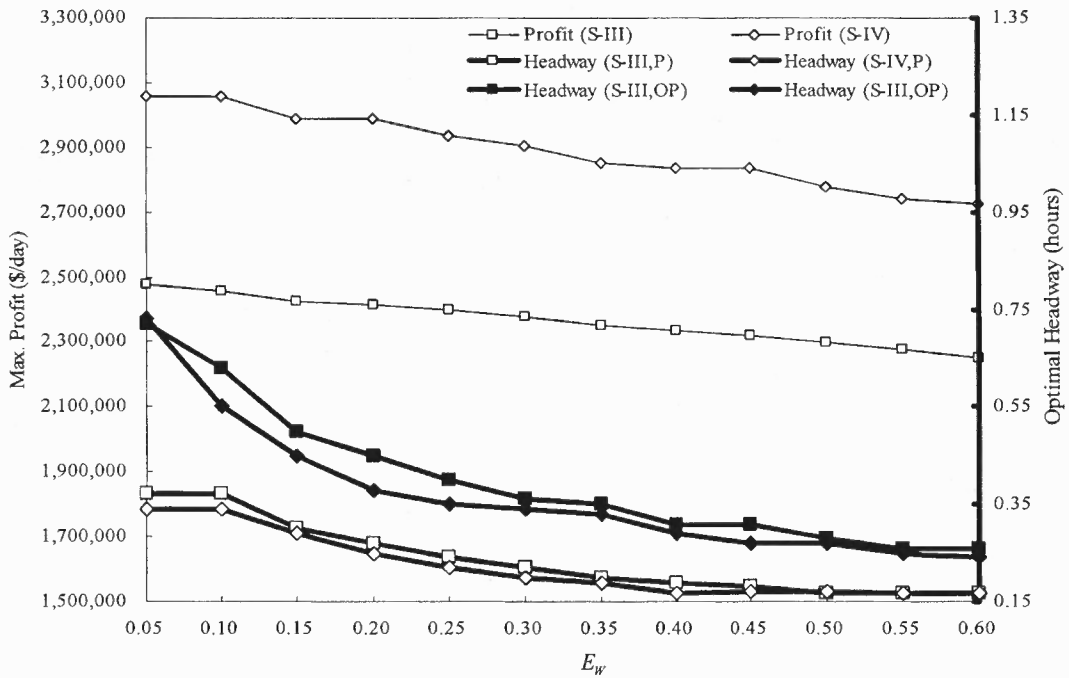


Figure 5.24 Maximized profit and optimal headway vs. E_w for Scenarios III and IV.

Figure 5.25 shows the variation of maximum profit and optimal headway for each RTD as the increase of demand multiplier in Scenarios I and II, while the optimal headway decreases to meet the increased demand. It was found that as the demand multiplier exceeds 1.8 in Scenarios I and II, the optimal headway is limited by H_{min} and

thus the profit becomes constant within each RTD. As a result, the profit is dominated by the operable fleet size of the transit system.

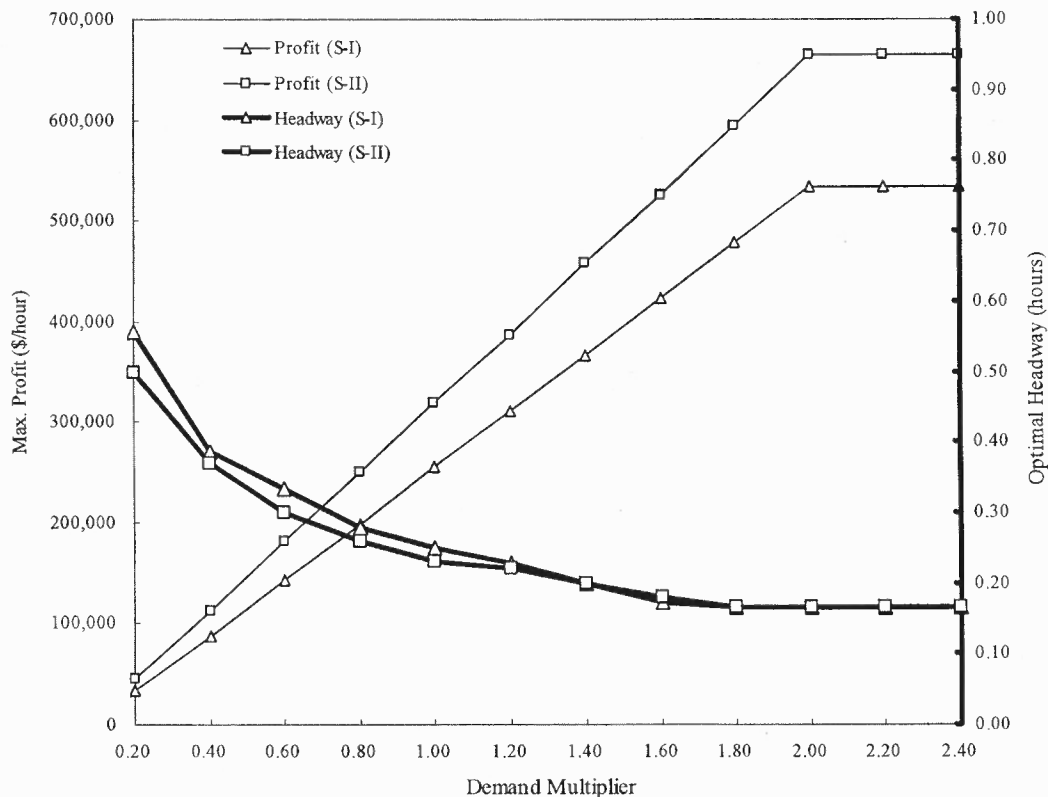


Figure 5.25 Maximized profit and optimal headway vs. demand multiplier for Scenarios I and II

Figure 5.26 indicates the changes of maximum profit and optimal headway versus demand increase in Scenarios III and IV. Similar to Figure 5.25, the optimal headway decreases to meet the increased demand. In Scenarios III and IV, the optimal headway during the peak hour reaches the H_{\min} when the demand multiplier increases to more than 2.2. However, the profit keeps increasing slowly since the optimal weighted unit fares and ridership keep increasing slightly during the off-peak hour. As a result, the profit is dominated by the operable fleet size of the transit system.

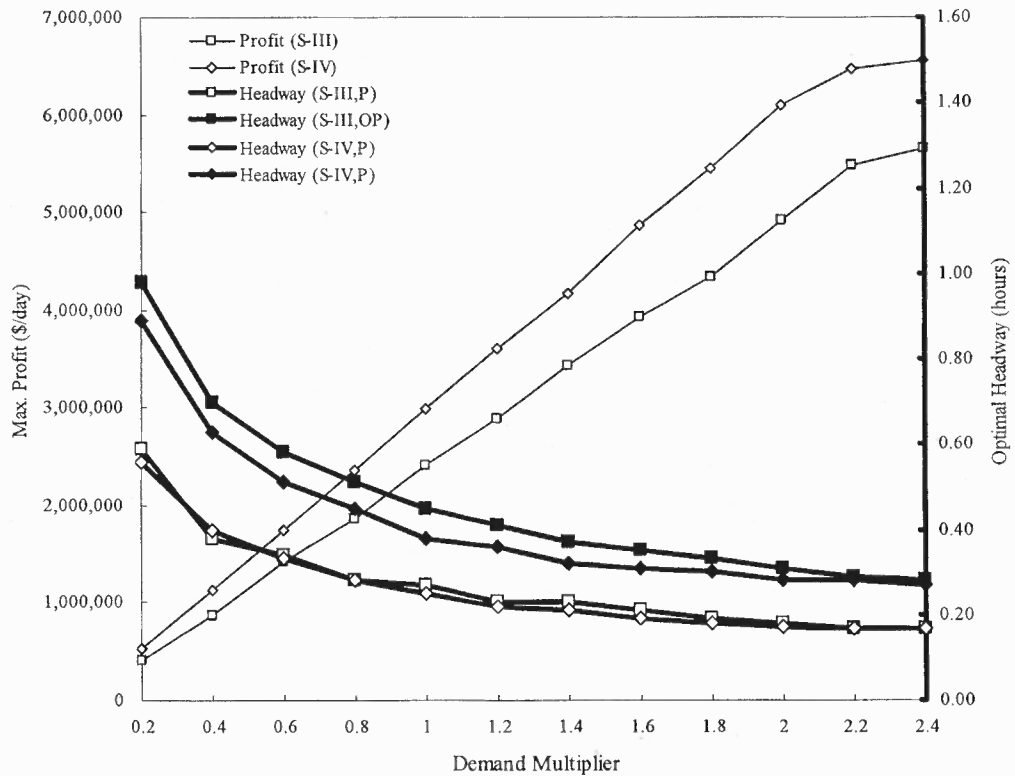


Figure 5.26 Maximized profit and optimal headway vs. demand multiplier for Scenarios III and IV.

The variation of optimal weighted unit fare for each RTD as the demand multiplier increase for Scenarios I and III is shown in Figure 5.27. It was found that the optimal weighted unit fare for each RTD increases to compensate for the increased operating cost. When the demand multiplier increases to more than 2.0, the transit service is constrained by the minimum headway (e.g., operable fleet size) and the optimal weighted unit fares during the peak hour are constant for short, medium and long travel distances.

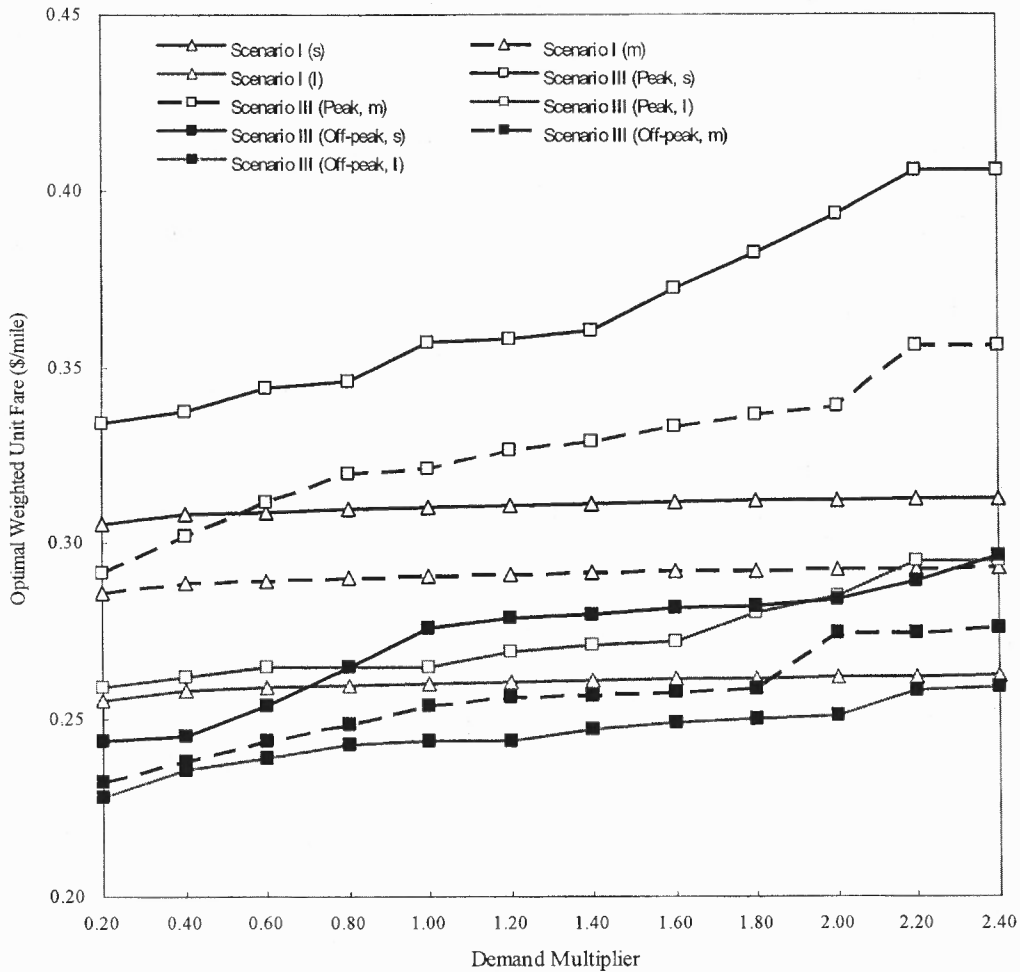


Figure 5.27 Optimal weighted unit fare vs. demand multiplier for Scenarios I and III.

Figure 5.28 shows the changes of the optimal unit fare versus the increases of demand for Scenarios II and IV. Similar to Figure 5.27, the optimal unit fare increases to compensate for the increased operating cost due to increased passenger demand. When the demand multiplier increases beyond 2.2, the transit service is constrained by the minimum headway during the peak hour and the optimal unit fares are constant for each RTD.

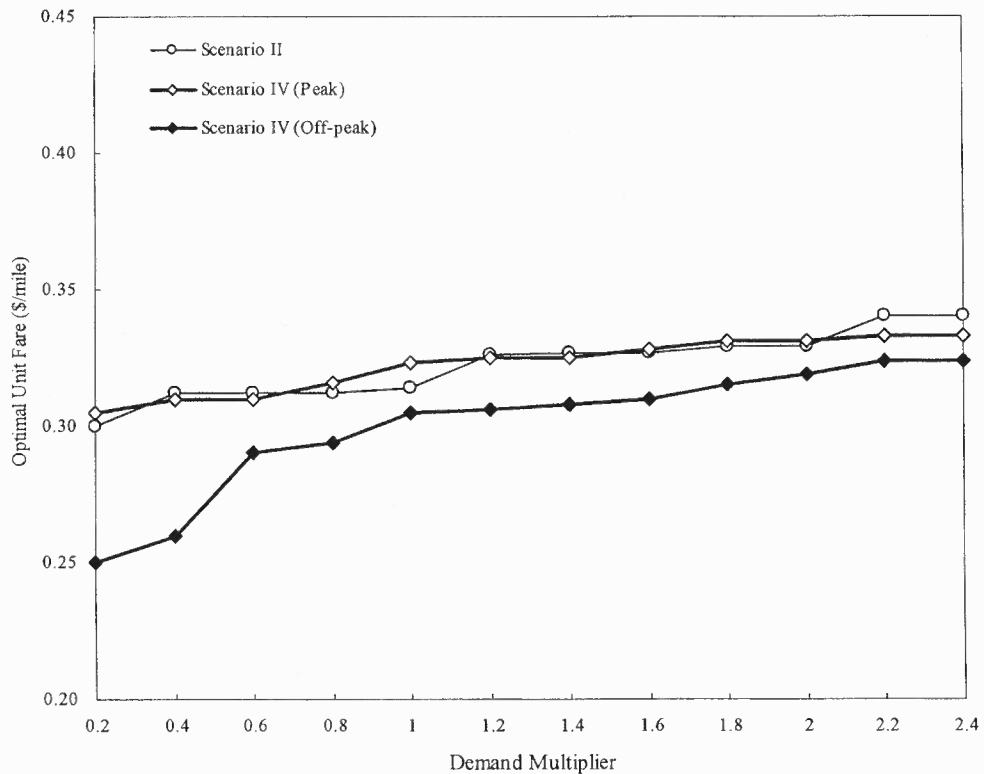


Figure 5.28 Optimal unit fare vs. demand multiplier for Scenarios II and IV.

Figure 5.29 shows the relationship of maximum profit and optimal fleet size versus demand for Scenario IV. As demand increases to more than 2.2 times (e.g., 220%) the current demand, the optimized fleet size exceeds the operable fleet size. Therefore, additional vehicles is needed to satisfy increasing demand as well as profit. The managerial decision can be made by considering the marginal profit gained by increasing the operable fleet size.

Maximum profit is achieved by the optimal fleet size of 20 vehicles in this case study. While increasing the demand by 20%, 40%, 60%, 80%, and 100%, the corresponding optimal fleet size increases to 23, 24, 27, 28, and 30, respectively. Therefore, the marginal profit for each extra vehicle can be achieved by \$203,457,

\$296,862, \$269,561, \$307,455, and \$311,097. It was found that if demand increases 40%, 80% and 100%, the operator could make more profit by adding extra vehicle service.

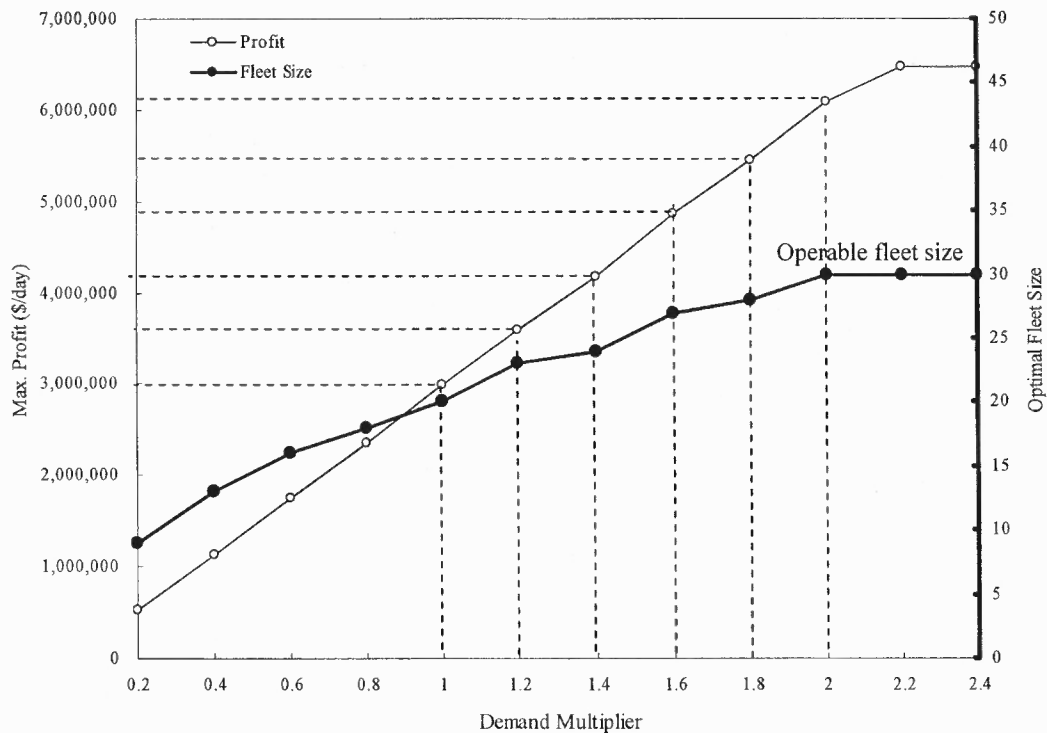


Figure 5.29 Maximized profit and optimal fleet size vs. demand multiplier for Scenario IV.

Finally, while investigating the relationship of maximum profit and optimal number of RTD versus demand in Figure 5.30, it was found that the maximum profit increases and the optimal number of RTD tends to decrease as demand multipliers increase from 0.2 to 2.4. However, the maximum profit remains constant when demand multiplier exceeds 2.2 due to the capacity constraint. By doubling the demand (e.g., demand multiplier equal to two), the optimal number of RTD decreases from seven and eight to five and four in Scenarios II and IV, respectively. Meanwhile, the maximum

profits increase 107% (from 313,268 \$/hour to 651,193 \$/hour) and 104% (from 2,965,860 \$/day to 6,055,368 \$/day) in Scenarios II and IV, respectively.

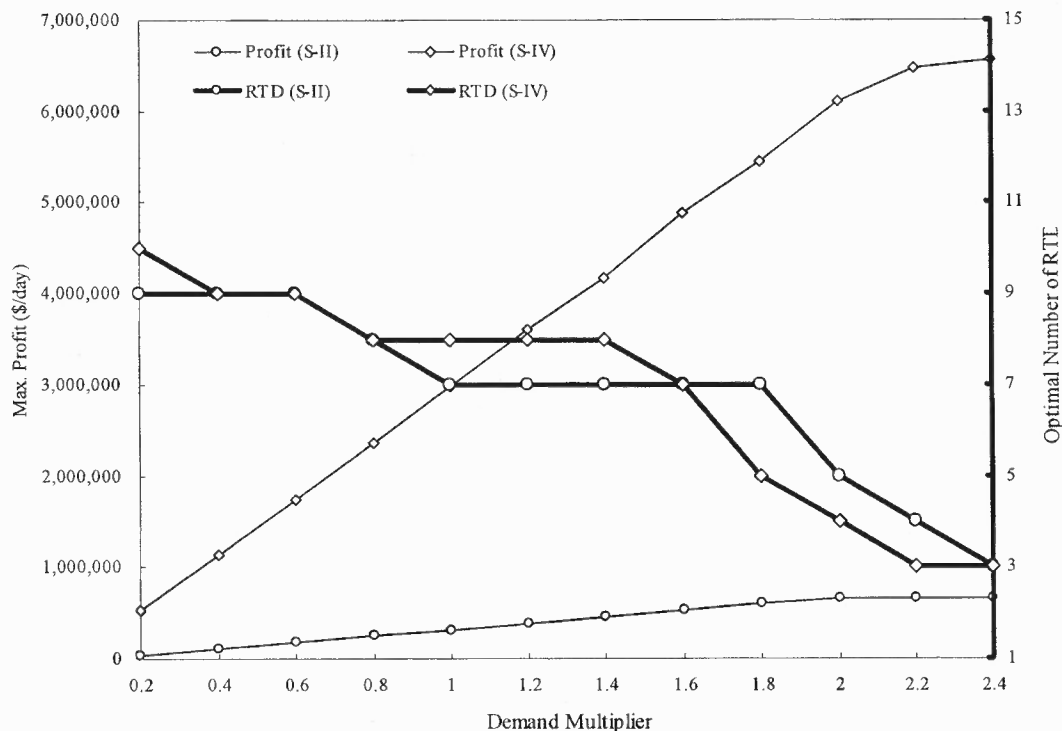


Figure 5.30 Maximized profit and optimal number of RTD vs. demand multiplier for Scenarios II and IV.

Due to demand heterogeneity, the optimized RTD vary with demand as shown in Figures 5.31 and 5.32. It was also found that as the number of RTD increase, the boundaries of RTD are concentrated in the range of shorter travel distances (e.g., travel distance less than 100 miles). One of the possible explanations behind this phenomenon is related to the demand distribution. The ridership for trips less than 100 miles in Scenario IV is 70% of the total ridership. The other possibility is that the optimal weighted unit fares for the shorter travel distance are higher than those of the longer

travel distance. In this case, more revenue can be generated by fares established with more RTD for short distance trips.

Travel Distance (miles)	Demand Multiplier											
	0.2	0.4	0.6	0.8	1.0	1.2	1.4	1.6	1.8	2.0	2.2	2.4
$0 < L_{ij} \leq 18.8$												
$18.8 < L_{ij} \leq 22.5$												
$22.5 < L_{ij} \leq 39.4$												
$39.4 < L_{ij} \leq 41.3$												
$41.3 < L_{ij} \leq 53.8$												
$53.8 < L_{ij} \leq 58.1$												
$58.1 < L_{ij} \leq 58.8$												
$58.8 < L_{ij} \leq 77.5$												
$77.5 < L_{ij} \leq 93.1$												
$93.1 < L_{ij} \leq 100.0$												
$100.0 < L_{ij} \leq 111.9$												
$111.9 < L_{ij} \leq 112.5$												
$112.5 < L_{ij} \leq 131.3$												
$131.3 < L_{ij} \leq 151.9$												
$151.9 < L_{ij} \leq 153.8$												
$153.8 < L_{ij} \leq 170.6$												
$170.6 < L_{ij} \leq 189.4$												
$189.4 < L_{ij} \leq 193.1$												
$193.1 < L_{ij} \leq 211.9$												
Optimized No. of RTD with GA	9	9	9	8	7	7	7	7	7	5	4	3

Figure 5.31 Optimized RTD for various demand multipliers for Scenario II.

Travel Distance (miles)	Demand Multiplier											
	0.2	0.4	0.6	0.8	1.0	1.2	1.4	1.6	1.8	2.0	2.2	2.4
$0 < L_{ij} \leq 18.8$												
$18.8 < L_{ij} \leq 22.5$												
$22.5 < L_{ij} \leq 39.4$												
$39.4 < L_{ij} \leq 41.3$												
$41.3 < L_{ij} \leq 53.8$												
$53.8 < L_{ij} \leq 58.1$												
$58.1 < L_{ij} \leq 58.8$												
$58.8 < L_{ij} \leq 77.5$												
$77.5 < L_{ij} \leq 93.1$												
$93.1 < L_{ij} \leq 100.0$												
$100.0 < L_{ij} \leq 111.9$												
$111.9 < L_{ij} \leq 112.5$												
$112.5 < L_{ij} \leq 131.3$												
$131.3 < L_{ij} \leq 151.9$												
$151.9 < L_{ij} \leq 153.8$												
$153.8 < L_{ij} \leq 170.6$												
$170.6 < L_{ij} \leq 189.4$												
$189.4 < L_{ij} \leq 193.1$												
$193.1 < L_{ij} \leq 211.9$												
Optimized No. of RTD with GA	10	9	9	9	8	8	8	7	5	4	3	2

Figure 5.32 Optimized RTD for various demand multipliers for Scenario IV.

CHAPTER 6

CONCLUSION AND FUTURE RESEARCH

A complex transportation fare and service frequency problem of an intercity transit system has been defined, formulated, optimized, and analyzed in this research. The objective total profit functions and sets of constraints were developed for Scenarios I through IV, while two solution algorithms were used to search for constrained optimal solutions. A modified Gauss-Southwell method was used to optimize fare and frequency for Scenarios I and III while RTD is treated as exogenous parameters. To optimize a combinatorial problem while considering RTD as decision variables, a Genetic Algorithm was developed. The methodology discussed in this study integrated the analytical approach and solution algorithms that jointly optimized differentiated fare and service headway for an intercity transit system.

Finally, a real world example of the Taiwan High Speed Rail (THSR) was introduced to demonstrate the efficiency and applicability of the developed models and solution algorithms to optimize the studied problem. Given a temporal, heterogeneous demand distribution, the differentiation of trip lengths and operator's costs were considered in the developed models which maximized total profit. The optimal results considering pre-specified and optimized RTD were obtained, and then sensitivity analyses were conducted for investigating the relationships among important decision variables and model parameters.

6.1 Conclusions

Subject to the time-dependent potential demand as well as various elasticity parameters of fare ($E_{F_{ij}}$) for each O-D pair, the optimal differentiated, temporal fare and headway corresponding to pre-specified and optimized RTD were obtained by a modified Gauss-Southwell method and a genetic algorithm, respectively. In summary, the major findings and conclusions are as follows:

(1) Methodology

- The developed models consider the differentiated fare based on passenger travel distance multiplied by the weighted unit fare. The weighted unit fare is determined by the product of unit fare (δ) and weight factor of unit fare ($\gamma_{z_{ij}}$) for all RTD with index z ($z= 1, 2, \dots, q$), while both δ and $\gamma_{z_{ij}}$ are decision variables in Scenarios I through IV. The optimal weighted unit fares of different O-D pairs show that passengers travel shorter distances will be charged a higher rate than those traveling longer distances.
- The fare optimization problem for an intercity transit system was analyzed under both capacity and fleet size constraints. In the numeric example, the capacity constraint affects train service for the baseline demand volumes. If the demand keeps increasing, the train service cannot satisfy the demand during the peak period (see Figure 5.33). Therefore, the optimal headway decreases in order to increase the train fleet size for serving more demand.
- A previous study (Hamacher and Schobel, 2004) focused on optimizing the number of zones by maximizing revenue. In this study, the optimization problem of distance-based fare, service headway, and RTD design is developed to maximize total profit. The optimized distance-based fare does not only consider the travel distance, but also optimize number of RTD and the distance of each RTD which might be affected by the elasticity parameters and demand. Therefore, the designed fares can reflect passengers' travel behavior for all O-D pairs.
- Since RTD is treated as a decision variable, the model becomes a combinatorial optimization problem due to the combination and interdependent relationships among the decision variables. Therefore, the total number of decision variables increases more than exponentially as the number of RTD increases.
- The developed models can be utilized to optimize the fare and headway of existing intercity transportation systems or a pre-planned transit route as soon as a

realistic demand function is available. In this study, a given demand function was adopted in the developed models.

(2) Solution algorithms

- The optimal results obtained by the successive substitution method were tested by substituting various sets of nonzero initial values of the decision variables, and all sets of initial values achieve the same maximum total profit (see Figure 5.9). By comparing the optimal results achieved by the developed GA and the successive substitution method, it was found that the maximum total profit is close. Therefore, the developed GA can be used to search for the optimal solution considering either pre-specified (e.g., for Scenarios I and III) or variable (e.g., for Scenarios II and IV) RTD.
- The developed GA is suitable for solving the combinatorial optimization problem formulated in this study, which has a nonlinear, integer and discontinuous objective function. The parameters of the developed GA, such as crossover and mutation ratios as well as population size, were determined by enumerating the ratios of production (R_P), mutation (R_M), and crossover (R_C). The best values of R_P , R_M , and R_C were determined based on initiating a large R_C to enable the global search and then increasing R_P , R_M to focus on a local search. The ratios of R_P , R_M , and R_C used were 0.125, 0.125, 0.75. Note that the ratios of production, mutation, and crossover must be $R_P + R_M + R_C = 1$.

(3) Optimal results and sensitivity analysis

- By comparing the optimal results among Scenarios I through IV, the maximum profits obtained by an optimized RTD were about 25% higher than those with pre-specified RTD. However, the ridership under the optimized fare setting for a pre-specified RTD was about 5% less than that under optimized RTD because of higher fare. It was also found that the highest RPM and RSM were all achieved at the shortest RTD since a great percentage of ridership contributed significantly to revenue within short travel distances.
- The load factors at each station-to-station link under the given RTD were generally greater than those under the optimized RTD since more ridership was generated from lower fare charged for each O-D pair.
- The profit surfaces for various headways, unit fares and weight factors of unit fare within short and medium travel ranges (as presented by their weight factors, γ_s and γ_m) are relatively flat near the optimum as shown in Figures 5.11 through 5.16. The managerial implication of this is that the decision variables can be adjusted marginally with only minor deviations from optimality. This is especially critical in setting the boundaries of the travel distance ranges.

- The results also indicate that there are diminishing returns to increase the fare differentiation, much of the gains coming from the initial attempts to reflect a differentiation principle and little coming from further fine tuning to hit on the exact optimum.
- The impact of fare elasticity parameters for given RTD (e.g., $E_{F_{ij}}$, where $z_{ij} = s, m, \text{ and } l$) in Scenarios I and III that the ridership significantly decreases for short distance travel due to passengers' sensitivity to fare; however, ridership slightly decreases for medium and long distance travel (see Figures 5.17 and 5.18) The managerial implication of this is that riders traveling long distances are critical for the financial health of the route. While increasing the elasticity parameter of fare ($E_{F_{ij}}$) for each O-D pairs in Scenarios II and IV (see Figures 5.19 and 5.20), the profit and ridership decreases because passengers become more sensitive to fare.
- The optimized RTD with corresponding differentiated fare and headway were determined based on maximum profit. As shown in the sensitivity analyses, the optimal numbers of RTD tend to increase when the elasticity parameter of fare increases and demand increases. It was found that the boundaries of RTD are concentrated in the range of shorter travel distances. Thus, the impact of fare to demand of each RTD can be considered into the optimization process.
- Results from the sensitivity analyses for the elasticity parameter of wait time (E_w) indicate that demand becomes more sensitive to wait time, which results in the reduction of service headway. Thus, the profit decreases due to increases in operation cost.
- While considering the demand keeps increasing, the optimized fleet size may exceed the operable fleet size. Therefore, an additional number of vehicles is needed to satisfy increasing demand as well as profit. The managerial decision can be made by considering the marginal profit gained by increasing the operable fleet size.

6.2 Future Research

Future research for the differentiated fare and service headway optimization problem can be extended but not limited to the following aspects:

- This study focused on an intercity transit system serving at each stop with a single user class. An immediate expansion of this study will integrate service patterns (i.e., skip stopping or express), while considering multiple-class users (i.e., business or economy class).

- Some other assumptions can be relaxed in further research efforts. For instance, the weight factors of unit fare for each RTD can be randomly assigned instead of decreasing as the index of RTD (z_{ij}) increases from a short to a long distance range.
- A multi-objective optimization problem can be extended by considering social welfare maximization as well as subsidy in addition to the total profit function. Thus, the researched profit maximization problem may also deal with subsidy minimization when the fare box revenue cannot cover the expenses of operating the service. There are many other issues that can be explored in future research, such as fare management, fare discount, coordination of fare and other marketing elements, and consideration of long-term profitability.
- The formulation of the operator's cost can be enhanced by considering the various operating cost between idle and on duty vehicles during peak and off-peak periods. Through this extension, the model can estimate operator's cost accurately based on a known operable vehicle fleet.
- The distance-based fares have the same value within the same O-D travel distance in the optimization models. While considering competing transportation modes, the pricing theory may take into account traveler's willingness to pay by setting differentiated fares for the same travel distance.
- A further extension of this study may focus on an intermodal transit service, such as rail and feeder buses which has been discussed by Chien and Schonfeld (1997). Moreover, optimization of timed transfer may be jointly optimized to yield the best performance of an integrated transit service, in terms of total social welfare and profit.
- The developed GA can be enhanced by generating a new chromosome with desired minor adjustment when the previous generation is close to the goal. It was found that the mutation tends to be more efficient than the crossover if a candidate solution is close to the real optimum solution. Therefore, the strategy of dynamically determining the ratio of three GA operations could further improved the results. (Wu and Shih, 2006)

REFERENCES

- Andrie, S., Kraus, J., Spielberg, F. (1991). "Lesson from the Broome County Distance-Based Fare Demonstration: Effects of Zone Fares and Off-Peak Discounts on Ridership, Revenue, Pass Sales, and Public Opinion." *Transportation Research Record* 1297, pp. 50-56.
- Babel, L., and Kellerer, H. (2003). "Design of Tariff Zones in Public Transportation Networks: Theoretical Results and Heuristics." *Mathematical Methods of Operations Research*, Vol. 58, pp. 359-374.
- Baum, H. J. (1973). "Free Public Transport." *Journal of Transportation Economics and Policy* 7, pp. 3-19.
- Bell, M. G., and Y. Iida (1997). *Transportation Network Analysis*. Chichester, U.K: John Wiley & Sons.
- Berechman, J. (1993). *Public Transit Economics and Deregulation Policy*. Netherlands: North-Holland.
- Bullnheimer B.; Hartl, R.; and Strauss, C. (1999). "An Improved Ant System Algorithm for the Vehicle Routing Problem." *Annals of Operations Research* 89: pp. 319-328.
- Cervero, R. (1981). "Flat versus Differentiated Transit Pricing: What's a Fair Fare?" *Transportation* 10, pp. 211-232.
- Cervero, R. (1985). "Experiences with Time-of-Day Transit Pricing in the United States." *Transportation Research Record* 1039, pp. 21-30.
- Cervero, R. (1990). "Transit Pricing Research – A Review and Synthesis." *Transportation* 17, pp. 117-139.
- Chang, S. W., and Schonfeld, P. (2004). "Optimized Schedules for Airline Routes." *Journal of Transportation Engineering*, Vol. 130, No. 4, pp. 412-418.
- Chang, S. K., and Schonfeld, P. (1991). "Multiple Period Optimization of Bus Transit Systems." *Transportation Research Part B*, Vol. 25, No. 6, pp. 453-478.
- Chien, S. I., and Schonfeld, P. (1997). "Joint Optimization of a Rail Transit Line and Its Feeder Bus System." *Journal of Advanced Transportation*, Vol. 32, No. 3, pp. 253-284.

- Chien, S.I., Yang, Z., and Hou, E. (2001) "A Genetic Algorithm Approach for Transit Route Planning and Design." *Journal of Transportation Engineering*, ASCE, Vol. 127, No. 3, pp. 200-207.
- Chien, S. I., and Spasovic, L. (2002). "Optimization of Grid Bus Transit Systems with Elastic Demand." *Journal of Advanced Transportation*, Vol. 36, No. 1, pp. 63–91.
- Chien, S. I., and Tsai, F. M. (2007). "Optimization of Fare Structure and Service Frequency for Maximum Profitability of Transit Systems." *Transportation Planning and Technology*, Vol. 30, No. 5, pp. 477-500.
- Chang, Y. H.(1999). *Transportation Economics*, No. 2. Taiwan: Hwa Tai Publishing.
- Cordeau, J.F.; Gendreau, M.; and Laporte, G. (1997). "A Tabu Search Heuristic for Periodic and Multi-Depot Vehicle Routing Problems." *Networks* 30, pp. 115-119.
- Cummings, C. P., Fairhurst, M., LaBelle, S., and Stuart, D. (1989). "Market Segmentation of Transit Fare Elasticities." *Transportation Quarterly* 43 (3), pp. 407-420.
- Curtin, J. F. (1968). "Effect of Fares on Transit Riding." *Highway Research Record* 213, pp. 8-20.
- Currie, G. and Phung, J. (2007). "Transit Ridership, Automobile Gas Prices, and World Events: New Drivers of Change?" *Transportation Research Record* 1992, pp. 3-10.
- Dandy, G. C. and Engelhardt, M. (2001). "Optimal Scheduling of Water Pipe Replacement Using Genetic Algorithms." *Journal of Water Resources Planning and Management*, Vol. 127, pp. 214-222.
- Daskin, M.S., Schofer, J.L., and Haghani, A.E. (1998). "A Quadratic Programming Model for Designing and Evaluating Distance-Based and Zone Fares for Urban Transit." *Transportation Research* 22B, pp. 25-44.
- Demery, L.W. (2006). "Japanese Railway Operating Cost Formulas." Retrieved June, 2006, from <http://www.publictransit.us>.
- Earl, P. E. (1995). *Microeconomics for Business and Marketing*. Vermont: Edward Elgar.
- Fleishman, D, Shaw, N., Joshi, A., Freeze, R., and Oram, R. (1996). "Fare Policies, Structures, and Technologies." *Transportation Research Board*, TCRP Report 10.
- Guenthner, R. P., and Jea, S. H. (1985). "Distance-Based Fare on Express Bus Routes." *Transportation Research Record* 1039, pp. 30-33.

- Gen, M., and Cheng, R. (1997). *Genetic Algorithms and Engineering Design*. New York: John Wiley and Sons.
- Hamacher, H. W., and Schobel, A. (2004). "Design of Zone Tariff Systems in Public Transportation." *Operations Research*, Vol. 52, No. 6, pp. 897-908.
- Henderson, J., and Fu, L. (2004). "Applications of Genetic Algorithms in Transportation Engineering." presentation in the Annual Meeting of Transportation Research Board, Washington, D.C., January 10-14.
- Herrera, F., Lozano, M., and Verdegay, J. L. (1994). "Applying Genetic Algorithms in Fuzzy Optimization Problems." *Fuzzy Systems and Artificial Intelligence*, Vol. 3, No. 1, pp. 39-52.
- Hestenes, M. R., and Stiefel, E. (1952). "Methods of Conjugate Gradients for Solving Linear Systems." *Journal of Research of the National Bureau of Standard*, Vol. 49, No.6, pp. 409-436.
- Ho, S. Y., Chen, H. M., and Shu, L. S. (1999). "Solving Large Knowledge Base Partitioning Problems Using the Intelligent Genetic Algorithm." in *Process Genetic and Evolutionary Computation Conference*, pp. 1567-1572.
- Holland, J. H. (1975). *Adaptation in Natural and Artificial Systems*. Cambridge, MA: MIT Press.
- Holland, J. H. (1992). *Adaptation in Natural and Artificial System: An Introductory Analysis with Applications to Biology, Control, and Artificial Intelligence*. Cambridge, MA: MIT press.
- Holroyd, E. M. (1967). "The Optimum Bus Service: A Theoretical Model for a Large Uniform Urban Area." *Vehicular Traffic Science*, pp 309-328.
- Hurdle, V. F. (1973). "Minimum Cost Schedules for a Public Transportation Route, I. Theory." *Transportation Science*, Vol. 7, pp. 109-137.
- Jorgensen, F., and Pedersen, P. A. (2004). "Travel Distance and Optimal Transport Policy." *Transportation Research Part B* 38, pp. 415-430.
- Kocur, G., and Hendrickson, C. (1982). "Design of Local Bus Service with Demand Equilibrium." *Transportation Science*, 16(2), pp. 149-170.
- LaBelle, S. J., and Fleishman, D. (1995). "Common Issues in Fare Structure Design." Retrieved January, 1995 from Federal Transit Administration: <http://www.fta.dot.gov/library/technology/sympops/LABELLE.htm>.

- Lam, W. H. K., and J. Zhou. (2000). "Optimal Fare Structure for Transit Networks with Elastic Demand." *Transportation Research Record* 1733, pp. 8–14.
- Lam, W., and Morrall, J. (1982). "Bus Passenger Walking Distances and Waiting Times: A Summer-Winter Comparison." *Transportation Quarterly*, Vol. 36, No. 3, pp. 407-421.
- Lave, L.B. (1972). "The Demand for Intercity Passenger Transportation." *Journal of Regional Science*, Vol. 12, No. 1, pp. 71-84.
- Lee, C. K. and Tsai, T. H. (2004). "Demand-Responsive Pricing Method for the Product Line of Taiwan High-Speed Rail." *Transportation Research Record* 1863, pp. 1–8.
- Lee, Y. J. and Vuchic, V. R. (2005). "Transit Network Design Variable Demand." *Journal of Transportation Engineering*, Vol. 131, No. 1, pp. 1-10.
- Link, H. and Polak, J. (2003). "Acceptability of Transportation Pricing Measures among Public and Professionals in Europe." *Transportation Research Record* 1839, pp. 34-44.
- Ling, J. H. (1995). "Transit Fare Differentials: A Theoretical Analysis." *Journal of Advanced Transportation*, Vol. 32, No. 3, pp. 297–314.
- Litman, T. (2004). "Transit Price Elasticities and Cross-Elasticities." *Journal of Public Transportation*, Vol. 7, No.2.
- Luenberger, D.G. (1989). *Linear and Non-Linear Programming, 2nd Edition*. Reading MA: Addison Wesley.
- Machado, P.; Tavares, J.; Pereira, F.; and Costa, E. (2002). Vehicle Routing Problem: Doing it the Evolutionary Way. In Proceedings of the Genetic and Evolutionary Computation Conference (GECCO'2002), New York, USA, pp. 9-13.
- Manheim, M.L. (1979). *Fundamentals of Transportation Systems Analysis*. Cambridge, MA: MIT Press.
- Mayworm, P., Lago, A., and McEnroe, J. (1980). "Patronage Impacts of Changes in Transit Fares and Services." Washington D.C.: Urban Mass Transportation Administrations (Report No. MD-06-0054-81-1).
- McFadden, D. (1974). "The Measurement of Urban Travel Demand." *Journal of Public Economics*, Vol. 3, No.4, pp. 303–328.
- Meyer, J. R. (1965). *The Urban Transportation Problem*. Cambridge, MA: Harvard University Press.

- Meyer, M.D., and Miller, E.J. (2001). *Urban Transportation Planning, 2nd edition*, New York: McGraw-Hill.
- Michalewicz, Z. (1999). *Genetic Algorithms + Data Structures = Evolution Programs, Third, Revised and Extended Edition*. New York: Springer- Verlag Berlin Heidelberg.
- Multisystem, INC., Mundle & Associates, INC., and Simon & Simon Research and Associated, INC. (2003). "Fare Policies, Structures, and Technologies: Update" *Transportation Research Board*, TCRP Report 94.
- Newell, G. F. (1971). "Dispatching Policies for a Transportation Route." *Transportation Science*, Vol.5 (1), pp. 91-105.
- Pham, D.T., and Karaboga, D. (2000). *Intelligent Optimisation Techniques-Genetic Algorithms, Tabu Search, Simulated Annealing and Neural Networks*. London: Springer- Verlag London Limited.
- Pham, L. (1991). "Effects of Fare Changes on Bus Ridership." American Public Transit Association, Washington, D.C.
- Powell, M.J.D. (1964). "An Efficient Method for Finding the Minimum of a Function of Several Variables without Calculating Derivatives." *Computer Journal*, Vol. 7, pp. 155-162.
- Pratelli, A. (2004). "The Combined Zone and Fare Planning Problem." Urban Transport X. Urban Transport and Environment in the 21st Century, WIT Press, pp. 311-320.
- Press, W. H. et al. (1992). *Numerical recipes*. New York: Cambridge University Press.
- Schmenner, R. (1976). "The Demand for Urban Bus Transit: A Route-by-route Analysis." *Journal of Transportation Economics and Policy* 10, pp. 68-86.
- Schobel, A. (2006). *Optimization in Public Transportation*. New York: Springer Science.
- Spasovic, L. N., Boile, M. P., and Bladikas, A. K. (1994). "Bus transit service coverage for maximum profit and social welfare." *Transportation Research Record 1451*, pp. 12-22.
- Su, C.H. et al. (2007). "Development of High-Speed Rail and Maglev Transportation System in Greater China Area." *Transportation Research Board 86th Annual Meeting*.

- O'Sullivan (2003). *Microeconomics: Principles and Tools*. Englewood Cliffs, NJ: Princeton Hall.
- Tang, K. S., Man, K. F., Liu, Z. F., and Kwong, S. (1998). "Minimal Fuzzy Memberships and Rules Using Hierarchical Genetic Algorithms," *IEEE Transaction on Industrial Electronics*, vol. 45, no. 1, pp. 162-169.
- Thomson, J. M. (1967). "An Evaluation of Two Proposals for traffic Restraint in Central London." *Journal of the Royal Statistical Society* 130, pp. 340-348.
- Tobin, R. L., and T. L. Friesz (1988). "Sensitivity Analysis for Equilibrium Flow." *Transportation Science*, Vol. 22, No. 4, pp. 242-250.
- Tsai, F. M., Chien, S. I., and Spasovic, L. N. (2007). "Optimizing Distance-based Fares and Headway of and Intercity Transportation System with Elastic Demand and Trip Length Differentiation." *Transportation Research Board 87th Annual Meeting*.
- Virginia Miller (2006). "Even with Decline in Gas Price in November, Strong Ridership Trend Continues As More Than 25 Agencies Show Double Digit Increases." Retrieved January 18, 2006, from American Public Transportation Association Web site: http://www.apta.com/media/releases/060118ridership_increases.cfm.
- Voith, R. (1991). "The Long-Run Elasticity of Demand for Commuter Rail Transportation." *Journal of Urban Economics*, Vol. 30, No. 3, pp. 360-372.
- Voith, R. (1997). "Fares, Service Levels, and Demographics: What Determines Commuter Rail Ridership in the Long Run?" *Journal of Urban Economics*, Vol. 41, No. 2, pp. 176-197.
- Vuchic, V. R. (2004). *Urban Transit: Operations, Planning, and Economics*. New York: John Wiley & Sons.
- Yang, H., and Lam, W.H. K. (1996). "Optimal Road Tolls Under Conditions of Queuing and Congestion." *Transportation Research*, Vol. 30A, pp. 463-486.
- Wu, Y. T., and Shih, F. Y. (2006). "Genetic Algorithm Based Methodology for Breaking the Steganalytic Systems." *IEEE Transactions on Systems, Man, and Cybernetics-Part B: Cybernetics*, Vol. 36, No. 1, pp. 24-31.
- Zolfaghari, S. and Liang, M. (2002). "Comparison Study of Simulated Annealing, Genetic Algorithms and Tabu Search for Solving Binary Comprehensive Machine Grouping Problems." *International Journal of Production Research*, Vol. 40 (9), pp. 2141-2148.